Aus dem Institut für Physiologische Chemie

Geschäftsführender Direktor: Prof. Dr. Hantschel

des Fachbereichs Medizin der Philipps-Universität Marburg

The Role of the Actin Regulator Cyclase-associated Protein 2 (CAP2) for Mammalian Skeletal Muscle Development

Inaugural-Dissertation

zur Erlangung des Doktorgrades

der gesamten Naturwissenschaften

(Dr. rer. nat.)

dem Fachbereich Medizin der Philipps-Universität Marburg

vorgelegt von

Lara-Jane Kepser

aus Goch

Marburg, 2020

Angenommen vom Fachbereich Medizin der Philipps-Universität Marburg am:

27.08.2020

Gedruckt mit Genehmigung des Fachbereichs Medizin

Dekan: Prof. Dr. Helmut Schäfer

Referent: Prof. Dr. Marco Rust

1. Korreferent: Prof. Dr. Thomas Worzfeld

"All our dreams can come true, if we have the courage to pursue them."

Walt Disney

TABLE OF CONTENTS

Summary

Actin is a structural protein that is a major component of the eukaryotic cytoskeleton. It is not only important for morphology and stability of cells, but also for dynamic processes such as cell migration, adhesion, growth or contraction. In muscle cells, the highly structured complex of myosin and actin filaments is essential for the coordinated contraction of muscle fibers, which ultimately generates muscle strength. In order to achieve this function, actin filaments have to build up and rebuilt dynamically during muscle development. However, the molecular mechanisms involved are still largely unknown. The need to elucidate these mechanisms arises from the finding that a large number of human myopathies are associated with defects in the actin cytoskeleton. Previous studies identified the transcription factor SRF (serum response factor) as a major regulator of skeletal muscle development in humans and mice. In a feedback mechanism, SRF is activated in an actin-dependent manner and in turn controls the expression of actin and actin-regulatory proteins. One of the main activators of SRF is MRTF (myocardin related transcription factor), which can be sequestered by actin monomers, thus preventing translocation and subsequent activation of SRF in the nucleus.

This cumulative dissertation presents two studies that aim to elucidate the underlying processes of myopathies during skeletal muscle development.

In the first publication, "CAP2 deficiency delays myofibril actin cytoskeleton differentiation and disturbs skeletal muscle architecture and function", we identified a previously unknown function for the actin-regulatory protein CAP2 (cyclase-associated protein 2) during skeletal muscle development in mammals. We showed that CAP2 controls the remodeling of actin filaments in developing skeletal muscle and is therefore essential for the differentiation of muscle fibers. As a consequence of CAP2 loss, mouse mutants developed structural changes in skeletal muscles, characterized by a frequent occurrence of ring fibers, internalized nuclei and disturbed mitochondrial distribution, as well as deficits in motor functions and moderate muscle weakness. These changes reflect symptoms of human myopathies.

In the second manuscript, "Cyclase-associated protein 2 (CAP2) controls MRTF-A localization and SRF activity in mouse embryonic fibroblasts", we reported that loss of CAP2 in mouse embryonic fibroblasts lead to disturbed SRF activity. Specifically, we found that CAP2 controls subcellular distribution of the SRF trans-activator MRTF in an actin-dependent mechanism. CAP2 inactivation was associated with reduced nuclear MRTF levels and impaired SRF-mediated gene expression. This suggests that CAP2-dependent actin dynamics may also control SRF activity during skeletal muscle development and that dysregulation of SRF may cause or at least contribute to the myopathy in CAP2 mutant mice.

Zusammenfassung

Das Strukturprotein Aktin stellt einen Hauptbestandteil des Zytoskeletts aller eukaryotischen Zellen dar. Als solches ist es nicht nur für die Morphologie und Stabilität von Zellen wichtig, sondern auch für dynamische Prozesse wie Zellmigration, Adhäsion, Wachstum oder Kontraktion. In Muskelzellen ist der hoch strukturierte Komplex aus Myosin- und Aktin-Filamenten essentiell für die koordinierte Kontraktion der Muskelfasern, welche letztendlich Muskelkraft erzeugen. Um diese Funktion zu bewerkstelligen, müssen Aktin-Filamente während der Muskelentwicklung dynamisch auf- und auch umgebaut werden. Die daran beteiligten molekularen Mechanismen sind allerdings noch weitestgehend unbekannt. Gleichzeitig existiert der Befund, dass eine Vielzahl humaner Muskelerkrankungen mit Defekten im Aktin-Zytoskelett assoziiert ist. Die daraus resultierende Notwendigkeit zur Aufklärung dieser Mechanismen bildet die Grundlage und das Ziel der vorliegenden Dissertation. Frühere Arbeiten anderer Arbeitsgruppen haben den Transkriptionsfaktor SRF (serum response factor) als einen wichtigen Regulator der Skelettmuskelentwicklung in Menschen und Mäusen identifiziert. In einem Rückkopplungsmechanismus wird SRF Aktin-abhängig aktiviert und kontrolliert wiederum die Expression von Aktin und Aktin-regulierenden Proteinen. Einer der Hauptaktivatoren von SRF ist MRTF (myocardin related transcription factor), welcher zumeist im Zytoplasma an Aktin-Monomere gebunden werden kann, wodurch seine Translokalisation in den Zellkern und die Aktivierung von SRF unterbunden werden.

Die vorliegende kumulative Dissertation präsentiert zwei Studien, die sich mit der Aufklärung von Prozessen beschäftigen, die Skelettmuskelentwicklungsdefekten zugrunde liegen.

In der ersten Publikation „CAP2 deficiency delays myofibril actin cytoskeleton differentiation and disturbs skeletal muscle architecture and function" wurde für das Aktin-regulierende Protein CAP2 (cyclase-associated protein 2) eine bislang unbekannte Funktion während der Entwicklung der Skelettmuskulatur in Säugetieren gezeigt.

Die Daten ergaben, dass CAP2 den Umbau von Aktin-Filamenten im sich entwickelnden Skelettmuskel kontrolliert und somit essentiell für die Differenzierung von Muskelfasern ist. Als Konsequenz eines CAP2-Funktionsverlusts entwickeln Mausmutanten strukturelle Veränderungen im Skelettmuskel, welche durch das gehäufte Auftreten von Ringbinden, internalisierten Zellkernen und durch eine gestörte Mitochondrien-Verteilung gekennzeichnet sind. Diese gehen mit Defiziten in motorischen Funktionen und einer moderaten Muskelschwäche einher. Diese Veränderungen spiegeln Symptome humaner Muskelerkrankungen wider.

Im zweiten Manuskript „Cyclase-associated protein 2 (CAP2) controls MRTF-A localization and SRF activity in mouse embryonic fibroblasts“ konnte gezeigt werden, dass der Verlust von CAP2 in embryonalen Maus-Fibroblasten zu einer gestörten SRF-Aktivität führt. Insbesondere wurde festgestellt, dass CAP2 die subzelluläre Verteilung des SRF-Transaktivators MRTF in einem Aktin-abhängigen Mechanismus steuert. Die Inaktivierung von CAP2 war mit reduzierter MRTF-Lokalisation im Kern und einer Beeinträchtigung der SRF-vermittelten Genexpression verbunden. Dies lässt uns vermuten, dass CAP2-abhängige Aktin-Dynamik die SRF-Aktivität auch während der Entwicklung der Skelettmuskulatur kontrollieren kann und dass eine Dysregulation von SRF die Myopathie bei CAP2-Mutanten verursachen oder zumindest zu ihr beitragen kann.

1. Introduction

1.1 The Actin Cytoskeleton

The actin cytoskeleton consists of a complex and dynamic network of actin filaments (F-actin) and actin-regulatory proteins (ARPs). Together with the other components of the eukaryotic cytoskeleton, the microtubules and intermediate filaments, it regulates crucial cellular processes such as adhesion, migration, division, organelle transport and contraction (Stricker et al. 2009). Since actin is essential for cellular functioning, its amino acid sequence is highly conserved throughout evolution. Actin has three main isotypes (α-actin, β-actin and γ-actin) which show different localization pattern (Perrin and Ervasti 2010; Tondeleir et al. 2009). While β- and γ-actin are ubiquitously expressed, the α-actin isoforms are abundant in those adult muscle tissues they were initially named after: α-skeletal muscle actin (α-SKA), α-cardiac actin (α-CAA) and α-smooth muscle actin (α-SMA). However, during skeletal muscle development occurs a switch in the expression of actin isoforms, from cytoplasmic to α-actin isoforms, that is crucial for proper structure and functioning of the adult muscle. To conduct all the different functions, the actin cytoskeleton undergoes permanent reorganization which requires a highly controlled regulation. Thereby, specific structures as stress fibers can be formed (Baum et al. 2006). An important key feature for the generation of these unique structures is the dynamic transition of actin itself from monomeric, globular actin (G-actin) to F-actin by the formation of non-covalent bonds as well as bundle formation by cross-linking proteins (Revenu et al. 2004). The assembly and disassembly of F-actin is known as actin treadmilling and is maintained by several ARPs.

1.1.1 Actin Treadmilling and Actin-regulatory Proteins

During the actin treadmilling mechanism, F-actin assembly and disassembly is maintained by ARPs. F-actin is a polar structure and can be assembled by addition of adenosine triphosphate (ATP)-bound G-actin at the barbed end.

Additionally, adenosine diphosphate (ADP)-bound actin can be dissociated from the pointed end (Baum et al. 2006; Pollard and Borisy 2003). The key players during these processes are members of the actin depolymerizing factor (ADF)/cofilin family, profilins and cyclase-associated proteins (CAPs). ADF, cofilin1 and cofilin2 are important depolymerizing factors that play a crucial role in F-actin disassembly by enhancing the dissociation rate of ADP-actin subunits from the pointed ends and by F-actin severing. While ADF and cofilin1 are expressed in almost all non-muscle tissues, cofilin2 is the predominant isoform in adult skeletal muscles (Vartiainen, et al. 2002; Thirion, et al. 2001; Ono et al. 1994). Profilin1-4 are important regulators of F-actin assembly since they are thought to be important for the nucleotide exchange from ADP-to-ATP on G-actin and the direction of ATP-actin to the barbed ends (Baum et al. 2006). Profilin1 is broadly expressed in non-muscle cells, profilin2 is expressed in adult skeletal muscles and profilin3 and 4 expression was described mainly in the testis (Witke et al. 1998; Honore et al. 1993; Ohshima et al. 1989). In mammals, there are two CAP isoforms that are known to interact with cofilins by enhancing F-actin disassembly and by releasing cofilin from G-actin for further treadmilling (Ono 2013). On the other side they have an impact on the nucleotide exchange similar to profilins. CAP1 is ubiquitously expressed and CAP2 is predominantly expressed in striated muscles and in the brain (Peche et al. 2007; Bertling et al. 2004).

1.2 Actin Dynamics in the Skeletal Muscle

There are three major muscle types in mammals: skeletal muscles, cardiac muscles and smooth muscles. Here, F-actin mainly consists of skeletal muscle actin (α-SKA), cardiac muscle actin (α-CAA) and smooth muscle actin (α-SMA) respectively. Skeletal and cardiac muscles belong to the striated muscle tissues for which sarcomeres, the basic functional units of the muscle fiber, are characteristic.

Sarcomeres are a highly organized structure that consist of actin and myosin filaments which are essential for muscle contraction. Consequently, the amount of G-actin in adult muscles is reduced to less than 1% of the total actin (Shimizu and Obinata 1986) implicating that the actin cytoskeleton has to be extremely stable. However, during skeletal muscle development this system is less organized and extremely receptive for disruptions that can result in several diseases.

1.2.1 Switch of Actin Isoforms during Skeletal Muscle Development

Unlike the strict correlation of actin isoforms to the respective muscle tissue in adulthood, there is a switch in the expression of different actin isoforms that goes ahead with specific stages and processes during skeletal muscle development (see Figure S9 in Kepser et al. 2019).

During early embryonic development (< embryonic day (E)12) β-cytoplasmic actin (β-CYA) and γ-cytoplasmic actin (γ-CYA), usually known to be expressed in non-muscle cells, are the main isoforms expressed in undifferentiated myoblasts (Hanft et al. 2006; Sonnemann et al. 2006; Tondeleir et al., 2009; Rybakova et al. 2000). Here, the actin cytoskeleton does not yet display any kind of striated organization and β-CYA and γ-CYA are part of actomyosin bundles called stress fibers. During this time, the actin cytoskeleton is highly dynamic with a high amount of G-actin. When myoblasts start to fuse to myotubes during primary myogenesis (E12 – E14), there is a switch from β-CYA and γ-CYA to α-SMA and α-CAA (Lloyd et al. 2004). Now, G-actin level decrease and newly formed F-actin starts to align and attach to so-called Z-discs through alpha-actinin, leading to a first striated pattern. During secondary myogenesis (E14 – E18), myotubes grow by addition of F-actin and form myofibrils which correlates with a second switch from α-SMA and α-CAA to the adult isoform α-SKA (Mizuno et al. 2009; McHugh et al. 1991; Chal and Pourquie 2017).

In mice, this process is known to be maintained by ARPs of the ADF/cofilin family and mutations in cofilin2 have been identified as a reason for the development of myopathies characterized by pathological skeletal muscles and muscle weakness, similar to human diseases (Gurniak et al. 2014; Agrawal et al. 2012).

1.2.2 Role of Actin-regulatory proteins for Skeletal Muscle Development and Maintenance

ARPs that were associated with skeletal muscle development and maintenance in the past are members of the ADF/cofilin family. While cofilin1 seems to have a broader role during early myogenesis, it is absent from late postnatal and adult skeletal muscles (Vartiainen et al. 2002; Thirion et al. 2001; Ono et al. 1994). A direct role for skeletal muscle development was not described so far as cofilin1 mutant mice died already during embryonic development (Gurniak et al. 2005). Nevertheless, cofilin1 was upregulated during early phases of regeneration after muscle injury (Thirion et al. 2001), suggesting that it may also have important functions during the early phases of myogenesis, as mechanisms of muscle regeneration are very similar to muscle developmental processes. When cofilin1 levels decrease during late embryonic/early postnatal development in mice, cofilin2 expression increases drastically and remains the only member of the ADF/cofilin family in adulthood (Vartiainen et al. 2002; Thirion et al. 2001; Ono et al. 1994). Cofilin2 is a known regulator of early postnatal skeletal muscle development, especially when the second actin switch takes place (Gurniak et al. 2014). Systemic cofilin2 mutants showed severe defects in skeletal muscle morphology during postnatal development and died around postnatal day (P)8 (Gurniak et al 2012; Agrawal et al. 2012). Morphological changes were characterized by internalized nuclei, disturbed distribution of mitochondria and F-actin aggregates; all features that were described for human myopathies as nemaline myopathy (Agrawal et al. 2007). Additionally, cofilin2 mutants displayed a delay in the second actin switch.

However, around birth they were indistinguishable from control littermates indicating again a more prominent role of cofilin2 for postnatal development.

Even though other ARPs as ADF, profilin1 and profilin2 were also identified to be expressed during different phases of skeletal muscle development, there are no studies implicating a specific and important role during these processes so far (Mohri et al. 2000; Ono 2010; Ohshima et al. 1989; Abe et al. 1989; Ono et al. 2003a; Nagaoka et al. 1996; Babcock and Rubenstein 1993; Ohshiama et al. 1989; Witke et al. 1998; Honore et al. 1993).

CAPs were not linked to skeletal muscle defects in the past, even though systemic CAP2 mutant mice showed severe defects in heart physiology (Peche et al. 2013; Xiong et al. 2019; Stöckigt et al. 2016). Beside enlarged hearts, fibrosis and dilated ventricles, CAP2 mutant hearts displayed disorganized myofibrils which might be a hint for a specific role during myofibrillogenesis. Systemic loss of CAP1 lead to embryonic lethality (Jang et al. 2019), giving no insight into specific functions for skeletal muscle development at all.

1.3 Serum Response Factor Pathway

Serum response factor (SRF) belongs to the MADS (MCM1, Agamous, Deficiens, and SRF) box superfamily of transcription factors and, with more than 200 downstream targets, controls multiple signaling pathways (Posern and Treisman 2006; Sun et al. 2006). SRF regulates several basic cellular processes as cell differentiation, apoptosis and growth as it controls the transcription of immediate early genes such as *c-Fos* (Arsenian et al. 1998). Beside this, SRF is a main regulator of cytoskeletal and muscle-specific genes and is accordingly an important player of myogenesis.

SRF can be activated by two different families of co-activators. The first one, the family of myocardin-related transcriptional factors (MRTF), can activate SRF in an actin-dependent manner (Posern and Treisman 2006).

When G-actin is present abundantly in the cell, MRTF is bound and due to that cannot translocate to the nucleus to activate SRF (Miralles et al. 2003; Olson and Nordheim 2010). As actin and actin regulators are downstream of SRF, this pathway is able to regulate itself at the transcriptional and post-transcriptional level. The MRTF family comprises two isoforms, MRTF-A and MRTF-B, which are both expressed ubiquitously. The second family of co-activators, the ternary complex factors (TCF), are regulated by the Ras/extracellular signal-regulated kinases (ERK) signaling pathway, mainly known to be involved in tumor development, and compete with MRTF for the SRF DNA-binding domain (Gualdrini et al. 2016).

1.3.1 Role during Skeletal Muscle Development

As SRF-dependent gene regulation is crucial for embryogenesis, systemic SRF mutants died due to gastrulation defects (Arsenian et al. 1998), giving no direct insights into its role for skeletal muscle development. First results were gathered a few years later after analysis of mice with a skeletal muscle-specific deletion of SRF (Li et al. 2004). Mutant mice were born at Medelian ratios but died perinatally due to severe skeletal muscle hypoplasia. When SRF was deleted in adult skeletal muscles, in a tamoxifen-inducible Cre mouse model, mice suffered from decreased muscle strength due to progressive loss of muscle mass (Lahoute et al. 2008). This implicates a crucial role of SRF for skeletal muscle differentiation and maintenance rather than early development.

Systemic loss of MRTF-A or MRTF-B did not show any effect on skeletal muscle development and morphology, even though both of them are activated after muscle injury (Mokalled et al. 2012). Interestingly, skeletal muscle-specific double knockout of both, MRTF-A and MRTF-B, lead to perinatal death (Cenik et al. 2016). Mice displayed reduced muscle fiber size and defects in sarcomere structure, implicating their importance for skeletal muscle differentiation and sarcomere formation.

Additionally, RNA sequencing revealed that genes known to be important for sarcomere formation and functioning were strongly downregulated and myoblasts showed reduced level of proliferation and an increased rate of apoptosis. Given the fact, that deletion of both, MRTF-A and MRTF-B, lead to such severe phenotypes in comparison to single mutations, it is likely that they are able to compensate for each other.

Together, the MRTF-SRF pathway has important functions for the differentiation of skeletal muscles and disturbances result in severe functional defects together with increased lethality of mice. On the other hand, disturbances of the TCF-SRF pathway were not specifically linked to skeletal muscle defects before, which is the reasons that we focus on the MRTF-SRF pathway in this dissertation as it seems to be the main player in the process of skeletal muscle development.

1.4 Aim of the Thesis

Aim of the thesis was to decipher the specific role of CAP2 for skeletal muscle development in mice. This was done by a characterization of muscle function in mutant mice together with histological, biochemical and molecular analysis of various skeletal muscle specimen, complemented with cell biological analysis. Given the fact that myogenesis is similar in hearts and skeletal muscles and that cofilin2 and CAP2 work together during the actin treadmilling mechanism, CAP2 might be an important player during skeletal muscle development and maintenance as well. Beside this, ARPs are important regulators of actin dynamics and changes in the expression of CAP2 might lead to dysregulated binding of MRTF to G-actin and consequently disruptions in SRF signaling.

2. Summary of Publications

2.1 CAP2 Deficiency delays Myofibril Actin Cytoskeleton Differentiation and disturbs Skeletal Muscle Architecture and Function

CAP2 mutant mice were born at expected Mendelian ratios. To assess whether loss of CAP2 leads to any behavioral abnormalities in newborn mice we analyzed physical landmarks and developmental milestones from P2 until P18. CAP2 mutants showed no abnormalities in the time points of eye opening and pinna detachment (Fig.1 A - B). Additionally, activity levels were equal to controls (Fig. 1 C), which leads to the impression that general development is unaffected. However, obvious differences were seen in all tests performed to study motor functions. CAP2 mutants showed a long-lasting tremor and significantly decreased performances in surface righting, level screen, vertical screen, negative geotaxis and bar holding (Fig.1 D - I and Movie S1). Tests for sensory functions or reflexes such as cliff avoidance, auditory and tactile startle, visual placing, grasping reflex and forelimb placing (Fig 1. J - O) were again unaffected. To investigate whether motor defects were still present in older mice, we performed several tests such as string test, grip strength and rotarod in juvenile and adult animals. Again, CAP2 mutants showed impairments in the string test, which is similar to bar holding in the developmental milestones testing (Fig. S1 A). Also, in the grip strength, which assesses maximal force generation of the animals, CAP2 mutants performed weaker, even after normalization to their reduced body weight (Fig. S1 B - C). Interestingly, CAP2 mutants did not display any defects in the rotarod or open field (Fig. S1 D - G) that we performed to assess motor coordination and activity. Hence, CAP2 mutants displayed specific defects in motor functions.

To test whether motor function defects were associated with skeletal muscle defects, we performed a thorough histological analysis of skeletal muscle specimen. After identification of CAP2 in multiple muscles (Fig. 2 A) we found several structural changes in CAP2 mutant *Musculus quadriceps femoris* (QUAD) muscles.

Stained cross-sections revealed a 12-fold increase in internalized nuclei, altered mitochondrial distributions in about 22% of fibers and a huge number of so-called ring fibers (Fig. 2 C - F). Ring fibers are a feature of several human myopathies and are characterized by reorientation of several myofibers that causes a ring-like structure in cross-sectioned myofibers (Fig. S2 B). These ring fibers can be nicely stained by fluorescent phalloidin, a phallotoxin that stably binds to F-actin, and were identified to be present in about 41% of the muscle cells in CAP2 mutants (Fig. 2 D, F). Co-labeling with antibodies against different myosin heavy chain (MHC) isoforms revealed that ring fibers were restricted to MHC IIB positive fibers, which are commonly called Type IIB fibers (Fig. S2 E, F). Further histological analysis did not reveal any hints towards other pathological conditions such as fibrosis or inflammation (Fig. S3). The described structural differences were also present in *Musculus tibialis anterior* (TA) and *Musculus extensor digitorum longus* (EDL), but not in *Musculus soleus* (SOL) (Fig. 2 F, Fig. S5, S6). Similar to QUAD, TA and EDL muscles consist mainly of Type IIB fibers and are so-called fast twitch muscles. In comparison, SOL muscles contain no Type IIB fibers at all, which is characteristic for slow twitch muscles. Despite the structural differences, we did not notice any kind of atrophy or malformation of leg muscles compared to control littermates (Fig. 2 B, Fig. S2 A). Further, staining of longitudinal sections with phalloidin and desmin, a protein that is located at the Z-discs, showed that general sarcomere structure was intact in CAP2 mutants (Fig. 2 G). Additionally, these findings were supported by analysis of muscle fibers on the ultrastructural level by electron microscopy (EM). Here, we confirmed the presence of ring fibers, mitochondrial abnormalities and a normal sarcomere structure (Fig. 2 H - K). Taken together, histological analysis of adult CAP2 mutant muscles exhibited several structural changes that can explain the defective motor functions and are similar to phenotypes seen in human myopathies caused by mutations in ARPs or actin itself.

Further, we were interested in early postnatal development of skeletal muscles, as first motor function deficits were already seen during that period. CAP2 is known to be expressed in adult skeletal muscles, but was never investigated during late fetal/early postnatal development. Western Blots of control QUAD muscles between E18 and P12 revealed CAP2 expression throughout development (Fig. 3 A). Additionally, structural changes comparable to ring fibers were not noted at P4, but at P8 and P12 we found a high amount of F-actin aggregates, ring fibers and an increased number of internalized nuclei similar to adults (Fig. 3 B). However, F-actin rich aggregates were no longer present at P21 and later stages. At P8, EM revealed disturbances as myofibril disarrangement and changes in mitochondrial distribution (Fig. S7 B - K). Notably, structural changes at P8 and P12 coincided with the strongest behavioral abnormalities during developmental milestone testing. During this time window, an important step of skeletal muscle development is happening – the second actin switch.

To test whether CAP2 has an impact on the switch of α-SMA and α-CAA to α-SKA, similar to cofilin2, we analyzed protein level of several actin isoforms in QUAD tissue (Fig. 3 C). First of all, we noticed with a pan-actin antibody that total actin levels were increased in CAP2 mutants throughout development and in adulthood. This increase was caused by elevated level of α-actin isoforms, as β- and γ-actin level were unchanged. In controls, α-SMA and α-CAA level dropped during postnatal development, similar to what was reported before. In CAP2 mutants, this drop was delayed and both isoforms were still present at P12 while they were already absent in age-matched control littermates. Interestingly, α-SKA levels were elevated throughout development in CAP2 mutant QUAD and were still increased in adult muscles. In contrast, mRNA levels of α-actin isoforms from CAP2 mutants were strongly reduced at E18 and unchanged at P4 (Fig. S8 A, B), indicating that the increase in protein level was not caused by elevated gene expression, but by delayed degradation of the proteins.

To examine whether the delay in the actin switch happened due to an impaired exchange of actin isoforms at the thin filaments, we made a fractionation of muscle proteins into a soluble and insoluble fraction. F-actin belongs to the insoluble fraction and we investigated whether α-SMA, α-CAA and/or α-SKA were still present in this fraction (Fig. S8 C). Indeed, we found the majority of α-SKA in the insoluble fractions in both, CAP2 mutants and controls, at P12. α-SMA and α-CAA were no longer detectable in controls, but in CAP2 mutants substantial level of both were detectable in the insoluble fraction. This implicates that both isoforms were indeed still incorporated in the thin filaments of sarcomeres. To validate this finding, we stained longitudinal sections with α-SMA (Fig. 3 D). As expected, we found α-SMA in a striated pattern that did not co-localize with desmin, while in controls the α-SMA signal was restricted to blood vessels, suggesting that in CAP2 mutants it was still present in sarcomeric F-actin. Hence, we identified CAP2 as an important regulator of the second actin switch at the level of thin filaments.

As innervation of skeletal muscles by motor neurons is significantly involved in the process of muscle contraction, defective motor functioning and structural deficits can also be caused due to developmental disruptions in this system. To check whether the described defects are caused by disruptions in the skeletal muscle itself or have a neurological origin, we re-expressed CAP2 in mutant QUAD muscles. Using a viral construct, we transduced green fluorescent protein (GFP)-tagged CAP2 in QUAD muscles at P0, before first structural defects were seen, and sacrificed the mice at P21 to check for ring fiber formation (Fig. 4 A). As a control, we expressed solely GFP in CAP2 mutant QUADs as well. As expected, ring fibers were present in GFP-CAP2-negative and in GFP-positive control muscle fibers, but were nearly absent in fibers that express GFP-CAP2 (Fig. 4 B, C). Additionally, the whole muscle seems to be more structured in regions expressing GFP-CAP2 as the interstitial space between muscle fibers was reduced and fibers were arranged more accurate.

These findings showed that the described skeletal muscle phenotype of CAP2 mutants is indeed skeletal muscle-specific and is not caused by disturbed innervation.

Taken together, our study revealed an important role for CAP2 in skeletal muscle development at the time point of the second actin switch during early postnatal development. When myofibril differentiation was disturbed, mutants suffered from several structural defects that resulted in motor deficits and decreased muscle strength. These changes commenced during early postnatal development and consisted until adulthood.

2.2 Cyclase-associated Protein 2 (CAP2) controls MRTF-A Localization and SRF Activity in Mouse Embryonic Fibroblasts

To study whether SRF activity is somehow controlled or influenced by CAP2, we generated immortalized MEFs from two control and two CAP2 mutant embryos. We could show by immunoblots that CAP2 was expressed solely in control MEFs (Fig. 1 A) and by transfection with CAP2-GFP we revealed that subcellular localization of CAP2 is mainly restricted to the cytosol (Fig. 1 B). By investigation of general appearance, proliferation and morphology (Fig. 1 C - E), we excluded any obvious general defects upon loss of CAP2 and identified MEFs as a suitable tool for our experiments.

As CAP2 is a known regulator of actin dynamics, we took a closer look at the actin cytoskeleton by staining the cells with phalloidin and DNase I, a marker that binds G-actin (Fig. 1 F - H). Quantification of fluorescence intensities revealed an increase in G- and F-actin level in CAP2 mutant MEFs. Interestingly, ratio of G- to F-actin was similar in both groups and by immunoblotting of G- and F-actin consisting fractions we did not see any difference as well (Fig. I - K). Hence, despite the increase in G- and F-actin levels, CAP2 mutant MEFs did not show any abnormalities in the actin cytoskeleton.

However, increased level of G-actin might have an impact on MRTF localization, as MRTF can be bound by G-actin and consequently cannot activate SRF in the nucleus. To study MRTF localization and translocation in more detail we generated cells that stably express MRTF-A-GFP (Fig. 2 A). We categorized MRTF-A localization into three categories: cytosolic, nuclear and equal distribution. Indeed, CAP2 mutant MEFs showed a striking increase in cytosolic MRTF-A compared to control cells (Fig. 2 C), probably reflecting the increase in G-actin levels in the cytosol. While MRTF-A localization was mainly restricted to the cytosol in CAP2 mutants, it was mostly nuclear in controls. Additionally, we analyzed endogenous MRTF-A localization and found a similar localization pattern for both groups, excluding that viral transduction of the cells had an impact on MRTF-A localization (Fig. 2 B, C). Taken together, these results suggest that CAP2 controls MRTF-A localization via an actin-dependent mechanism as increased level of G-actin go ahead with an increased cytosolic MRTF-A localization in CAP2 mutants.

To verify this hypothesis, we manipulated the actin cytoskeleton by specific drugs. As Latrunculin B (LATB) leads to an elevation of the G-actin pool and consequently increases the binding with MRTF, more MRTF-A should be located in the cytosol after treatment. Treatment with Jasplakinolide (JASP) leads to stabilization of F-actin that in the end results in a decrease in G-actin level and consequently less MRTF binding, which should result into translocation of MRTF-A into the nucleus. Indeed, control cells showed increased cytosolic MRTF-A localization after LATB treatment and more nuclear MRTF-A after treatment with JASP (Fig. 2 D, E). Interestingly, MRTF-A localization in CAP2 mutant cells did not change upon LATB treatment. In contrast, JASP treatment resulted in an increased fraction of nuclear MRTF-A which, in the end, was similar to MRTF-A localization in untreated control cells. Hence, reduction of G-actin by JASP treatment rescued the phenotype seen in CAP2 mutants, supporting again the hypothesis that CAP2 controls MRTF-A localization via regulation of the actin cytoskeleton.

To identify whether CAP2 was additionally relevant for serum-induced nuclear translocation of MRTF, we performed live-cell imaging to quantify translocation performance and speed. It is known that upon serum stimulation, MRTF is translocated within minutes to the nucleus. After starving of MEFs for 48 h, which lead to an increased cytosolic localization of MRTF-A, we added fetal calf serum (FBS) to cells and analyzed MRTF-A translocation kinetics. To do so, we only examined cells that, prior to stimulation, showed only cytosolic localization of MRTF-A and similar fluorescence intensities. By analyzing the time MRTF-A needed to translocate completely to the nucleus, we revealed that there was no significant difference in the translocation kinetics between CAP2 mutants and controls (Fig. 3 A, B; Movies S1 - 2). Additionally, we investigated the distribution of MRTF-A under starving and after serum stimulation, similar to the previous experiments. As expected, control MEFs showed an increase in cytosolic MRTF-A under starving condition compared to basal condition and a complete translocation to the nucleus after serum stimulation (Fig. 3 C, D). In contrast, MRTF-A localization under starving condition did not change in CAP2 mutant cells and after serum stimulation there were still cells left where MRTF-A was distributed equally. Hence, even though MRTF-A localization was changed upon loss of CAP2, the kinetics of translocation was unchanged between mutant and control cells.

Next, we examined whether altered MRTF distribution in CAP2 mutants affects SRF activity. We generated another cell line which stably expressed an SRF reporter for luciferase measurements. Here, the firefly luciferase is controlled by three minimal c-Fos promotor sequences including serum response elements (SRE). In order to investigate effects coming from MRTF-A itself, this promotor is lacking TCF binding sites. Indeed, luciferase activity was significantly reduced in CAP2 mutant cells compared to controls under basal conditions (Fig. 4 A), implicating that MRTF-A mis-localization directly influences and reduces SRF activity.

To investigate whether reduced SRF activity can be directly linked to changes in SRF-dependent gene expression in CAP2 mutants, we investigated whether established SRF target genes were reduced as well. To do so, we performed qPCR with several targets as the immediate early genes cysteine-rich angiogenic inducer 61 (*Cyr61*) and *c-Fos*, the cytoskeletal genes actin alpha 2 (*Acta2*, encoding α-SMA) and vinculin (*vcl*), and SRF (*Srf*) itself. As a control we used early growth response protein 2 (*Egr2*), a MRTF-independent but SRF-dependent target. As expected, mRNA levels of SRF targets and *Srf* itself were strongly downregulated in CAP2 mutants, while *Egr2* levels were unchanged (Fig. 4 B). Hence, SRF activity and SRF-dependent gene expression is reduced as a consequence of changed MRTF-A localization upon loss of CAP2. Interestingly, similar to MRTF-A translocation kinetics, induced SRF activity upon serum stimulation in the luciferase assay was similar in CAP2 mutants and controls as well (Fig. 4 C).

Taken together, lack of CAP2 lead to elevated level of G-actin which consequently resulted in an increased cytosolic MRTF-A localization that in the end lead to decreased MRTF-SRF-dependent gene regulation in CAP2 mutant MEFs.

2.3 Description of own Contribution

For the first publication “CAP2 deficiency delays myofibril actin cytoskeleton differentiation and disturbs skeletal muscle architecture and function” I performed all behavioral experiments, qPCRs, preparations of the muscle specimen, slicing, immunohistochemical staining, confocal microscopy and all data analysis. Histological staining and electron microscopy was performed in collaboration with A. Pagenstecher. Western Blots were done together with the MSc student F. Damar that I supervised. Virus production and transduction in CAP2 mutant QUAD was carried out by T. De Cicco in T. J. Prószyński’s laboratory. The manuscript was written by M. B. Rust and me.

For the second manuscript “Cyclase-associated protein 2 (CAP2) controls MRTF-A localization and SRF activity in mouse embryonic fibroblasts” I performed all experiments and data analysis. Generation of the stable cell lines expressing MRTF-A and luciferase constructs was done together with L. S. Hinojosa in R. Grosse’s laboratory. The same applies for live-cell imaging. The manuscript was written by M. B. Rust and me.

3. Discussion

3.1 The Role of CAP2 for Skeletal Muscle Development

In “CAP2 deficiency delays myofibril actin cytoskeleton differentiation and disturbs skeletal muscle architecture and function” we revealed a new function of CAP2 for skeletal muscle development in mammals. We showed that CAP2 is a novel and important regulator of the second actin switch, where α-SMA and α-CAA are replaced by α-SKA at the level of thin filaments during early postnatal development. During this phase, the actin cytoskeleton is extremely susceptible for disruptions and the development of myopathies. Upon loss of CAP2, mice develop deficits in motor functions and structural abnormalities during the early postnatal phase that consist until adulthood. These structural abnormalities were characterized by a high amount of ring fibers, an increased number of internalized nuclei and abnormally distributed mitochondria. However, general appearance of the muscle was inconspicuous as we didn’t notice any kind of atrophy and additionally sarcomere structure appeared completely normal. Interestingly, first occurrence of structural changes and behavioral deficits appeared at the same time as the delayed second switch of actin isoforms.

Similar phenotypes were seen in cofilin2 mutant mice (Gurniak et al. 2014, Agrawal et al. 2012). Here, the second actin switch was delayed as well, but phenotypes were more severe as cofilin2 mutant mice died during early postnatal development due to defects in skeletal muscle maturation. Given the fact that the actin switch depends on CAP2 functioning, we propose a model in which CAP2 and cofilin2 work together on the exchange of actin subunits at the level of thin filaments (Fig. S9 B). For this exchange, there needs to be a coordinated release of α-SMA and α-CAA from F-actin and at the same time point an incorporation of α-SKA. When this exchange is not working properly, thin filaments remain in an undifferentiated stage as they still comprise the “wrong” actin isoforms.

We claim that, when first excessive voluntary movements in mice start, thin filaments built up from α-SMA and α-CAA cannot withstand the forces of muscle contraction, myofibrils become disrupted and the structural changes together with motoric dysfunctions appear. It is known, that F-actin built up from different isoforms show different characteristics. F-actin consisting of α-SKA is known to be more stable as they show a higher resistance to heat denaturation compared to α-CAA-composed F-actin (Orban et al. 2008). Additionally, force generation is reduced in cardiac myofibrils compared to skeletal myofibrils (Linke et al. 1994).

Another fact that supports our hypothesis is the finding, that ring fibers were restricted to Type IIB fibers. As these are the fast twitching fibers, they have to resist higher mechanical forces than Type I and Type IIA fibers (MacIntosh et al. 2006). This was not only shown by us, but also in a publication using mice with mutations in α-SKA (Ravenscroft et al. 2011). Here, mutant mice showed muscle weakness, features of nemaline myopathy and ring fibers restricted to Type IIB fibers as well.

Taken together, our data for the first time showed a critical function for CAP2 during skeletal muscle development. Together with cofilin2, CAP2 is a critical regulator of actin cytoskeleton refinement during myofibril development. As humans and mice show many similarities in the phenotypes of myopathies caused by actin or ARP mutations (Ravenscroft et al. 2011, Agrawal et al. 2012, Crawford et al. 2002, Gurniak et al. 2014), CAP2 might also cause or contribute to human myopathies of unknown origin. In humans, the CAP2 gene is located in the chromosomal region 6p22.3 and deletion of this region were implicated with developmental delays, heart defects and hypotonia (Bremer et al. 2009; Di Benedetto et al. 2013; Celestino-Soper et al. 2012). Mutations in CAP2 might contribute to the described pathological conditions and additionally might be the reason for human myopathies as well.

3.2 SRF Dysregulation in CAP2 mutant MEFs and how it could explain the Skeletal Muscle Phenotype of Mice lacking CAP2

In “Cyclase-associated protein 2 (CAP2) controls MRTF-A localization and SRF activity in mouse embryonic fibroblasts” we revealed a novel function of CAP2 as a regulator of SRF-dependent gene regulation in MEFs. We used fibroblasts to get a first hint whether SRF signaling is disturbed in CAP2 mutants because the impact of actin dynamics on SRF signaling was shown extensively in MEFs by other research groups before (Miralles et al. 2003, Sotiropoulos et al. 1999).

Analysis of CAP2 mutant MEFs showed no obvious abnormalities in morphology, proliferation, growth and general organization of the actin cytoskeleton. CAP2 is a known regulator of actin dynamics and we could already show in Kepser et al. 2019 that CAP2 depletion results in altered actin expression. Indeed, we found an increase in G- and F-actin level in CAP2 mutant MEFs. Given the fact, that the SRF co-activator MRTF can be bound by G-actin in the cytosol and thereby prevents the translocation into the nucleus and the resulting activation of SRF-dependent gene transcription, we suggested that MRTF subcellular localization might be disturbed in CAP2 mutant MEFs due to the elevated level of G-actin in the cytosol. Studies in NIH3T3 cells already linked increased level of G-actin through changes of cofilin activity, another important regulator of actin dynamics that is known to interact directly with CAP2, to a defective localization of MRTF (McGee et al. 2011). Indeed, CAP2 mutant MEFs displayed an increased fraction of MRTF-A in the cytosol compared to control cells under basal conditions. But can this be explained solely by the changes in G-actin level? Nuclear import of MRTF is another important part of the process that is thought to be mainly actin-dependent (Pawlowski et al. 2010). Interestingly, disturbed nuclear translocation can be excluded as a cause of MRTF-A mis-localization in CAP2 mutant MEFs, as translocation speed and the response to serum stimulation was similar compared to control cells.

Indeed, recent studies could show that nuclear import of MRTF after serum stimulation is not exclusively actin-dependent as Ddx19, a mRNA export factor, is able to change the conformation of MRTF to initiate nuclear import in an actin-independent manner (Rajakylä et al. 2015). Additionally, after manipulation of G-actin level by JASP, we showed that MRTF-A mis-location can be rescued. After treatment, MRTF-A localization was similar to control cells under basal conditions, implying that disturbed levels of G-actin were indeed the cause of altered MRTF localization similar to what was seen upon changes in cofilin level. These experiments revealed that CAP2 controls the subcellular localization of MRTF-A by regulation of G- and F-actin level in MEFs.

Increased subcellular localization of MRTF in the cytosol is known to result in reduced SRF-dependent gene regulation. Recent studies already demonstrated that loss of CAP2 leads to downregulation of the SRF target genes *Acta2* and *c-Fos* in MEFs (Xiong et al. 2019). We could verify these results and additionally showed that *Cyr61*, *Vcl* and even *Srf* itself were strongly downregulated as well. Additionally, we included *Egr2*, a target gene that is SRF-dependent but MRTF-independent. *Egr2* expression was similar in CAP2 mutant cells compared to controls and from these findings we can suggest that mainly the MRTF part of the SRF pathway is disturbed in CAP2 mutant MEFs. This makes sense as CAP2 is a regulator of actin dynamics and activation of SRF by MRTF is an actin-dependent mechanism.

Another case where dysregulation of actin dynamics leads to disruptions in MRTF-SRF signaling in mice is the leiomodin3 (Lmod3) mouse model. Here, loss of Lmod3, a tropomodulin-related protein that promotes actin nucleation, caused a strong reduction in MRTF and resulted in the development of nemaline myopathy (Cenik et al. 2015). As it is known that SRF is an important regulator of myogenesis, the skeletal muscle phenotype seen in our CAP2 mutant mice might result from disturbances in the SRF pathway as well.

Nowadays, it is known that SRF is more important for hypertrophic growth of skeletal muscles than for early myogenic differentiation (Li et al. 2005), as SRF mutant mice die during early postnatal development due to non-functional skeletal muscle formation. This was exactly the time-point where phenotypes in our CAP2 mutants occurred. Beside this, skeletal-muscle specific deletion of SRF, using the human skeletal actin promotor, lead to impaired growth and a striking loss of muscle mass (Chavret et al. 2006). Additionally, these mice showed reduced level of α-SKA and contractile genes as nebulin on mRNA level.

Taken similarities to recent publications on SRF and MRTF mutant mice into account, the skeletal muscle phenotype of CAP2 mutants could be caused due to changes in SRF-MRTF signaling after disruptions in actin dynamics similar to what we found in MEFs. One first step to verify this hypothesis is to evaluate the level of G- and F-actin and the expression of SRF downstream targets in skeletal muscles of CAP2 mutants. Even though Xiong and co-workers (Xiong et al. 2019) claimed that SRF activity is unchanged in CAP2 mutant skeletal muscles after preliminary experiments, a more detailed and comprehensive study is needed. Indeed, loss of CAP2 in heart muscles revealed an upregulation of SRF target genes as *Acta2* which is opposite to our findings (Xiong et al. 2019). Given the fact, that SRF can be regulated differently in several tissues, these findings do not exclude a dysregulation of SRF in CAP2 mutant skeletal muscles. In Kepser et al. 2019 we already showed on mRNA level, that the expression of actin isoforms is indeed reduced even though we reported an increase on protein level. Additionally, delayed development of CAP2 mutant skeletal muscles together with changes in proliferation and an increase in G-actin level (unpublished data) support our hypothesis, that loss of CAP2 indeed leads to reduced SRF signaling in skeletal muscles.

If this holds true, CAP2-dependent myopathies could be linked to SRF dysregulation and this might give insight into new therapeutic strategies. By inhibition of SRF with the synthesized drug CCG-1423-8u, Xiong and co-workers were recently able to increase survival of cardiac muscle-specific CAP2 mutant animals by roughly 2 weeks (Xiong et al. 2019). These results provide a promising strategy for treatment of diseases caused by dysregulation of the actin cytoskeleton, because targeting of actin directly mostly results in cardiac toxicity.

References

Abe, H., S. Ohshima and T. Obinata (1989). "A cofilin-like protein is involved in the regulation of actin assembly in developing skeletal muscle." J Biochem **106**(4): 696-702.

Agrawal, P.B., Greenleaf, R.S., Tomczak, K.K., Lehtokari, V.L., Wallgren-Pettersson, C., Wallefeld, W., Laing, N.G., Darras, B.T., Maciver, S.K., Dormitzer, P.R., et al. (2007). Nemaline myopathy with minicores caused by mutation of the CFL2 gene encoding the skeletal muscle actin-binding protein, cofilin-2. Am J Hum Genet **80**(1), 162-7.

Agrawal, P. B., M. Joshi, T. Savic, Z. Chen and A. H. Beggs (2012). "Normal myofibrillar development followed by progressive sarcomeric disruption with actin accumulations in a mouse Cfl2 knockout demonstrates requirement of cofilin-2 for muscle maintenance." Hum Mol Genet **21**(10): 2341-2356.

Arsenian, S., B. Weinhold, M. Oelgeschlager, U. Ruther and A. Nordheim (1998). "Serum response factor is essential for mesoderm formation during mouse embryogenesis." Embo j **17**(21): 6289-6299.

Babcock, G. and P. A. Rubenstein (1993). "Control of profilin and actin expression in muscle and nonmuscle cells." Cell Motil Cytoskeleton **24**(3): 179-188.

Baum, J., A. T. Papenfuss, B. Baum, T. P. Speed and A. F. Cowman (2006). "Regulation of apicomplexan actin-based motility." Nat Rev Microbiol **4**(8): 621-628.

Bertling, E., P. Hotulainen, P. K. Mattila, T. Matilainen, M. Salminen and P. Lappalainen (2004). "Cyclase-associated protein 1 (CAP1) promotes cofilin-induced actin dynamics in mammalian nonmuscle cells." Mol Biol Cell **15**(5): 2324-2334.

Bremer, A., J. Schoumans, M. Nordenskjold, B. M. Anderlid and M. Giacobini (2009). "An interstitial deletion of 7.1Mb in chromosome band 6p22.3 associated with developmental delay and dysmorphic features including heart defects, short neck, and eye abnormalities." Eur J Med Genet **52**(5): 358-362.

Celestino-Soper, P. B., C. Skinner, R. Schroer, P. Eng, J. Shenai, M. M. Nowaczyk, D. Terespolsky, D. Cushing, G. S. Patel, L. Immken, A. Willis, J. Wiszniewska, R. Matalon, J. A. Rosenfeld, R. E. Stevenson, S. H. Kang, S. W. Cheung, A. L. Beaudet and P. Stankiewicz (2012). "Deletions in chromosome 6p22.3-p24.3, including ATXN1, are associated with developmental delay and autism spectrum disorders." Mol Cytogenet **5**: 17.

Cenik, B. K., A. Garg, J. R. McAnally, J. M. Shelton, J. A. Richardson, R. Bassel-Duby, E. N. Olson and N. Liu (2015). "Severe myopathy in mice lacking the MEF2/SRF-dependent gene leiomodin-3." J Clin Invest **125**(4): 1569-1578.

Cenik, B. K., N. Liu, B. Chen, S. Bezprozvannaya, E. N. Olson and R. Bassel-Duby (2016). "Myocardin-related transcription factors are required for skeletal muscle development." Development **143**(15): 2853-2861.

Chal, J. and O. Pourquie (2017). "Making muscle: skeletal myogenesis in vivo and in vitro." Development **144**(12): 2104-2122.

Charvet, C., C. Houbron, A. Parlakian, J. Giordani, C. Lahoute, A. Bertrand, A. Sotiropoulos, L. Renou, A. Schmitt, J. Melki, Z. Li, D. Daegelen and D. Tuil (2006). "New role for serum response factor in postnatal skeletal muscle growth and regeneration via the interleukin 4 and insulin-like growth factor 1 pathways." Mol Cell Biol **26**(17): 6664-6674.

Crawford, K., R. Flick, L. Close, D. Shelly, R. Paul, K. Bove, A. Kumar and J. Lessard (2002). "Mice lacking skeletal muscle actin show reduced muscle strength and growth deficits and die during the neonatal period." Mol Cell Biol **22**(16): 5887-5896.

Di Benedetto, D., G. Di Vita, C. Romano, M. L. Giudice, G. A. Vitello, M. Zingale, L. Grillo, L. Castiglia, S. A. Musumeci and M. Fichera (2013). "6p22.3 deletion: report of a patient with autism, severe intellectual disability and electroencephalographic anomalies." Mol Cytogenet **6**(1): 4.

Gualdrini, F., C. Esnault, S. Horswell, A. Steward, N. Matthews and R. Treisman (2016). "SRF Co-factors Control the Balance between Cell Proliferation and Contractility." Mol Cell **64**: 1048-1061

Gurniak, C. B., F. Chevessier, M. Jokwitz, F. Jonsson, E. Perlas, H. Richter, G. Matern, P. P. Boyl, C. Chaponnier, D. Furst, R. Schroder and W. Witke (2014). "Severe protein aggregate myopathy in a knockout mouse model points to an essential role of cofilin2 in sarcomeric actin exchange and muscle maintenance." Eur J Cell Biol **93**(5-6): 252-266.

Gurniak, C. B., E. Perlas and W. Witke (2005). "The actin depolymerizing factor n-cofilin is essential for neural tube morphogenesis and neural crest cell migration." Dev Biol **278**(1): 231-241.

Hanft, L. M., I. N. Rybakova, J. R. Patel, J. A. Rafael-Fortney and J. M. Ervasti (2006). "Cytoplasmic gamma-actin contributes to a compensatory remodeling response in dystrophin-deficient muscle." Proc Natl Acad Sci U S A **103**(14): 5385-5390.

Honore, B., P. Madsen, A. H. Andersen and H. Leffers (1993). "Cloning and expression of a novel human profilin variant, profilin II." FEBS Lett **330**(2): 151-155.

Jang, H. D., S. E. Lee, J. Yang, H. C. Lee, D. Shin, H. Lee, J. Lee, S. Jin, S. Kim, S. J. Lee, J. You, H. W. Park, K. Y. Nam, S. H. Lee, S. W. Park, J. S. Kim, S. Y. Kim, Y. W. Kwon, S. H. Kwak, H. M. Yang and H. S. Kim (2020). "Cyclase-associated protein 1 is a binding partner of proprotein convertase subtilisin/kexin type-9 and is required for the degradation of low-density lipoprotein receptors by proprotein convertase subtilisin/kexin type-9." Eur Heart J **41**(2): 239-252.

Kepser, L. J., F. Damar, T. De Cicco, C. Chaponnier, T. J. Proszynski, A. Pagenstecher and M. B. Rust (2019). "CAP2 deficiency delays myofibril actin cytoskeleton differentiation and disturbs skeletal muscle architecture and function." Proc Natl Acad Sci U S A **116**(17) 8397-8402

Lahoute, C., A. Sotiropoulos, M. Favier, I. Guillet-Deniau, C. Charvet, A. Ferry, G. Butler-Browne, D. Metzger, D. Tuil and D. Daegelen (2008). "Premature aging in skeletal muscle lacking serum response factor." PLoS One **3**(12): e3910.

Li, S., M. P. Czubryt, J. McAnally, R. Bassel-Duby, J. A. Richardson, F. F. Wiebel, A. Nordheim and E. N. Olson (2005). "Requirement for serum response factor for skeletal muscle growth and maturation revealed by tissue-specific gene deletion in mice." Proc Natl Acad Sci U S A **102**(4): 1082-1087.

Linke, W. A., V. I. Popov and G. H. Pollack (1994). "Passive and active tension in single cardiac myofibrils." Biophys J **67**(2): 782-792.

Lloyd, C. M., M. Berendse, D. G. Lloyd, G. Schevzov and M. D. Grounds (2004). "A novel role for non-muscle gamma-actin in skeletal muscle sarcomere assembly." Exp Cell Res **297**(1): 82-96.

McGee, K. M., M. K. Vartiainen, P. T. Khaw, R. Treisman and M. Bailly (2011). "Nuclear transport of the serum response factor coactivator MRTF-A is downregulated at tensional homeostasis." EMBO Rep **12**(9): 963-970.

McHugh, K. M., K. Crawford and J. L. Lessard (1991). "A comprehensive analysis of the developmental and tissue-specific expression of the isoactin multigene family in the rat." Dev Biol **148**(2): 442-458.

Miralles, F., G. Posern, A. I. Zaromytidou and R. Treisman (2003). "Actin dynamics control SRF activity by regulation of its coactivator MAL." Cell **113**(3): 329-342.

Mizuno, Y., M. Suzuki, H. Nakagawa, N. Ninagawa and S. Torihashi (2009). "Switching of actin isoforms in skeletal muscle differentiation using mouse ES cells." Histochem Cell Biol **132**(6): 669-672.

Mohri, K., H. Takano-Ohmuro, H. Nakashima, K. Hayakawa, T. Endo, K. Hanaoka and T. Obinata (2000). "Expression of cofilin isoforms during development of mouse striated muscles." J Muscle Res Cell Motil **21**(1): 49-57.

Mokalled, M. H., A. N. Johnson, E. E. Creemers and E. N. Olson (2012). "MASTR directs MyoD-dependent satellite cell differentiation during skeletal muscle regeneration." Genes Dev **26**(2): 190-202.

Nagaoka, R., N. Minami, K. Hayakawa, H. Abe and T. Obinata (1996). "Quantitative analysis of low molecular weight G-actin-binding proteins, cofilin, ADF and profilin, expressed in developing and degenerating chicken skeletal muscles." J Muscle Res Cell Motil **17**(4): 463-473.

Ohshima, S., H. Abe and T. Obinata (1989). "Isolation of profilin from embryonic chicken skeletal muscle and evaluation of its interaction with different actin isoforms." J Biochem **105**(6): 855-857.

Olson, E. N. and A. Nordheim (2010). "Linking actin dynamics and gene transcription to drive cellular motile functions." Nat Rev Mol Cell Biol **11**(5): 353-365.

Ono, K., M. Parast, C. Alberico, G. M. Benian and S. Ono (2003). "Specific requirement for two ADF/cofilin isoforms in distinct actin-dependent processes in Caenorhabditis elegans." J Cell Sci **116**(Pt 10): 2073-2085.

Ono, S. (2010). "Dynamic regulation of sarcomeric actin filaments in striated muscle." Cytoskeleton (Hoboken) **67**(11): 677-692.

Ono, S. (2013). "The role of cyclase-associated protein in regulating actin filament dynamics - more than a monomer-sequestration factor." J Cell Sci **126**(Pt 15): 3249-3258.

Ono, S., N. Minami, H. Abe and T. Obinata (1994). "Characterization of a novel cofilin isoform that is predominantly expressed in mammalian skeletal muscle." J Biol Chem **269**(21): 15280-15286.

Orban, J., D. Lorinczy, M. Nyitrai and G. Hild (2008). "Nucleotide dependent differences between the alpha-skeletal and alpha-cardiac actin isoforms." Biochem Biophys Res Commun **368**(3): 696-702.

Pawlowski, R., E. K. Rajakylä, M. K. Vartiainen and R. Treisman (2010). "An actin-regulated importin α/β-dependent extended bipartite NLS directs nuclear import of MRTF-A." Embo j **29**(20): 3448-3458.

Peche, V., S. Shekar, M. Leichter, H. Korte, R. Schroder, M. Schleicher, T. A. Holak, C. S. Clemen, Y. B. Ramanath, G. Pfitzer, I. Karakesisoglou and A. A. Noegel (2007). "CAP2, cyclase-associated protein 2, is a dual compartment protein." Cell Mol Life Sci **64**(19-20): 2702-2715.

Peche, V. S., T. A. Holak, B. D. Burgute, K. Kosmas, S. P. Kale, F. T. Wunderlich, F. Elhamine, R. Stehle, G. Pfitzer, K. Nohroudi, K. Addicks, F. Stockigt, J. W. Schrickel, J. Gallinger, M. Schleicher and A. A. Noegel (2013). "Ablation of cyclase-associated protein 2 (CAP2) leads to cardiomyopathy." Cell Mol Life Sci **70**(3): 527-543.

Perrin, B. J. and J. M. Ervasti (2010). "The actin gene family: function follows isoform." Cytoskeleton (Hoboken) **67**(10): 630-634.

Pollard, T. D. and G. G. Borisy (2003). "Cellular motility driven by assembly and disassembly of actin filaments." Cell **112**(4): 453-465.

Posern, G. and R. Treisman (2006). "Actin' together: serum response factor, its cofactors and the link to signal transduction." Trends Cell Biol **16**(11): 588-596.

Rajakylä, E.K., T. Viita, S. Kyheröinen, G. Huet, R. Treisman and M. K. Vartiainen (2015). "RNA export factor Ddx19 is required for nuclear import of the SRF coactivator MKL1." Nat Commun **6**: 5978.

Ravenscroft, G., C. Jackaman, S. Bringans, J. M. Papadimitriou, L. M. Griffiths, E. McNamara, A. J. Bakker, K. E. Davies, N. G. Laing and K. J. Nowak (2011). "Mouse models of dominant ACTA1 disease recapitulate human disease and provide insight into therapies." Brain **134**(Pt 4): 1101-1115.

Revenu, C., R. Athman, S. Robine and D. Louvard (2004). "The co-workers of actin filaments: from cell structures to signals." Nat Rev Mol Cell Biol **5**(8): 635-646.

Rybakova, I. N., J. R. Patel and J. M. Ervasti (2000). "The dystrophin complex forms a mechanically strong link between the sarcolemma and costameric actin." J Cell Biol **150**(5): 1209-1214.

Shimizu, N. and T. Obinata (1986). "Actin concentration and monomer-polymer ratio in developing chicken skeletal muscle." J Biochem **99**(3): 751-759.

Sonnemann, K. J., D. P. Fitzsimons, J. R. Patel, Y. Liu, M. F. Schneider, R. L. Moss and J. M. Ervasti (2006). "Cytoplasmic gamma-actin is not required for skeletal muscle development but its absence leads to a progressive myopathy." Dev Cell **11**(3): 387-397.

Sotiropoulos, A., D. Gineitis, J. Copeland and R. Treisman (1999). "Signal-regulated activation of serum response factor is mediated by changes in actin dynamics." Cell **98**(2): 159-169.

Stockigt, F., V. S. Peche, M. Linhart, G. Nickenig, A. A. Noegel and J. W. Schrickel (2016). "Deficiency of cyclase-associated protein 2 promotes arrhythmias associated with connexin43 maldistribution and fibrosis." Arch Med Sci **12**(1): 188-198.

Stricker, J., T. Falzone and M. L. Gardel (2010). "Mechanics of the F-actin cytoskeleton." J Biomech **43**(1): 9-14.

Sun, Q., G. Chen, J. W. Streb, X. Long, Y. Yang, C. J. Stoeckert, Jr. and J. M. Miano (2006). "Defining the mammalian CArGome." Genome Res **16**(2): 197-207.

Thirion, C., R. Stucka, B. Mendel, A. Gruhler, M. Jaksch, K. J. Nowak, N. Binz, N. G. Laing and H. Lochmuller (2001). "Characterization of human muscle type cofilin (CFL2) in normal and regenerating muscle." Eur J Biochem **268**(12): 3473-3482.

Tondeleir, D., D. Vandamme, J. Vandekerckhove, C. Ampe and A. Lambrechts (2009). "Actin isoform expression patterns during mammalian development and in pathology: insights from mouse models." Cell Motil Cytoskeleton **66**(10): 798-815.

Vartiainen, M. K., T. Mustonen, P. K. Mattila, P. J. Ojala, I. Thesleff, J. Partanen and P. Lappalainen (2002). "The three mouse actin-depolymerizing factor/cofilins evolved to fulfill cell-type-specific requirements for actin dynamics." Mol Biol Cell **13**(1): 183-194.

Witke, W., A. V. Podtelejnikov, A. Di Nardo, J. D. Sutherland, C. B. Gurniak, C. Dotti and M. Mann (1998). "In mouse brain profilin I and profilin II associate with regulators of the endocytic pathway and actin assembly." Embo j **17**(4): 967-976.

Xiong, Y., K. Bedi, S. Berritt, B. K. Attipoe, T. G. Brooks, K. Wang, K. B. Margulies and J. Field (2019). "Targeting MRTF/SRF in CAP2-dependent dilated cardiomyopathy." JCI Insight **4**(6): e124629.

Reprints of Original Publications

CAP2 Deficiency delays Myofibril Actin Cytoskeleton Differentiation and disturbs Skeletal Muscle Architecture and Function

Kepser LJ, Damar F, De Cicco T, Chaponnier C, Prószyński TJ, Pagenstecher A, Rust MB

PNAS, 2019, 116 (17): 8397-8402

DOI: https://doi.org/10.1073/pnas.1813351116

Cyclase-associated Protein 2 (CAP2) controls MRTF-A Localization and SRF Activity in Mouse Embryonic Fibroblasts

Kepser LJ, Soto Hinojosa L, Grosse R, Rust MB

In preparation

CAP2 deficiency delays myofibril actin cytoskeleton differentiation and disturbs skeletal muscle architecture and function

Lara-Jane Kepser[a], Fidan Damar[a], Teresa De Cicco[b], Christine Chaponnier[c], Tomasz J. Prószyński[b], Axel Pagenstecher[d], and Marco B. Rust[a,e,f,1]

[a]Molecular Neurobiology Group, Institute of Physiological Chemistry, University of Marburg, 35032 Marburg, Germany; [b]Laboratory of Synaptogenesis, Nencki Institute of Experimental Biology PAS, 02-093 Warsaw, Poland; [c]Department of Pathology and Immunology, University of Geneva, 1211 Geneva, Switzerland; [d]Institute of Neuropathology, University of Marburg, 35032 Marburg, Germany; [e]Center for Mind, Brain and Behavior, Research Campus of Central Hessen, 35032 Marburg, Germany; and [f]DFG Research Training Group "Membrane Plasticity in Tissue Development and Remodeling," GRK 2213, University of Marburg, 35032 Marburg, Germany

Edited by Yale E. Goldman, University of Pennsylvania/PMI, Philadelphia, PA, and approved March 14, 2019 (received for review August 7, 2018)

Actin filaments (F-actin) are key components of sarcomeres, the basic contractile units of skeletal muscle myofibrils. A crucial step during myofibril differentiation is the sequential exchange of α-actin isoforms from smooth muscle (α-SMA) and cardiac (α-CAA) to skeletal muscle α-actin (α-SKA) that, in mice, occurs during early postnatal life. This "α-actin switch" requires the coordinated activity of actin regulators because it is vital that sarcomere structure and function are maintained during differentiation. The molecular machinery that controls the α-actin switch, however, remains enigmatic. Cyclase-associated proteins (CAP) are a family of actin regulators with largely unknown physiological functions. We here report a function for CAP2 in regulating the α-actin exchange during myofibril differentiation. This α-actin switch was delayed in systemic CAP2 mutant mice, and myofibrils remained in an undifferentiated stage at the onset of the often excessive voluntary movements in postnatal mice. The delay in the α-actin switch coincided with the onset of motor function deficits and histopathological changes including a high frequency of type IIB ring fibers. Our data suggest that subtle disturbances of postnatal F-actin remodeling are sufficient for predisposing muscle fibers to form ring fibers. Cofilin2, a putative CAP2 interaction partner, has been recently implicated in myofibril actin cytoskeleton differentiation, and the myopathies in cofilin2 and CAP2 mutant mice showed striking similarities. We therefore propose a model in which CAP2 and cofilin2 cooperate in actin regulation during myofibril differentiation.

ringbinden | spiral annulets | actin dynamics | 6p22.3 | Srv2

Ring fibers are muscle fibers containing myofibrils in a perpendicular orientation to the main group of normal, longitudinally orientated myofibrils (1, 2). In cross-sections, ring fibers show circular myofibrils around or serpentine myofibrils crossing the normally orientated myofibrils. Ring fibers have been reported for congenital myopathies (e.g., myotonic dystrophy, limb-girdle dystrophy, inclusion body myositis), for myopathies of unknown etiology (3–5), and for disease mouse models (6, 7). While previous studies suggested the involvement of hypertonic muscle state, aberrant synthesis of myofibril proteins, or cytoskeletal defects (7, 8), the natural cause of ring fiber formation remained elusive.

Cyclase-associated proteins (CAPs) are evolutionary conserved proteins with largely unknown physiological function. CAPs interact with monomeric and filamentous actin, suggesting a role in actin dynamics, the spatiotemporally controlled F-actin assembly and disassembly (9). Indeed, CAP1 and its yeast homolog Srv2 mediated fast F-actin disassembly in vitro (10), and CAP1 accelerates ADF/cofilin-mediate F-actin disassembly in nonmuscle cells (11). Most species express only a single CAP isoform, but vertebrates have two family members, CAP1 and CAP2, encoded by distinct genes (9). Expression of CAP2 is restricted to only a few tissues including brain and striated muscles (11, 12), where it may have acquired specific functions. While previous analyses of mutant mice demonstrated a role of CAP2 in neuron morphology and heart physiology (13–15), its function in skeletal muscles has not been investigated, yet.

We here report a function for CAP2 in skeletal muscle development. We found that CAP2 controls the exchange of α-actin isoforms during myofibril differentiation. In systemic CAP2-deficient mice, the "α-actin switch" was delayed and coincided with motor function deficits and a myopathy characterized by a large number of ring fibers in type IIB muscle fibers. Our findings highlight CAP2 as a regulator of myofibril actin cytoskeleton differentiation that is critical for skeletal muscle structure and function.

Results

Delayed Maturation of Motor Functions and Reduced Muscle Strength in CAP2 Mutants. To generate CAP2-deficient mice (KO), we intercrossed heterozygous mutants (HET) obtained from the European Conditional Mouse Mutagenesis Program (EUCOMM). Genotyping at postnatal week 2–3 revealed 24% KO among all offspring ($n = 77$), demonstrating that KO were viable and born at

Significance

Displaced myofibrils termed ring fibers have been reported for human congenital myopathies and for myopathies of unknown etiology, but their natural cause largely remained elusive. Cyclase-associated protein 2 (CAP2) is an actin regulator with unknown physiological function. We identified CAP2 as a regulator for the exchange of α-actin isoforms during myofibril differentiation. In CAP2 mutant mice, myofibrils remained in an undifferentiated stage at the onset of excessive voluntary muscle contractions, predisposing them to form ring fibers that compromise skeletal muscle function. Our data confirm that subtle cytoskeletal changes can cause ring fibers. Moreover, they led us to propose that CAP2 inactivation contributes to defects of human 6p22.3 deletion syndrome such as developmental delay and hypotonia.

Author contributions: L.-J.K., T.J.P., A.P., and M.B.R. designed research; L.-J.K., F.D., T.D.C., and A.P. performed research; C.C. contributed new reagents/analytic tools; L.-J.K. and M.B.R. analyzed data; and A.P. and M.B.R. wrote the paper.

The authors declare no conflict of interest.

This article is a PNAS Direct Submission.

[1]To whom correspondence should be addressed. Email: marco.rust@staff.uni-marburg.de.

This article contains supporting information online at www.pnas.org/lookup/suppl/doi:10.1073/pnas.1813351116/-/DCSupplemental.

Published online April 8, 2019.

the expected Mendelian ratio. To study whether CAP2 inactivation compromised postnatal development, we assessed physical landmarks and developmental milestones in newborn mice. Occurrence of eye opening or pinna detachment as well as activity was similar to wild-type (WT) littermates (Fig. 1 *A*–*C*), excluding severe developmental defects in KO. However, KO showed higher tremor levels in particular between postnatal days (P) 10 and 18 (Fig. 1*D*). Moreover, KO displayed a delayed maturation in motor function tests including surface righting, level screen, vertical screen, negative geotaxis, or bar holding (Fig. 1 *E*–*I* and Movie S1). Motor deficits were similar in male and female KO, and we therefore pooled data of both sexes. Motor skills were not impaired in HET. Notably, KO performed similar to WT in other tests that evaluated visual and auditory performance, tactile perception, or reflexes (Fig. 1 *J*–*O*). Together, male and female KO showed normal activity, sensation, and reflexes, while maturation of motor functions was delayed. We conclude that CAP2 is specifically relevant for motor function development.

To test whether motor functions were impaired at later stages, we performed the string test that measures forelimb strength by determining the time mice need to pull themselves up when hanging on a bar (16). This latency was increased in both juvenile (3–4 wk) and adult (6–8 wk) KO (*SI Appendix*, Fig. S1*A*). We also determined maximal force generation by performing the grip strength (GS) test. Because KO body weight (BW) was reduced by roughly 20% throughout development (*SI Appendix*, Fig. S1*B*), we normalized GS to BW. Normalized GS of either the forepaws or all four paws was reduced by 25% in juvenile and 20% in adult KO (*SI Appendix*, Fig. S1 *C* and *D*). KO showed normal motor coordination in the rotarod and normal locomotor activity and exploratory behavior in the open field (*SI Appendix*, Fig. S1 *E*–*G*), reflecting their overall healthy appearance. Hence, juvenile and adult KO displayed specific defects in muscle strength.

Myopathy in CAP2 Mutants Is Characterized by Frequent Ring Fibers. We found CAP2 present in all WT skeletal muscles tested (Fig. 2*A*). We therefore tested whether muscle weakness was associated with altered muscle histology. In KO, skeletal muscles did not appear atrophic (Fig. 2*B*), which was also evident from normal weight of the *Musculus* (*M.*) *quadriceps femoris* (QUAD; *SI Appendix*, Fig. S2*A*). We studied skeletal muscle histology by performing a thorough analysis of cross-sectioned adult QUAD. Hematoxylin-eosin (HE) staining revealed an overall normal QUAD architecture in KO, but we noted a 12-fold increase in

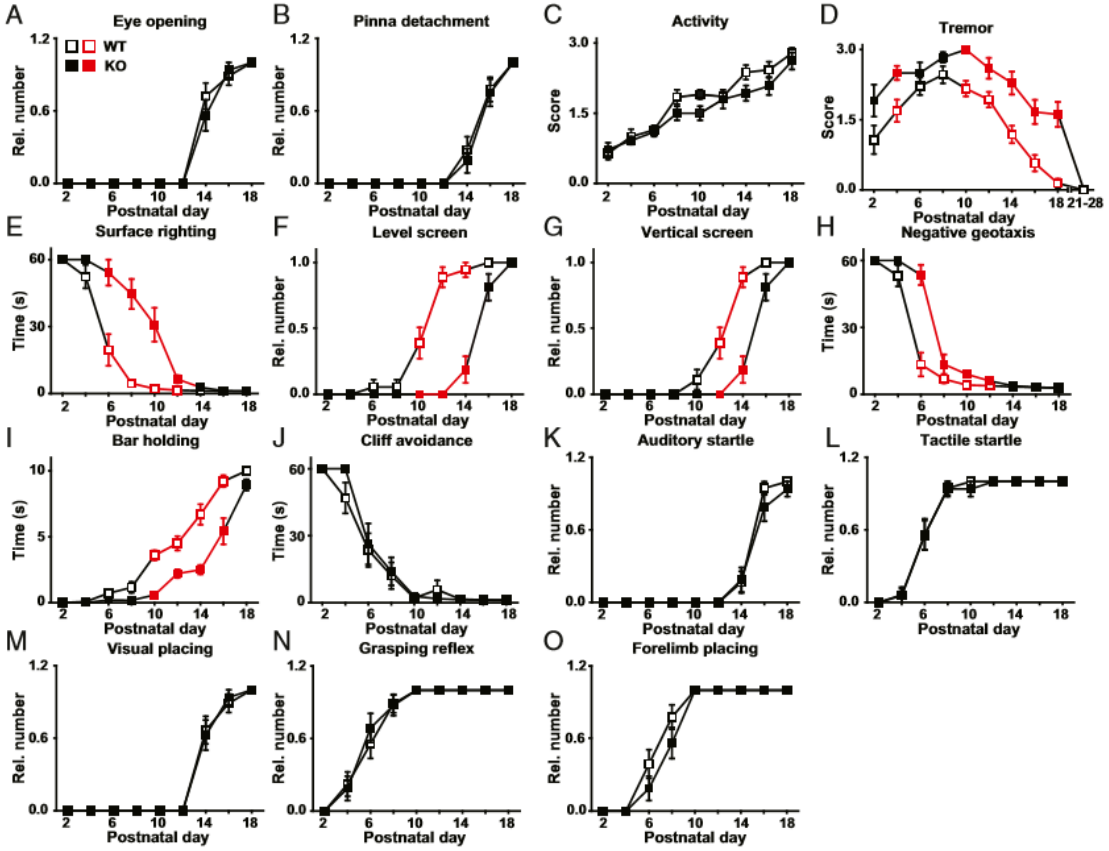

Fig. 1. Motor function deficits in neonatal CAP2 mutants. (*A*–*C*) Graphs showing that eye opening, pinna detachment, and activity were unchanged in CAP2 mutants. (*D*) Instead, CAP2 mutants showed increased levels of tremulous movements. (*E*–*I*) Moreover, they performed weaker in various motor function tests. (*J*–*O*) No changes were noted in cliff avoidance, auditory startle, tactile startle, visual placing, grasping reflex, or forelimb placing. For *A*–*O*: $n = 18$ WT and 16 KO. If mean values (MV) were significantly different between groups ($P < 0.05$), squares indicating MV and error bars indicating SEMs are shown in red.

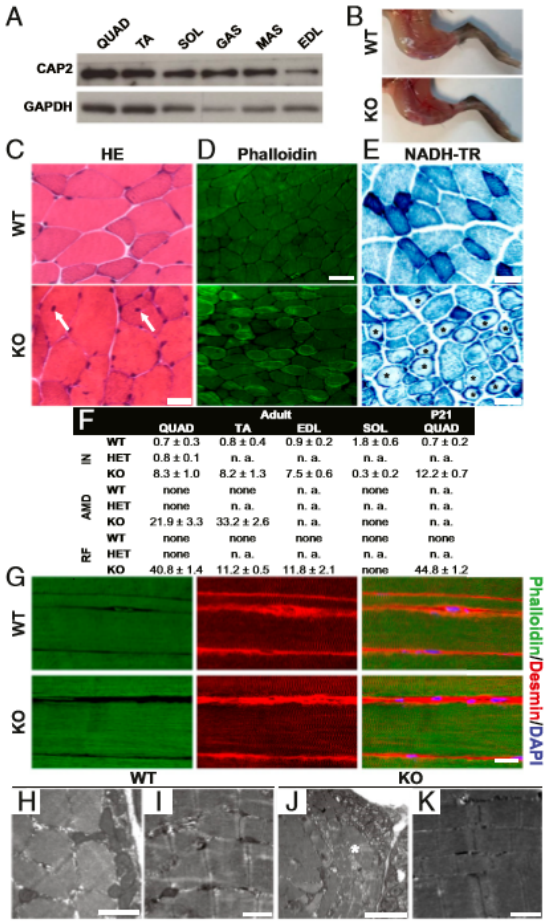

Fig. 2. Myopathy in CAP2 mutants. (*A*) Immunoblots demonstrating presence of CAP2 in all skeletal muscles tested (GAS, *M. gastrocnemius*; MAS, *M. masseter*). GAPDH was used as a loading control. (*B*) Micrographs showing skinned hind legs from age-matched WT and KO. (*C*) HE-stained adult QUAD cross-sections. White arrows indicate internalized nuclei in KO. (*D*) Phalloidin staining revealed frequent occurrence of ring fibers in KO. (*E*) NADH-TR staining revealed altered mitochondrial distribution in KO (asterisks). (*F*) Quantification of histopathological changes in adult skeletal muscles and in P21 QUAD. Muscle fibers (%) with internalized nuclei (IN), altered mitochondrial distribution (AMD), and ring fibers (RF). n.a., not analyzed. For each analysis, at least nine micrographs of 0.6 mm^2 from three mice per genotype have been used. (*G*) Antibody staining against desmin (red) in longitudinal TA sections. Sections were counterstained with phalloidin (green) and Hoechst 33342 (blue). (*H–K*) EM of adult WT and KO QUAD cross- and longitudinal sections. Asterisk in *J* indicates a ring fiber. Scale bar (μm): 1.0 (*H*, *I*, and *K*), 2.5 (*J*), 20 (*C* and *G*), 50 (*D*), 30 (*E*).

the fraction of internalized nuclei and the occurrence of ring fibers (Fig. 2*C* and *SI Appendix*, Fig. S2*B*). We exploited fluorescent phalloidin that labels F-actin to better visualize ring fibers and confirmed their presence in 41% of muscle fibers (Fig. 2 *D* and *F* and *SI Appendix*, Fig. S2*C*). In QUAD cross-sections, ring fibers were equally distributed. Staining of sequential sections with either phalloidin or antibodies against myosin heavy chain (MHC) isoforms revealed presence of ring fibers in MHC IIB-labeled, but not in MHC IIA-labeled muscle fibers (*SI Appendix*, Fig. S2 *E* and *F*). MHC isoform-specific antibodies further allowed a quantification of fiber-type fractions, which was unchanged in KO (*SI Appendix*, Fig. S2*G*). Staining of nicotinamide adenine dinucleotide tetrazolium reductase (NADH-TR) or succinate dehydrogenase/cytochrome oxidase II (SDH/COXII) revealed that mitochondrial distribution was severely disturbed in 22% of muscle fibers (Fig. 2 *E* and *F* and *SI Appendix*, Fig. S3*A*). A closer inspection revealed a normal number of intensively labeled "oxidative" (type I) muscle fibers in KO QUAD, suggesting that altered mitochondrial distribution was present in lighter "less oxidative" (type II) muscle fibers, which are mainly of type IIB (*SI Appendix*, Fig. S2*G*). Gömöri trichrome staining confirmed the presence of internalized nuclei, and ATPase and periodic acid-Schiff (PAS) staining confirmed the occurrence of ring fibers (*SI Appendix*, Figs. S2*D* and S3*B–C*). Apart from that, we did not find any additional changes in Gömöri trichrome staining, PAS staining, oil red O staining, van Gieson's staining, or acid phosphatase staining (*SI Appendix*, Fig. S3 *B–F*), thereby demonstrating the absence of lipid deposits or macrophages as well as normal patterns of glycogen and connective tissue in KO mice. In summary, our QUAD analyses revealed internalized nuclei, disturbed mitochondrial distribution, and a high frequency of ring fibers that were restricted to type IIB muscle fibers. Histopathological changes were very similar in QUAD from female and male KO, while no such changes were present in HET (*SI Appendix*, Fig. S4). We further analyzed *M. tibialis anterior* (TA), *M. soleus* (SOL), and *M. extensor digitorum longus* (EDL). Similar to QUAD, type IIB muscle fibers predominate in TA and EDL (17). Instead, type I and IIA muscle fibers predominate in SOL, which do not possess type IIB muscle fibers. Very similar to QUAD, we frequently found ring fibers, internalized nuclei, and muscle fibers with disturbed mitochondrial distribution in TA and EDL (Fig. 2*F* and *SI Appendix*, Figs. S5 and S6). Conversely, the number of internalized nuclei was not increased in SOL, and we did not find ring fibers or mitochondrial distribution defects. Together, histopathological changes were present in all "type IIB muscle fiber predominated" skeletal muscles examined, but not in SOL.

We next performed immunohistochemistry on longitudinal sections to examine sarcomere structure. We performed these experiments on TA, in which immunohistochemistry was superior to QUAD. Phalloidin staining revealed a regular striated F-actin pattern that was very similar in WT and KO (Fig. 2*G*). We confirmed an overall normal sarcomere structure in KO by antibody staining against desmin that surrounds Z-discs. To characterize muscle fibers on the ultrastructural level, we performed electron microscopy (EM) on adult QUAD (Fig. 2 *H–K*). EM confirmed both presence of ring fibers in numerous KO muscle fibers as well as subsarcolemmal accumulation of mitochondria. Moreover, sarcomere ultrastructure appeared normal in KO QUAD. Hence, KO myopathy was not associated with obvious defects in sarcomere structure.

CAP2 Controls Postnatal Skeletal Muscle Differentiation. Because motor function deficits were present in KO neonates, we tested developmental CAP2 expression in skeletal muscles and found similar levels throughout QUAD development (Fig. 3*A*). We therefore tested whether onset of myopathy coincided with motor function deficits in neonatal KO. We noted no differences between WT and KO QUAD cross-sections at P4 (Fig. 3*B*). Instead, ring fibers were present during the second postnatal week. They appeared together with phalloidin-labeled, F-actin–rich aggregates that were not present at later stages (P21, adult). Phalloidin and HE staining at P21 revealed frequent occurrence of ring fibers and internalized nuclei, very similar to adult QUAD (Figs. 2*F* and 3*B* and *SI Appendix*, Fig. S7*A*). EM analyses on QUAD longitudinal and cross-sections confirmed the presence of ultrastructural changes at P8 including irregular arrangement of myofibrils and abnormal distribution of mitochondria, as well as the occasional

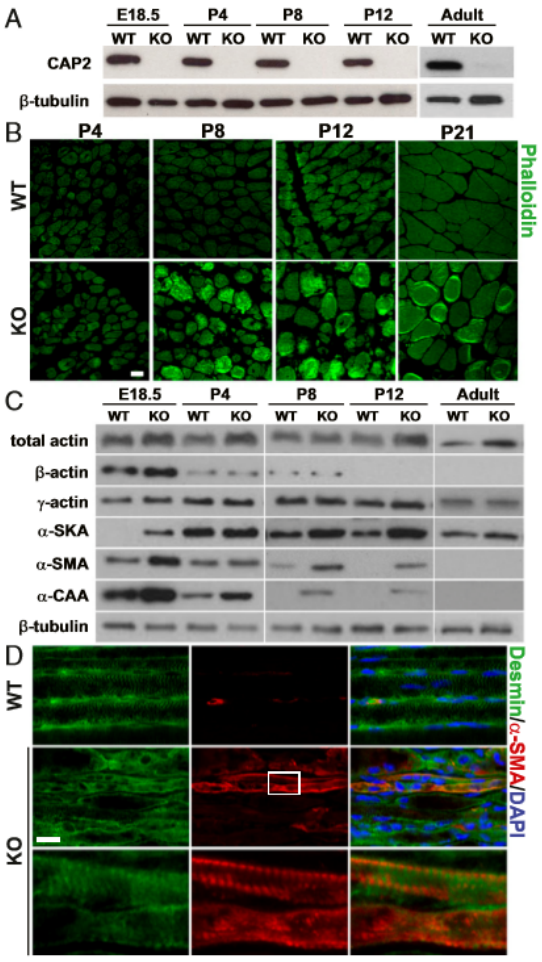

Fig. 3. Myopathy onset coincides with delay in α-actin switch. (*A*) Immunoblots demonstrating CAP2 expression throughout QUAD development. β-tubulin was used as a loading control. (*B*) Micrographs showing phalloidin-stained QUAD cross-sections. (*C*) Immunoblots showing levels of total actin (pan-actin), skeletal muscle (α-SKA), smooth muscle (α-SMA), and cardiac α-actin (α-CAA), β-actin, and γ-actin throughout QUAD development. β-tubulin was used as a loading control. (*D*) Antibody staining against desmin (green) and α-SMA (red) in longitudinal TA sections from P12 mice. Sections were counterstained with DAPI (blue). White box indicates area in KO TA shown at higher magnification. Scale bars (μm): 20 (*B* and *D*).

occurrences of abnormal undulation of Z-bands, dilated tubulus systems, and subsarcolemmal accumulation of lipid droplets (*SI Appendix*, Fig. S7 *B–K*). Together, histopathology started during the first week of life and coincided with the onset of motor dysfunction. These findings reveal a pivotal function of CAP2 for early postnatal skeletal muscle development.

A crucial step during early postnatal skeletal muscle development is the replacement of smooth muscle (α-SMA) and cardiac muscle (α-CAA) α-actin by skeletal muscle (α-SKA) α-actin (18, 19). This exchange requires the coordinated release of actin subunits, and cofilin2, a putative CAP2 interaction partner (9), has been implicated therein (20). To test whether CAP2 is critical for this exchange, we quantified levels of α-actin isoforms by exploiting isoform-specific antibodies (21). Additionally, a pan-actin antibody was used to assess total actin levels. Compared with WT, total actin levels were higher in KO at all postnatal stages examined and remained increased in adult mice (Fig. 3*C*). This increase was due to elevated α-actin because β-actin and γ-actin levels were unchanged. Indeed, compared with controls, α-SKA levels were higher in KO throughout development. In WT, α-SMA and α-CAA levels gradually declined postnatal, similar to previous studies (20). However, their decline was delayed in KO. Consequently, α-SMA and α-CAA levels were elevated at postnatal stages and still detectable in P12 KO (Fig. 3*C*). In sharp contrast to elevated protein levels, mRNA levels of *Acta1*, *Acta2*, and *Actc1*, which encode α-SKA, α-SMA, and α-CAA, respectively, were reduced at E18.5, but unaltered at P4 (*SI Appendix*, Fig. S8 *A* and *B*). Hence, elevated protein levels in KO were not caused by increased gene expression. We therefore suspected a delayed removal from F-actin and degradation of α-SMA and α-CAA. If this holds true, α-SMA and α-CAA should be present in the F-actin–enriched insoluble protein fraction in P12 KO. To test this, we separated soluble (containing actin monomers) and insoluble protein fractions and determined levels of α-actin isoforms in both fractions. As expected, the majority of α-SKA was found in the insoluble WT fraction, and we found a very similar distribution in KO (*SI Appendix*, Fig. S8*C*). However, while α-SMA and α-CAA were not detectable in either WT fraction, the vast majority of both proteins was present in the insoluble KO fraction. These data suggested that α-SMA and α-CAA were still integrated in F-actin in P12 KO. To prove this, we performed antibody staining on longitudinal TA sections. In this analysis, we were limited to α-SMA because of unspecific α-CAA signals. As expected, α-SMA immunoreactivity was restricted to blood vessels in P12 WT (Fig. 3*D*). Conversely, we frequently found α-SMA–positive muscle fibers in KO. Notably, these muscle fibers showed a striated α-SMA pattern, demonstrating that α-SMA was an integral component of sarcomere F-actin. Together, our data revealed a delayed α-actin switch in KO sarcomeres, and they implicated CAP2 in the exchange of α-actin isoforms during myofibril differentiation.

CAP2 Reexpression Rescues Ring Fiber Myopathy in CAP2 Mutants. Because the delayed α-actin switch coincided with the onset of ring fibers, we hypothesized that the pathology was caused by a primary defect in skeletal muscles. To test our hypothesis, we reexpressed GFP-CAP2 in KO QUAD by viral transduction at P0, before onset of myopathy, and killed mice at P21 to screen for ring fibers that we used as a readout (Fig. 4*A*). In this experiment, expression of GFP-CAP2 was restricted to peripheral QUAD regions (Fig. 4*B*), which allowed us to compare ring fiber formation between CAP2 reexpressing and CAP2-deficient muscle fibers in the same QUAD. We additionally performed control experiments, in which we expressed GFP in KO QUAD. As expected, the fraction of muscle fibers with ring fibers was independent of GFP expression in control KO QUAD (Fig. 4*C*). Similarly, ring fibers were frequently present in KO muscle fibers not expressing GFP-CAP2. Conversely, we hardly found any ring fibers in GFP-CAP2 expressing muscle fibers in KO QUAD. These findings proved our hypothesis that loss of CAP2 activity in skeletal muscles caused ring fiber myopathy in KO.

Discussion

In the present study, we report a function for the actin regulator CAP2 in skeletal muscle development. We found that CAP2 is crucial for the exchange of α-actin isoforms during myofibril differentiation. In CAP2 mutant mice, this α-actin switch was delayed and coincided with the onset of a myopathy characterized by type IIB ring fibers and motor dysfunction. Rescue experiments in alive mutants proved that loss of CAP2 activity in skeletal muscles caused the myopathy. Our data indicate that the

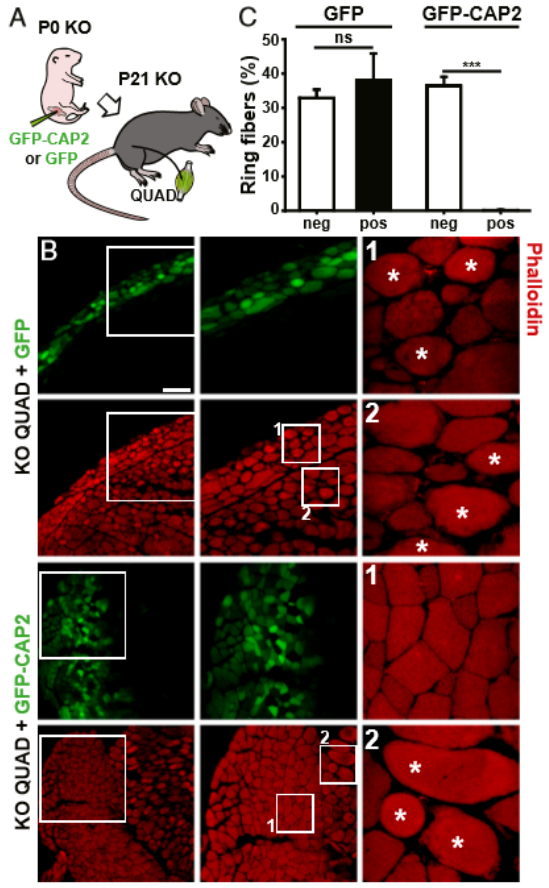

Fig. 4. CAP2 reexpression rescued ring fiber myopathy in KO. (*A*) Scheme showing experimental approach for rescue experiments in KO QUAD. (*B*) Micrographs from P21 KO QUAD cross-sections upon viral transduction of either GFP or GFP-CAP2. Sections were counterstained with phalloidin (red) to screen for ring fibers. White boxes indicate areas shown at higher magnification. Asterisks indicate ring fibers. Scale bar (μm): 100. (*C*) Graph showing fractions of GFP-negative or GFP-positive muscle fibers displaying ring fibers in P21 KO QUAD upon viral induction of either GFP or GFP-CAP2. GFP: negative, 32.8 ± 1.8%; positive, 38.0 ± 5.5%, $P = 0.547$. GFP-CAP2: negative, 36.5 ± 2.3%; positive, 0.2 ± 0.1, $P < 0.001$. $n = 6$ images from three mice. MV ± SEM are shown in *C*. ns, not significant, ***$P < 0.001$.

early postnatal period constitutes a vulnerable phase, in which delayed differentiation of the sarcomere actin cytoskeleton leads to the development of ring fibers.

Apart from ring fibers, KO displayed an elevated number of internalized nuclei and a disturbed distribution of mitochondria. While sarcomere structure was preserved in the majority of muscle fibers, we only very rarely noted moderate Z-band streaming. Accordingly, we did not find Z-band protein-containing remnants (nemaline bodies, ref. 22). KO skeletal muscles did not appear atrophic, and they showed a normal fiber-type proportion. Further, we did not find inclusion bodies, myofibrillar accumulations, sarcoplasmic bodies, (central) cores, fiber necrosis, increased connective tissue, or fat cells—characteristic features for myopathies including myofibrillar myopathies, inclusion body myopathy, central core disease, or dystrophies. Hence, a large fraction of ring fibers characterized the myopathy in CAP2 mutants. Myopathic changes became apparent during early postnatal life, increased until the third postnatal week, and were stable thereafter. Likewise, motor function deficits were present in newborn mutants, and muscle weakness was similar in juvenile and young adult mutants. Our data imply that CAP2 is relevant specifically for skeletal muscle development. The inheritance of the pathological phenotype is autosomal recessive, since HET were indistinguishable from WT.

What could cause ring fiber formation in CAP2 mutants? One important aspect of myofibril differentiation is the assembly and precise alignment of F-actin (23). This includes the sequential exchange of α-actin isoforms that, in mice, occurs during early postnatal life (*SI Appendix*, Fig. S9*A*, refs. 18 and 19). Specifically, α-SKA replaces α-SMA and α-CAA to become the major α-actin in differentiated myofibrils. This α-actin switch requires the coordinated release of actin subunits (20), a process that might depend on proper function of CAP2. In agreement with recent literature (20), we observed a gradual increase of α-SKA in skeletal muscles during early postnatal life and a concomitant decline in α-CAA and α-SMA levels, which were both absent from WT at P12. At this stage, substantial levels of α-CAA and α-SMA were still present in KO. The striated pattern of α-SMA immunoreactivity in muscle fibers, together with its occurrence in the insoluble protein fraction indicated that α-SMA was an integral component of sarcomere F-actin in mutant myofibrils at P12. Notably, α-CAA distribution between soluble and insoluble protein fractions was similar to α-SKA or α-SMA in P12 KO, suggesting that α-CAA was also a component of F-actin. Together, we found a delayed α-actin switch in mutant sarcomeres, suggesting that mutant myofibrils remained in an undifferentiated stage at the onset of the often excessive voluntary muscle contraction around P10 (24). Hence, we identified CAP2 as a critical α-actin exchange factor during myofibril differentiation. A similar function has been proposed for cofilin2 (20), and the myopathy in cofilin2 mutant mice showed some similarities to that of CAP2 mutants (20, 25). We therefore propose a model in which CAP2 and cofilin2 cooperate in regulating the exchange of α-actin isoforms during myofibril differentiation (*SI Appendix*, Fig. S9*B*). In line with our model, a cooperative activity in F-actin turnover in nonmuscle cells has been shown for their close homologs CAP1 and cofilin1 (11, 26), which share similar biochemical functions with CAP2 and cofilin2, respectively (9, 27).

Could a delayed α-actin switch explain the myopathy in KO? Previous studies reported functional differences between myofibrils containing either α-CAA or α-SKA, although both α-actin isoforms are 99% identical and vary only at four amino acid residues (28). They showed that (*i*) force generation in isolated cardiac myofibrils was fourfold smaller than in skeletal muscle myofibrils, (*ii*) heart contractility was increased in BALB/c mice expressing unusual low α-CAA and high α-SKA levels, and (*iii*) maximal specific force was reduced in α-SKA null mice expressing α-CAA in skeletal muscles (29–32). Importantly, in vitro studies further demonstrated that α-CAA filaments were less stable than α-SKA filaments (33). In WT, the switch to the more stable α-SKA that exerts higher mechanical force occurs before mice start strong voluntary movements and in particular pass through the phase of hopping movements during the second to third postnatal week (24). In CAP2-deficient mice, the retarded α-actin switch leads to the simultaneous presence of all three α-actin isoforms in skeletal muscle during this phase of sharply increasing force exertion. We propose that undifferentiated, α-SMA– and α-CAA–containing myofibrils disrupted and reassembled in a random manner thereby leading to ring fibers. This scenario would also explain our observation that ring fibers were restricted to fast twitching type IIB muscle fibers that, compared with type I or IIA fibers, are exposed to higher mechanical forces during muscle contraction (34). In line with this scenario, type IIB ring fiber have been reported for transgenic mice expressing a mutant α-SKA variant that weakened

the interaction between actin subunits (7). Hence, our data and other studies suggest that subtle changes in sarcomere F-actin composition increase the vulnerability of muscle fibers to form ring fibers.

In summary, our study unraveled a critical function for CAP2 in refining the actin cytoskeleton during myofibril differentiation. Given that skeletal muscle differentiation is similar in humans, we propose a crucial function for CAP2 in human myofibril differentiation. In fact, transgenic mouse lines displayed myopathies similar to those associated with mutations in human actin-related genes (7, 25, 35). We therefore propose that mutations in human CAP2 gene may cause ring fiber myopathy. Notably, human *CAP2* has been localized to 6p22.3, and interstitial deletions of variable sizes encompassing the *CAP2* locus have been associated with clinical symptoms including developmental delay, hypotonia, and heart defects (36–38). While we showed here developmental delay and hypotonia for CAP2 mutant mice, others previously reported heart defects (13, 14, 39). We therefore propose that loss of *CAP2* causes or contributes to the pathology of 6p22.3 deletion syndrome.

Materials and Methods

Mice. CAP2 mutants were obtained from the European Conditional Mouse Mutagenesis Program (EUCOMM). See *SI Appendix* for more information on mice and their husbandry. Behavioral experiments and killing of mice were approved by internal animal welfare authorities of the University of Marburg and the Regierungspräsidium Giessen (references: AK-6-2014-Rust, V54-19c2015h01M20/29 Nr. G27/2016, V54-19c2015h01M20/30 Nr. G65/2016). Virus infection was approved by the First Warsaw Local Ethics Committee for Animal Experimentation (reference: 36/2017).

Developmental Milestones. A test battery to assess developmental milestones has been previously described (40). See *SI Appendix* for detailed description.

Histology. Mice were killed by cervical dislocation or decapitation. Upon dissection, skeletal muscle specimens were snap-frozen in isopentane-cooled liquid nitrogen and stored at −80 °C until further processing. Histochemical stains were performed as described (41). See *SI Appendix* for detailed description and antibody list.

Electron Microscopy. EM was performed as described (42). See *SI Appendix* for detailed description.

Immunoblot Analyses. See *SI Appendix* for a detailed description of methods and a list of all antibodies.

Virus Production and Pup Treatment. See *SI Appendix* for a detailed description.

Statistics. Significance was calculated using Student's *t* test. All experiments were conducted by experimenters blind to the genotype. If not specified (histology, immunoblots), all experiments have been conducted in at least three independent experiments (three biological replicates).

ACKNOWLEDGMENTS. We thank the EUCOMM for providing CAP2 mutant mice; Katja Gessner and Isabell Metz for generating graphical schemes; and Karlheinz Burk, Bettina Kowalski, Denis Grabski, Sylvia Stanek, and Heidrun Jennemann for excellent technical support. L.-J.K. was supported by the DFG Research Training Group 2213 "Membrane Plasticity in Tissue Development and Remodeling." This work was supported by a research grant (MR 24/20147) from the University Medical Center Giessen Marburg (UKGM) and by a research grant (ACAciA) from the Fondazione Cariplo (to M.B.R.), as well as a grant from Polish National Science Center (UMO-2016/21/B/NZ3/03638) (to T.J.P.).

1. Banker BQ, Engel AG (1986) Basic reactions of muscle. *Myology. Basic and Clinical*, eds Banker BQ, Engel AG (McGraw-Hill, New York), pp 845–907.
2. Carpenter S, Karpati G (1984) *Pathology of Skeletal Muscle* (Churchill Livingston, New York), pp 216–220.
3. Bethlem J, Vanwijngaarden GK (1963) The incidence of ringed fibres and sarcoplasmic masses in normal and diseased muscle. *J Neurol Neurosurg Psychiatry* 26:326–332.
4. Del Bigio MR, Jay V (1992) Inclusion body myositis with abundant ring fibers. *Acta Neuropathol* 85:105–110.
5. Joyce NC, Oskarsson B, Jin LW (2012) Muscle biopsy evaluation in neuromuscular disorders. *Phys Med Rehabil Clin N Am* 23:609–631.
6. Mankodi A, et al. (2000) Myotonic dystrophy in transgenic mice expressing an expanded CUG repeat. *Science* 289:1769–1773.
7. Ravenscroft G, et al. (2011) Mouse models of dominant ACTA1 disease recapitulate human disease and provide insight into therapies. *Brain* 134:1101–1115.
8. Peña J, Luque E, Noguera F, Jimena I, Vaamonde R (2001) Experimental induction of ring fibers in regenerating skeletal muscle. *Pathol Res Pract* 197:21–27.
9. Ono S (2013) The role of cyclase-associated protein in regulating actin filament dynamics - more than a monomer-sequestration factor. *J Cell Sci* 126:3249–3258.
10. Johnston AB, Collins A, Goode BL (2015) High-speed depolymerization at actin filament ends jointly catalysed by Twinfilin and Srv2/CAP. *Nat Cell Biol* 17:1504–1511.
11. Bertling E, et al. (2004) Cyclase-associated protein 1 (CAP1) promotes cofilin-induced actin dynamics in mammalian nonmuscle cells. *Mol Biol Cell* 15:2324–2334.
12. Peche V, et al. (2007) CAP2, cyclase-associated protein 2, is a dual compartment protein. *Cell Mol Life Sci* 64:2702–2715.
13. Peche VS, et al. (2013) Ablation of cyclase-associated protein 2 (CAP2) leads to cardiomyopathy. *Cell Mol Life Sci* 70:527–543.
14. Field J, et al. (2015) CAP2 in cardiac conduction, sudden cardiac death and eye development. *Sci Rep* 5:17256, and erratum (2016) 6:26640.
15. Kumar A, et al. (2016) Neuronal actin dynamics, spine density and neuronal dendritic complexity are regulated by CAP2. *Front Cell Neurosci* 10:180.
16. Deacon RM (2013) Measuring motor coordination in mice. *J Vis Exp* 75:e2609.
17. Augusto V, Padovani CR, Campos GER (2004) Skeletal muscle fiber types in C57BL6J mice. *Braz J Morphol Sci* 21:89–94.
18. Tondeleir D, Vandamme D, Vandekerckhove J, Ampe C, Lambrechts A (2009) Actin isoform expression patterns during mammalian development and in pathology: Insights from mouse models. *Cell Motil Cytoskeleton* 66:798–815.
19. Mizuno Y, Suzuki M, Nakagawa H, Ninagawa N, Torihashi S (2009) Switching of actin isoforms in skeletal muscle differentiation using mouse ES cells. *Histochem Cell Biol* 132:669–672.
20. Gurniak CB, et al. (2014) Severe protein aggregate myopathy in a knockout mouse model points to an essential role of cofilin2 in sarcomeric actin exchange and muscle maintenance. *Eur J Cell Biol* 93:252–266.
21. Chaponnier C, Gabbiani G (2016) Monoclonal antibodies against muscle actin isoforms: Epitope identification and analysis of isoform expression by immunoblot and immunostaining in normal and regenerating skeletal muscle. *F1000 Res* 5:416.
22. Luther PK (2009) The vertebrate muscle Z-disc: Sarcomere anchor for structure and signalling. *J Muscle Res Cell Motil* 30:171–185.
23. Ono S (2010) Dynamic regulation of sarcomeric actin filaments in striated muscle. *Cytoskeleton (Hoboken)* 67:677–692.
24. Fuller JL, Wimer RE (1966) Neural, sensory, and motor functions. *Biology of the Laboratory Mouse*, ed Green EL (Dover Publ, New York), 2nd Ed.
25. Agrawal PB, Joshi M, Savic T, Chen Z, Beggs AH (2012) Normal myofibrillar development followed by progressive sarcomeric disruption with actin accumulations in a mouse Cfl2 knockout demonstrates requirement of cofilin-2 for muscle maintenance. *Hum Mol Genet* 21:2341–2356.
26. Moriyama K, Yahara I (2002) Human CAP1 is a key factor in the recycling of cofilin and actin for rapid actin turnover. *J Cell Sci* 115:1591–1601.
27. Hild G, Kalmár L, Kardos R, Nyitrai M, Bugyi B (2014) The other side of the coin: Functional and structural versatility of ADF/cofilins. *Eur J Cell Biol* 93:238–251.
28. Chaponnier C, Gabbiani G (2004) Pathological situations characterized by altered actin isoform expression. *J Pathol* 204:386–395.
29. Linke WA, Popov VI, Pollack GH (1994) Passive and active tension in single cardiac myofibrils. *Biophys J* 67:782–792.
30. Hewett TE, Grupp IL, Grupp G, Robbins J (1994) Alpha-skeletal actin is associated with increased contractility in the mouse heart. *Circ Res* 74:740–746.
31. Jackaman C, et al. (2007) Novel application of flow cytometry: Determination of muscle fiber types and protein levels in whole murine skeletal muscles and heart. *Cell Motil Cytoskeleton* 64:914–925.
32. Nowak KJ, et al. (2009) Rescue of skeletal muscle alpha-actin-null mice by cardiac (fetal) alpha-actin. *J Cell Biol* 185:903–915.
33. Orbán J, Lorinczy D, Nyitrai M, Hild G (2008) Nucleotide dependent differences between the alpha-skeletal and alpha-cardiac actin isoforms. *Biochem Biophys Res Commun* 368:696–702.
34. MacIntosh BR, Gardiner PF, McComas AJ (2006) *Skeletal Muscle: Form and Function* (Human Kinetics, Champaign, IL), 2nd Ed.
35. Crawford K, et al. (2002) Mice lacking skeletal muscle actin show reduced muscle strength and growth deficits and die during the neonatal period. *Mol Cell Biol* 22:5887–5896.
36. Bremer A, Schoumans J, Nordenskjöld M, Anderlid BM, Giacobini M (2009) An interstitial deletion of 7.1Mb in chromosome band 6p22.3 associated with developmental delay and dysmorphic features including heart defects, short neck, and eye abnormalities. *Eur J Med Genet* 52:358–362.
37. Celestino-Soper PB, et al. (2012) Deletions in chromosome 6p22.3-p24.3, including ATXN1, are associated with developmental delay and autism spectrum disorders. *Mol Cytogenet* 5:17.
38. Di Benedetto D, et al. (2013) 6p22.3 deletion: Report of a patient with autism, severe intellectual disability and electroencephalographic anomalies. *Mol Cytogenet* 6:4.
39. Stöckigt F, et al. (2016) Deficiency of cyclase-associated protein 2 promotes arrhythmias associated with connexin43 maldistribution and fibrosis. *Arch Med Sci* 12:188–198.
40. Heyser CJ (2004) Assessment of developmental milestones in rodents. *Curr Protoc Neurosci*, Chapter 8, Unit 8.18.
41. Dubowitz V, Sewry C, Oldfors A (2013) *Muscle Biopsy: A Practical Approach* (Saunders Ltd., Philadelphia), pp 21–27.
42. Kraushaar T, et al. (2015) Interactions by the fungal Flo11 adhesin depend on a fibronectin type III-like adhesin domain girdled by aromatic bands. *Structure* 23:1005–1017.

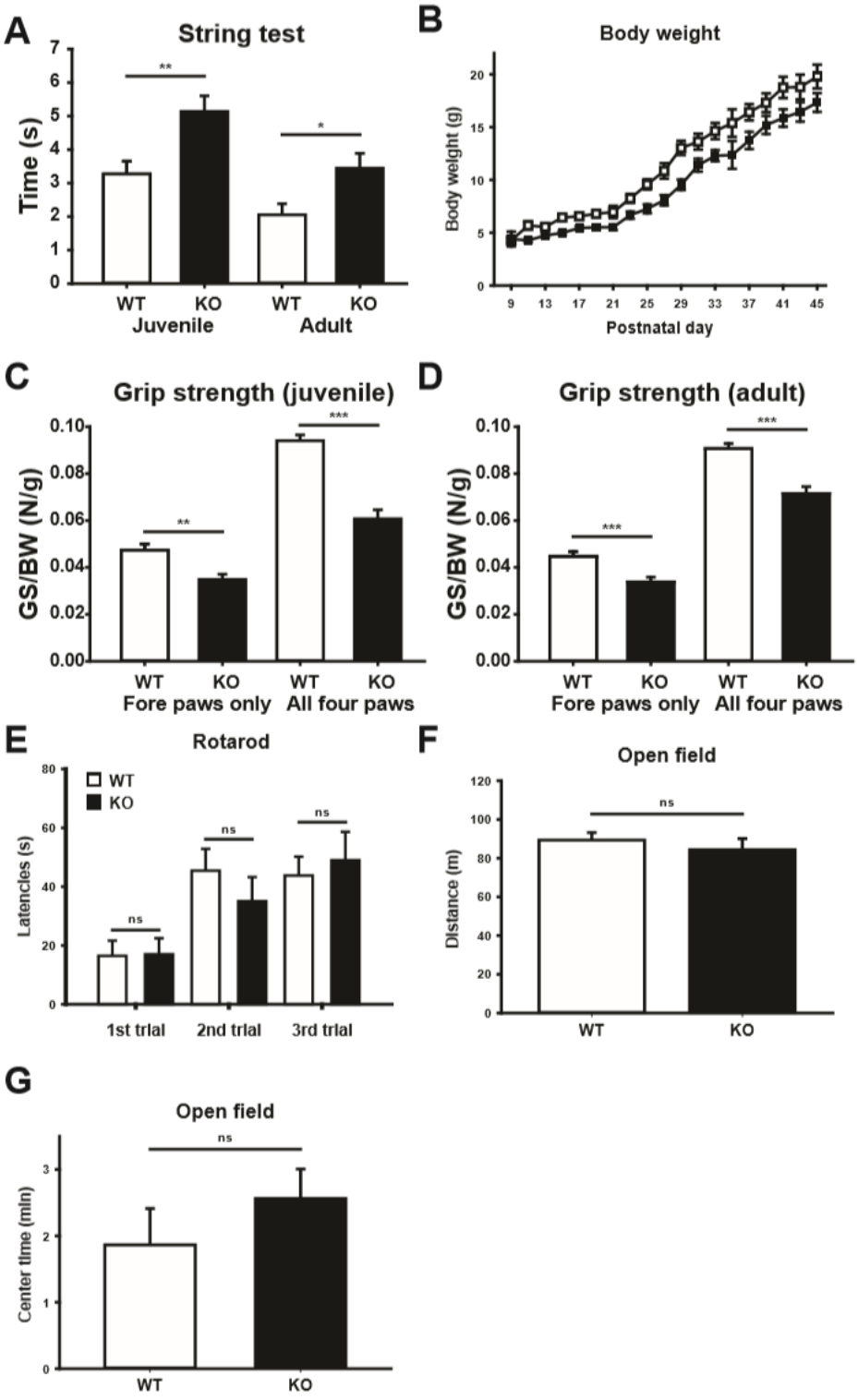

www.pnas.org/cgi/doi/10.1073/pnas.1813351116

Figure S1

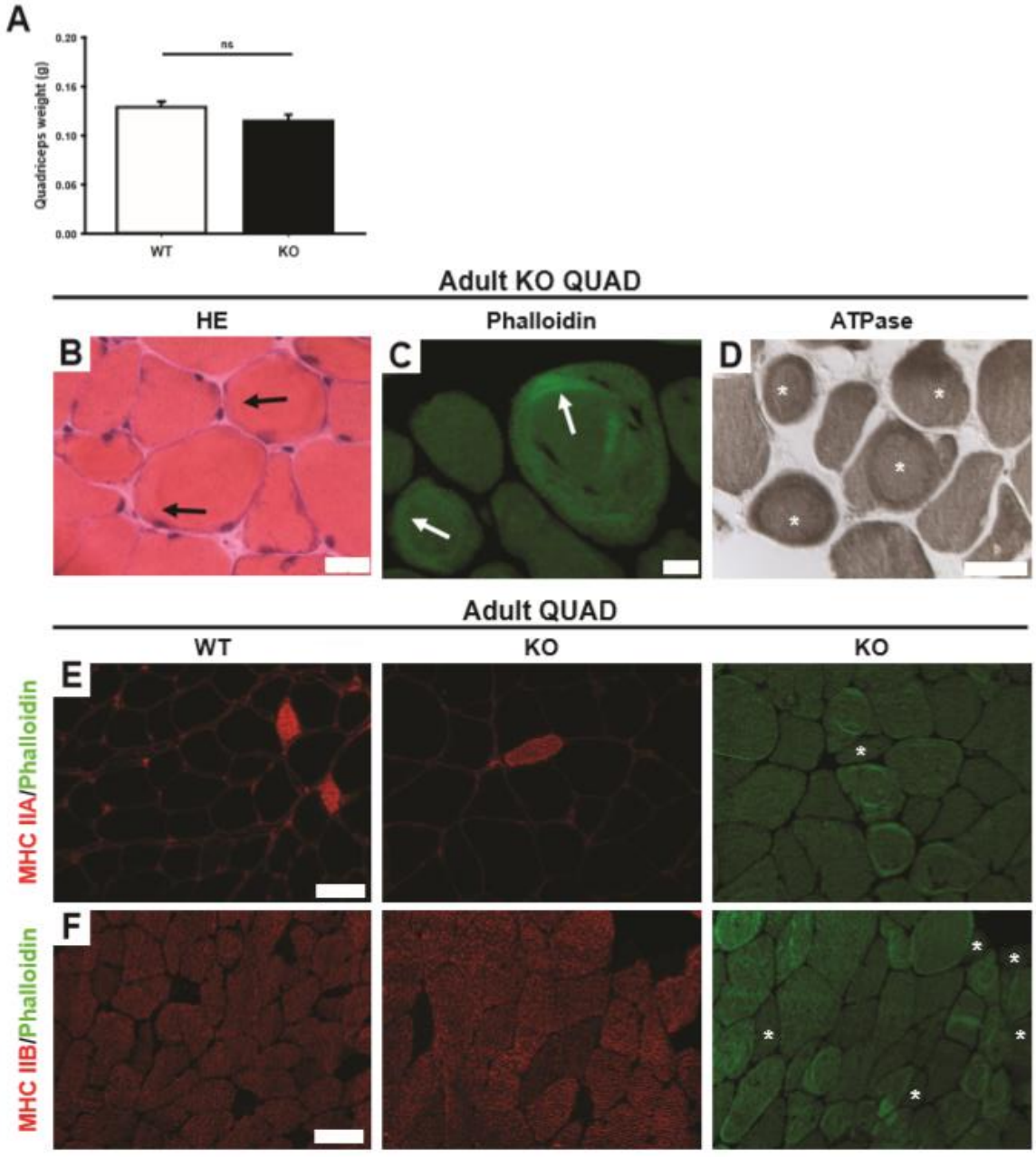

G

		Muscle fibers (%)		
		QUAD	TA	SOL
MHC I	WT	none	0.05 ± 0.04	37.14 ± 4.97
	KO	none	0.73 ± 0.60	45.40 ± 1.04
MHC IIA	WT	1.37 ± 1.12	7.80 ± 1.95	48.03 ± 2.15
	KO	4.81 ± 3.65	5.36 ± 1.08	38.83 ± 3.24
MHC IIB	WT	84.41 ± 5.88	66.87 ± 7.85	none
	KO	92.17 ± 3.58	62.57 ± 5.05	none

Figure S2

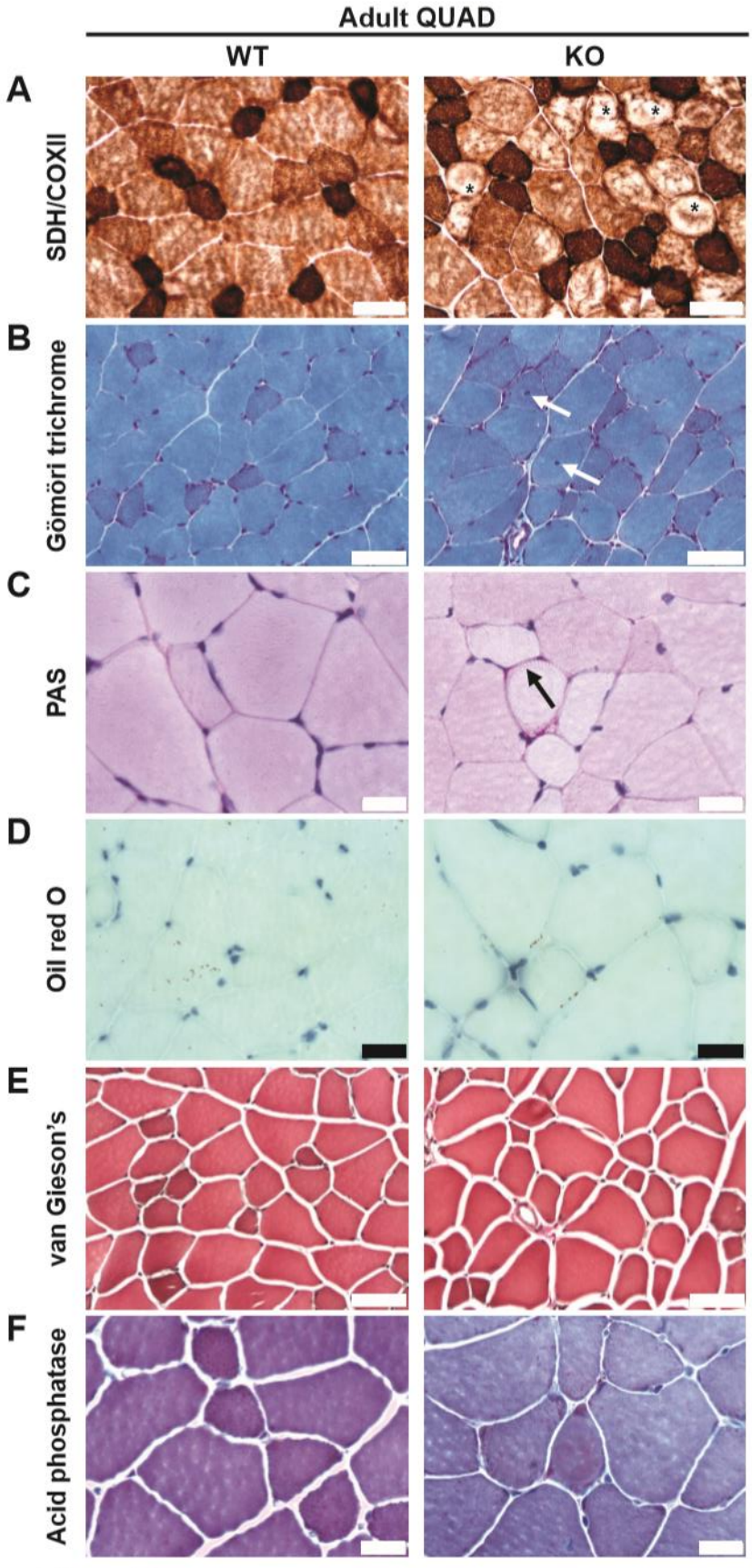
Adult QUAD
WT
KO
A
SDH/COXII
B
Gömöri trichrome
C
PAS
D
Oil red O
E
van Gieson's
F
Acid phosphatase

Figure S3

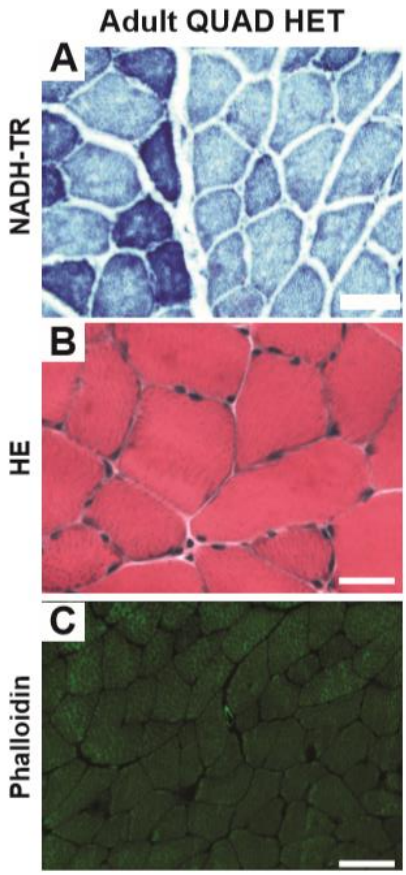

Figure S4

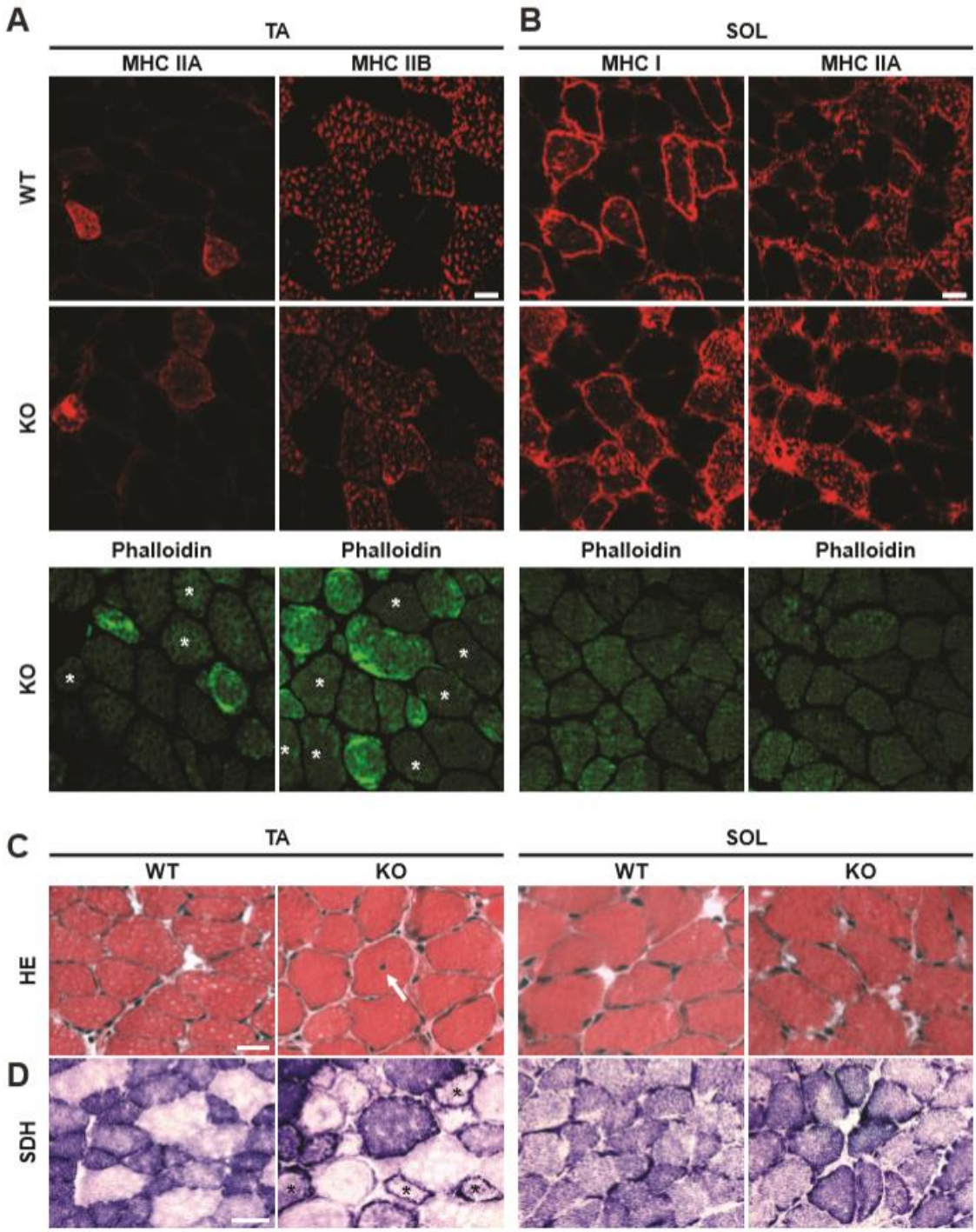
A
TA
MHC IIA
MHC IIB
WT
KO
B
SOL
MHC I
MHC IIA
Phalloidin
Phalloidin
KO
Phalloidin
Phalloidin
C
TA
WT
KO
SOL
WT
KO
HE
D
SDH

Figure S5

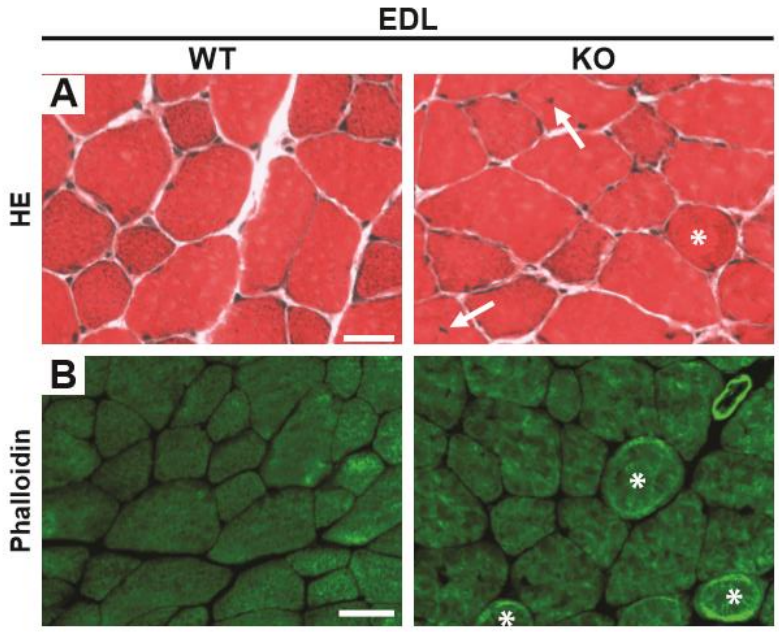

Figure S6

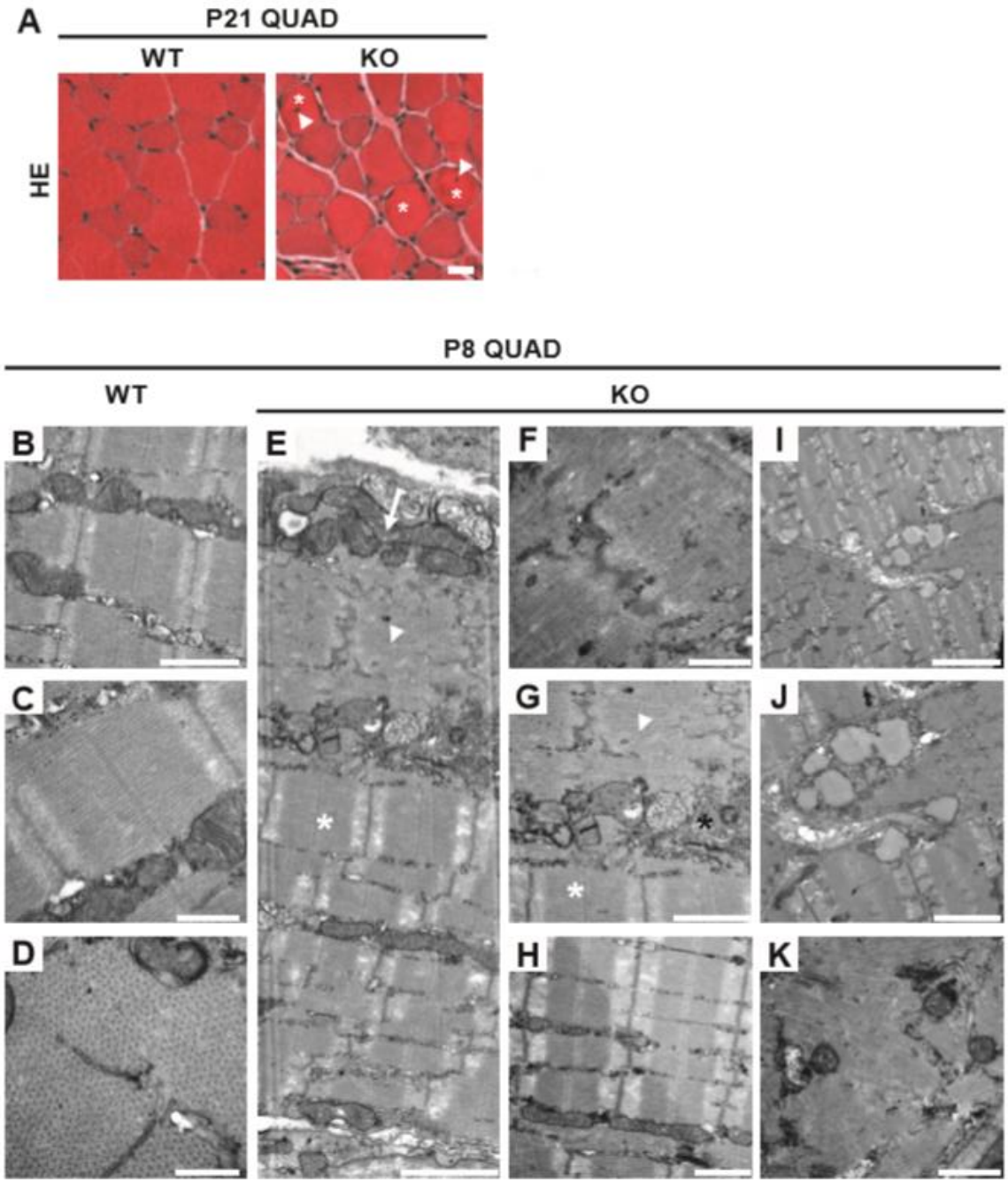

Figure S7

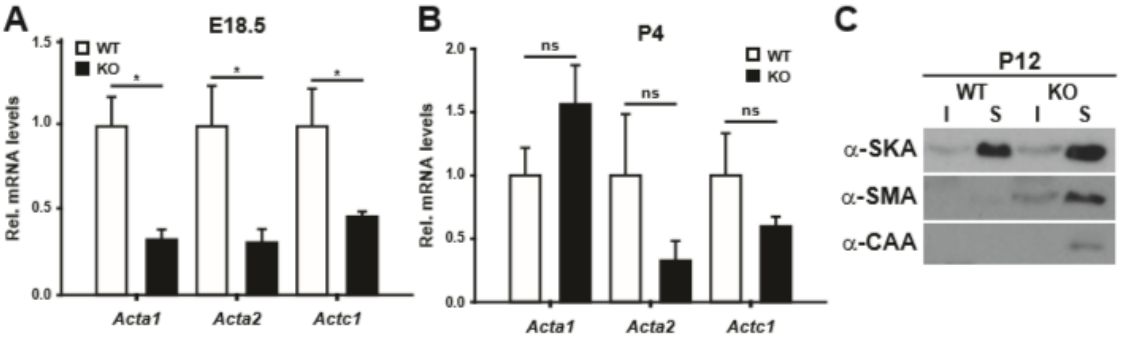
A
E18.5
WT
KO
Rel. mRNA levels
1.5
1.0
0.5
0.0
*
*
*
Acta1
Acta2
Actc1
B
P4
WT
KO
Rel. mRNA levels
2.0
1.5
1.0
0.5
0.0
ns
ns
ns
Acta1
Acta2
Actc1
C
P12
WT
KO
I
S
I
S
α-SKA
α-SMA
α-CAA

Figure S8

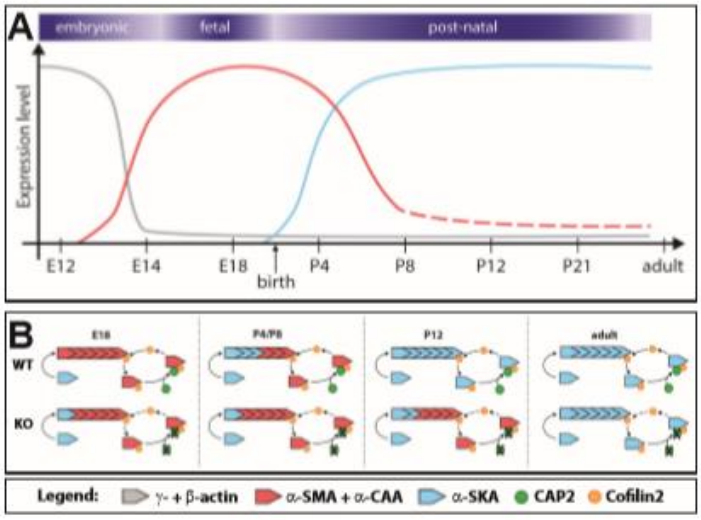
A
embryonic
fetal
post-natal
Expression level
E12
E14
E18
birth
P4
P8
P12
P21
adult
B
E18
P4/P8
P12
adult
WT
KO
Legend:
γ- + β-actin
α-SMA + α-CAA
α-SKA
CAP2
Cofilin2

Figure S9

Figure Legends

Movie S1 shows P8 mice during surface righting testing. In contrast to WT (below), the KO (top) was not able to turn around within 60 s.

Fig. S1. (A) KO performed weaker in string test ((in s) juvenile: WT: 3.3±0.4, n=11; KO: 5.1±0.5, n=12; P<0.01; adult: WT: 2.1±0.3; KO: 3.5±0.4; n=12; P<0.05). **(B)** Graph showing reduced body weight (BW) of male KO (n≥12 for each stage). **(C)** Graph showing reduced grip strength (GS) normalized to BW in juvenile KO ((in N/g) fore paws: WT: 0.047±0.003, n=11; KO: 0.035±0.002, n=12; P<0.01; all paws: WT: 0.094±0.002; KO: 0.064±0.004; P<0.001). **(D)** Graph showing reduced GS/BW in adult KO ((in N/g) fore paws: WT: 0.045±0.002, n=18; KO: 0.034±0.002, n=19; P<0.001; all paws: WT: 0.090±0.002; KO: 0.072±0.003; P<0.001). For P-R: MV±SEM, *: P<0.05, **: P<0.01, ***: P<0.001. **(E)** KO showed normal performance in rotarod testing (e.g. 3rd trial: WT: 43.8±6.1 s; KO: 49.0±9.1 s, n=10, P=0.665). In the open field, **(F)** total distance travelled (WT: 89.4±3.7 m; KO: 84.4±5.5 m; n=12; P=0.467) as well as **(G)** time in center region (WT: 1.9±0.5 min; KO: 2.6±0.4 min; P=0.340) was unchanged in KO. MV±SEM, ns: not significant.

Fig. S2. (A) Graph showing unchanged QUAD weight in adult KO (WT: 0.13±0.01 g, n=11; KO: 0.12±0.01 g, n=12; P=0.118. MV±SEM are shown, ns: not significant. **(B)** Hematoxylin-eosin (HE)-stained adult QUAD cross-sections. Black arrows indicate ring fibers. **(C)** High magnification of KO muscle fibers containing ring fibers (white arrows). **(D)** ATPase-stained QUAD cross-section. **(E-F)** Antibody staining against the type IIA muscle fiber marker MHC IIA and the type IIB muscle fiber marker MHC IIB. For KO, serial sections were stained with phalloidin to label ring fibers. Asterisk in E indicates MHC IIA-positive muscle fiber. Asterisks in F indicate MHC-IIB-negative muscle fibers. **(G)** Quantification of muscle fiber composition in QUAD, TA and SOL. For each analysis, at least 9 micrographs of 0.6 mm^2 from 3 adult mice per genotype have been used. Scale bar (in µm): 20 (B), 10 (C), 50 (D, E, F)

Fig. S3. (A) Succinate dehydrogenase (SDH)/cytochrome oxidase II (COXII) staining confirmed altered mitochondrial distribution in KO muscle fibers (asterisks). **(B)** Gömöri

trichrome staining confirmed increased number of internalized nuclei (arrows). No obvious changes were noted in **(C)** periodic acid-Schiff (PAS) staining, **(D)** oil red O staining, **(E)** van Gieson's staining or **(F)** acid phosphatase staining. Arrow in C indicates a ring fiber in PAS staining. Scale bars (in µm): 50 (A, B, E), 20 (C, D, F).

Fig. S4. (A-C) Representative micrographs of QUAD cross-sections from adult HET showing normal appearance in NADH-TR, HE or phalloidin staining. Scale bar (in µm): 30 (A), 20 (B), 50 (C).

Fig. S5. (A) Representative micrographs of TA cross-sections stained with antibodies against MHC IIA or MHC IIB (red). KO sections were counterstained with phalloidin (green). Asterisks indicate MHC IIA-labeled muscle fiber in left micrograph and MHC IIB-negative muscle fibers in right micrograph. **(B)** Representative micrographs of SOL cross-sections stained with antibodies against MHC I or MHC IIA (red). KO sections were counterstained with phalloidin (green). **(C)** Representative micrographs of HE-stained TA and SOL cross-sections. Arrow indicates an internalized nucleus in KO TA. **(D)** Representative micrographs of SDH-stained TA and SOL cross-sections. Asterisks indicate muscle fibers with altered mitochondrial distribution in KO TA. Scale bar (in µm): 20 (A, B, C, D)

Fig. S6. (A) Representative micrographs of HE-stained EDL cross-sections. Arrows indicate internalized nuclei and asterisk a ring fiber. **(B)** Representative micrographs of phalloidin-stained EDL cross-sections. Asterisks indicate muscle fibers with ring fibers. Scale bar (in µm): 20 (A, B)

Fig. S7. (A) Micrographs of HE-stained P21 QUAD cross-sections. Arrowheads indicate internalized nuclei and asterisks ring fibers. Scale bar (µm): 20. **(B-D)** EM of QUAD longitudinal sections and cross-section from P8 WT. **(E-K)** EM of QUAD longitudinal sections and cross-sections from P8 KO showed a fraction of fibers with partially normal morphology (white asterisks) adjacent to disturbed sarcomeres (E, G, arrowheads). Note the subsarcolemmal accumulation of mitochondria accompanied by too little mitochondria in the inner parts of the fibers (E, arrow), Z-bands revealed

abnormal undulation (E-G) and the tubulus system was dilated (G, black asterisk). Occasional muscle fibers had subsarcolemmal accumulation of lipid droplets and irregular arrangement of myofibrils (I-J). Scale bars (in nm): 3,500 (I), 2,000 (J), 1,500 (E), 1,000 (B, G, H), 500 (C, F, K), 250 (D).

Fig. S8. (A) Bar graphs showing relative mRNA levels of *Acta1* (encodes α-SKA), *Acta2* (encodes α-SMA) and *Actc1* (encodes α-CAA) in E18.5 QUAD (*Acta1:* 0.33±0.05, *Acta2:* 0.31±0.06, *Actc1:* 0.46±0.02; n=3 for all genes, P<0.05 for all genes). **(B)** Bar graphs showing relative mRNA levels of *Acta1*, *Acta2* and *Actc1* in P4 QUAD (*Acta1:* 1.56±0.27, n=4, P=0.188; *Acta2:* 0.33±0.13, n=5 WT, 4 KO, P=0.343; *Actc1:* 0.60±0.07, n=5 WT, 4 KO, P=0.659). MV±SEM are shown, ns: not significant, *: P<0.05. **(C)** Immunoblots showing distribution of α-SKA, α-SMA and α-CAA in soluble (S) and insoluble protein fractions (I) from P12 QUAD.

Fig. S9. Model for CAP2 function during myofibril differentiation. (A) Expression of actin isoforms during skeletal muscle development (1-3). During embryonic myogenesis (E10-E12), when myoblasts fuse to form primary myotubes, γ- and β-actin (grey line) are the dominant actin isoforms. During secondary myotube formation (fetal myogenesis), expression levels of γ- and β-actin decline, while α-SMA and α-CAA (red line) become expressed. At postnatal stages (P1-P21), during muscle fiber formation, α-SKA (blue line) expression increases and it becomes the major actin isoform. Instead, expression of α-SMA and α-CAA decrease. **(B)** Schematic drawing showing how CAP2 may control the 'α-actin switch' during skeletal muscle differentiation, as suggested by data from us and others (4). Upper row: In WT, CAP2 (green) and cofilin2 (orange) cooperate in regulating F-actin turnover. Consisting with other studies (5), CAP2 may release cofilin2 from the actin complex and thereby accelerates cofilin2-mediated F-actin turnover. In the absence of CAP2 (lower row), actin-depolymerizing activity of cofilin2 may be impaired (dashed lines), thereby causing a delay in the 'α-actin switch'.

Material and methods

Mice

We obtained gene-targeted mice (*Cap2*$^{tm1e(EUCOMM)Wtsi}$) from the European Conditional Mouse Mutagenesis Program (EUCOMM) that have been generated from the embryonic stem (ES) cell clone GSF-EPD0155_4_B07 (EMMA ID: 04444). Genotyping of offspring from *Cap2*$^{+/-}$ breeding pairs has been performed by standard PCR protocols on genomic DNA from tail biopsies using the following primers: Cap2-5'arm (TACCTGGAAGAGCTACAGAGG), Cap2-3'arm (GTTCACAGGGACTTTGTTG G), and LAR3 (CAACGGGTTCTTCTGTTAGTCC). PCR with Cap2-5'arm and Cap2-3'arm resulted in a product of 561 bp in the wildtype (WT), but not in the recombinant allele. Instead, PCR with Cap2-5'arm and LAR3 resulted in a product of 617 bp in the recombinant, but not in the WT allele. All mice were housed in the animal facility of the University of Marburg on 12-hour dark-light cycles with food and water available *ad libitum*. Behavioral experiments were conducted during the light cycle. Treatment of mice was in accordance with the German law for conducting animal experiments and followed the guidelines for the care and use of laboratory animals of the U.S. National Institutes of Health. Behavioral experiments and killing of mice were approved by internal animal welfare authorities and the Regierungspräsidium Giessen (references: AK-6-2014-Rust, V54-19c2015h01M20/29 Nr. G27/2016, V54-19c2015h01M20/30 Nr. G65/2016).

Developmental milestones. A test battery to assess developmental milestones has been previously described (6). For eye opening, pinna detachment, auditory startle, tactile startle, visual placing, grasping reflex, forelimb placing, level screen, vertical screen, 'first day of appearance/performance' was noted. For surface righting, negative geotaxis, cliff avoidance and bar holding, time to perform the task was measured. After 60 s (10 s for bar holding), experiments were stopped, non-performing mice were scored with the maximum time. Activity and tremor were scored with values ranging from 0-3.

Muscle strength. Muscle strength was recorded with a self-made grip strength meter, which was generated by equipping a power razor (Sauter, FK25) with a metal grid. Experiments were performed with juvenile and adult mice as previously described (7). Briefly, mice were allowed to grab the grid with either their fore paws only or all 4 paws, and maximal force was recorded. Each mouse was tested 3 times, mean value of each

mouse was considered for further analyses. String test was performed as described (8). Briefly, mice were allowed to grab a thin metal bar with their fore paws and time until they lifted themselves up was recorded. For each mouse, mean value was calculated from 3 independent trials.

Open field

Adult mice (8 weeks) were placed for 30 min in a squared open field arena with 50 cm edge length (TSE Systems), similar to our previous studies (9, 10). Locomotion and time in center region were analyzed automatically using VideoMot2 package (TSE Systems).

Rotarod

During rotarod testing, mice were placed on a self-made rotarod (rod diameter 5 cm), which continuously increases its speed from 4 to 40 rpm within 4 minutes. The test phase consists of 3 trials (15 min inter-trial intervals) without prior training. To allow placing of mice, the rod rotated with 4 rpm until acceleration was started. The latency of falling from the rod was stopped manually.

Electron microscopy

EM was performed as described (11). Briefly, muscle specimens were dissected and tied immediately to the bone. Muscles were fixed in Sörensen-buffer (77 mM Na_2HPO_4 x 2 H_2O, 23 mM KH_2PO_4, pH 7.45) containing 2.5% glutaraldehyde and 0.5% sodium acide for 24 hours. Afterwards, muscles were cut into small specimen (1 x 1 x 5 mm). After osmication and contrasting with uranyl acetate and lead citrate, samples were embedded in Epon resin. Thin sections were analyzed using a Zeiss EM 902.

Virus production and pup treatment GFP-CAP2 cDNA was subcloned from pGFP-CAP2 into pAAV-CMV (a gift from Connie Cepko [Addgene plasmid #67634; http://n2t.net/addgene: 67634; RRID:Addgene_67634]) using HindIII and BglII restriction sites. scAAV-GFP from SignaGen Laboratories (Plasmid #SL100840-SC) was used for control virus production. AAV2/9 particles were prepared by the Nencki Institute Core Facility (Laboratory of Animal Models). P0 pups were subjected to hypothermic anesthesia by placing them on ice for 5 min. Muscles were injected with 1.02 x 109 vg and animals were sacrificed at P21 by isoflurane inhalation and dislocation. QUAD were dissected as described.

Histology

Mice were sacrificed by cervical dislocation or decapitation. Upon dissection, skeletal muscle specimens were snap-frozen in isopentane-cooled liquid nitrogen and stored at -80°C until further processing. Sections from skeletal muscle specimen were generated by using a Leica CM 3050 S cryostate. 7 µm-thick sections (for rescue experiments 20 µm) were collected on Ultra Plus microscope slides (Thermo Scientific), dried and subsequently stored at -20°C. Histochemical stains were performed as described (12). For immunohistochemistry, sections were treated for 1 hour with blocking solution (2% bovine serum albumin (BSA), 3% normal goat serum (NGS), 0.5% NP40 in phosphate-buffered saline (PBS)). Sections were incubated over night at 4°C in carrier solution (2% BSA, 0.5% NP40 in PBS) containing the primary antibody and/or phalloidin. After three washing steps of 5 min in PBS, sections were incubated for 2 hours at room temperature (RT) in carrier solution containing Alexa-488 and/or Alexa-546-conjugated secondary antibodies (1:200, Life Technologies). Afterwards, sections were counterstained for 10 min at RT with the intercalating dye Hoechst 33342 (Invitrogen) diluted 1:1,000 in PBS. After two washing steps of 5 min in PBS, sections were embedded in self-made embedding medium containing 2.5% Dabco (Sigma Aldrich). Images were acquired with a Leica SP5 confocal microscope using 20x and 40x objectives (N.A. 0.7, N.A. 1.3, respectively). Images were processed with Fiji software (ImageJ 1.51w) and analyzed by exploiting the cell counter plug-in (13).

Primary antibodies used for immunohistochemistry: mouse anti-Desmin (1:200, #M0760, Dako), mouse anti-Myosin Heavy Chain Type I (1:10, #BA-D5, obtained from Developmental Studies Hybridoma Bank (DSHB), mouse anti-Myosin Heavy Chain Type IIA (1:10, #SC-71, DSHB), mouse anti-Myosin Heavy Chain Type IIB (1:10, #BF-F3, DSHB), α-SMA (14). To label F-actin, we exploited either Alexa-488- (1:100, #A12379, Invitrogen) or Alexa-647-conjugated phalloidin (1:40, #8940S, Cell Signaling).

Immunoblot analyses

To generate total protein from skeletal muscles, tissues were homogenized in lysis buffer (50 mM Tris-HCl, 150 mM NaCl, 0.5% NP-40, 0.1% SDS) containing protease inhibitor (Complete, Roche). Separation of soluble and insoluble fractions from muscle tissues has been conducted as described before (15). Briefly, samples were homogenized in cold lysis buffer 1 (10 mM K_2HPO_4, 100 mM NaF, 50 mM KCl, 2 mM

$MgCl_2$, 1 mM EGTA, 0.2 mM DTT, 0.5% Triton X-100, 1 mM sucrose, pH 7.0) and centrifuged with 15,000 g for 30 min at 4°C. Supernatant was transferred to a new tube and the remaining pellet was suspended in lysis buffer 1 and an equal volume of lysis buffer 2 (1.5 mM guanidine hydrochloride, 1 mM sodium acetate, 1 mM $CaCl_2$, 1 mM ATP, 20 mM Tris-HCl, pH 7.5). After that, samples were centrifuged with 15,000 g for 30 min at 4°C and the supernatant was transferred to a new tube. Samples were loaded either with the same protein concentration.

Protein extracts were denatured at 95°C in Laemmli buffer, separated by SDS-page and blotted onto a polyvinylidene difluoride membrane (Merck) by using a Wet/Tank Blotting System (Biorad). Membranes were blocked in Tris-buffered saline (TBS) containing 5% milk powder, 0,5% Tween-20 and 0,02% sodium acid for 1 hour and afterwards incubated with primary antibodies in blocking solution over night at 4°C. As secondary antibodies, horseradish peroxidase (HRP)-conjugated antibodies (1:20,000, Thermo Fisher Scientific) were used and detected by chemiluminescence with ECL Plus Western Blot Detection System (GE Healthcare).

Primary antibodies used for immunoblots: polyclonal antibodies against CAP2 were generated against two CAP2 epitopes (peptide #1: VTDDKKTYKNPSLRA, peptide #2: WDGSKLVTEPAEIMA) in rabbits by performing the Speedy 28-day polyclonal package (Eurogentec). Sera were used for immunoblots (1:1,000), and antibodies recognized a band of 53 kDa in WT tissues, which was absent from KO tissues. Further antibodies: mouse anti-actin (1:5,000, #NB600-535, Novus Biologicals), mouse anti-β actin (1:5,000, #A5441, Sigma Aldrich), rabbit anti-γ actin (1:5,000, #PA513467, Thermo Fisher), mouse anti-β tubulin (1:5,000, #T5201, Sigma Aldrich), anti-α-SKA (1:500, (14)), mouse anti-α-CAA (1:500, (14)), mouse anti-α-SMA (1:500, (14)).

Quantitative PCR

Total RNA from skeletal muscle tissues was isolated using peqGold Trifast (VWR) according to the manufacturer's instructions. To exclude DNA contamination, samples were treated with the TURBO DNA-free kit (Invitrogen), followed by reverse transcription using iScript cDNA synthesis kit (Bio-Rad) according to the manufacturer's protocol. Quantitative PCR (qPCR) was performed in the STEP-One Light cycler (ABI Systems) using the iTaq SYBR Green Supermix (Bio-Rad) for detection of target genes. Three technical replicates were averaged and normalized to U6 in order to determine mRNA levels. Relative changes were calculated using the

ΔΔCt method (16). Primer sequences: *Acta1* (forward (f): CCAAGTCCTGCAAGTGAACAAG, reverse (r): GTCGCACATGGTGTCTAGTTTC), *Acta2* (f: GGCATCCACGAAACCACCTAT, r: CTGTGATCTCCTTCTGCATCCT), *Actc1* (f: TGGTATGGAATCTGCTGGCATT, r: CCTTTTGCATACGATCGGCAAT), *U6* (f: CTCGCTTCGGCAGCACA, r: AACGCTTCACGAATTTGCGT).

References

1. Khaitlina SY (2001) Functional specificity of actin isoforms. *Int Rev Cytology* 202:35-98.
2. Imbriano C & Molinari S (2018) Alternative Splicing of Transcription Factors Genes in Muscle Physiology and Pathology. *Genes* 9(2).
3. Relaix F & Zammit PS (2012) Satellite cells are essential for skeletal muscle regeneration: the cell on the edge returns centre stage. *Development* 139(16):2845-2856.
4. Gurniak CB, *et al.* (2014) Severe protein aggregate myopathy in a knockout mouse model points to an essential role of cofilin2 in sarcomeric actin exchange and muscle maintenance. *Eur J Cell Biol* 93(5-6):252-66.
5. Ono S (2013) The role of cyclase-associated protein in regulating actin filament dynamics - more than a monomer-sequestration factor. *J Cell Sci* 126(15):3249-3258.
6. Heyser CJ (2004) Assessment of developmental milestones in rodents. Curr Protoc Neurosci Chapter 8:Unit 8 18.
7. Bonetto A, Andersson DC, & Waning DL (2015) Assessment of muscle mass and strength in mice. Bonekey Rep 4:732.
8. Deacon RM (2013) Measuring motor coordination in mice. J Vis Exp (75):e2609.
9. Goodson M, *et al.* (2012) Cofilin-1: a modulator of anxiety in mice. *PLoS Genet* 8(10):e1002970.
10. Zimmermann AM, *et al.* (2015) Attention-Deficit/Hyperactivity Disorder-like Phenotype in a Mouse Model with Impaired Actin Dynamics. *Biol Psychiatry* 78(2):95-106.
11. Kraushaar T, et al. (2015) Interactions by the Fungal Flo11 Adhesin Depend on a Fibronectin Type III-like Adhesin Domain Girdled by Aromatic Bands. Structure 23(6):1005-1017.
12. Dubowitz, Sewry, & Oldfors (2013) Muscle Biopsy: A Practical Approach. (Saunders Ltd.), pp 21-27.
13. Schindelin J, *et al.* (2012) Fiji: an open-source platform for biological-image analysis. *Nat Methods* 9(7):676-682.
14. Chaponnier C & Gabbiani G (2016) Monoclonal antibodies against muscle actin isoforms: epitope identification and analysis of isoform expression by immunoblot and immunostaining in normal and regenerating skeletal muscle. *F1000Res* 5:416.
15. Huang W, *et al.* (2013) mTORC2 controls actin polymerization required for consolidation of long-term memory. *Nat Neurosci* 16(4):441-448.
16. Livak KJ & Schmittgen TD (2001) Analysis of relative gene expression data using real-time quantitative PCR and the 2(-Delta Delta C(T)) Method. *Methods* 25(4):402-408.

Cyclase-associated protein 2 (CAP2) controls MRTF-A localization and SRF activity in mouse embryonic fibroblasts

Lara-Jane Kepser[1,2], Laura Soto Hinojosa[2,3], Robert Grosse[2,3], Marco B. Rust[1,2,4]

[1]Molecular Neurobiology Group, Institute of Physiological Chemistry, University of Marburg, 35032 Marburg, Germany; [2]DFG Research Training Group, Membrane Plasticity in Tissue Development and Remodeling, GRK 2213, Philipps-University of Marburg, 35032 Marburg, Germany; [3]Institute of Pharmacology, University of Marburg, 35032 Marburg, Germany; [4]Center for Mind, Brain and Behavior (CMBB), University of Marburg and Justus-Liebig-University Giessen, Hans-Meerwein-Strasse 6, 35032 Marburg, Germany

***Correspondence to**

Marco B. Rust

Institute of Physiological Chemistry

Philipps-University of Marburg

35032 Marburg, Germany

Phone: +49-6421-2865020

E-Mail: marco.rust@staff.uni-marburg.de

Abstract

Recent studies identified cyclase-associated proteins (CAPs) as important regulators of actin dynamics that control assembly and disassembly of actin filaments (F-actin). While these studies significantly advanced our knowledge of their molecular functions, the physiological relevance of CAPs largely remained elusive. Gene targeting in mice implicated CAP2 in heart physiology and skeletal muscle development. Heart defects in CAP2 mutant mice were associated with altered activity of serum response factor (SRF), a transcription factor involved in multiple biological processes including heart function, but also skeletal muscle development. By exploiting mouse embryonic fibroblasts (MEFs) from CAP2 mutant mice, we aimed at deciphering the CAP2-dependent mechanism relevant for SRF activity. Reporter assays and mRNA quantification by qPCR revealed reduced SRF-dependent gene expression in mutant MEFs. Reduced SRF activity was associated with moderately increased G-actin levels and an altered subcellular distribution of MRTF-A, a transcriptional SRF coactivator that is shuttled out of the nucleus and, hence, inhibited upon G-actin binding. Moreover, pharmacological actin manipulation restored MRTF-A distribution in mutant MEFs. Our data are in line with a model in which CAP2 controls the MRTF-SRF pathway via an actin-dependent mechanism. While MRTF-A localization and SRF activity was impaired under basal conditions, serum stimulation induced nuclear MRTF-A translocation and SRF activity in mutant MEFs similar to controls. In summary, our data revealed that in MEFs CAP2 controls MRTF-A localization and SRF activity in an actin-dependent mechanism, while it was dispensable for serum-induced nuclear MRTF-A translocation and SRF stimulation.

Introduction

Cyclase-associated proteins (CAPs) have been recognized as actin-binding proteins (ABP) two decades ago (Freeman and Field 2000; Hubberstey and Mottillo 2002; Balcer et al. 2003; Bertling et al. 2004), but significant progress in their molecular function has been achieved only recently (Chaudhry et al. 2010; Jansen et al. 2014; Johnston et al. 2015; Kotila et al. 2018; Kotila et al. 2019; Mu et al. 2019; Shekhar et al. 2019). These studies unraveled a role for yeast and mammalian CAPs in disassembly of actin filaments (F-actin) and in the ATP-for-ADP-exchange on actin monomers (G-actin) that is essential for F-actin assembly. Hence, CAPs emerged as important regulators of F-actin dynamics, the spatiotemporally controlled assembly and disassembly of F-actin. While these studies advanced our knowledge of their molecular functions, the physiological relevance of mammalian CAPs largely remained elusive, also because appropriate animal models were lacking. This holds true specifically for the ubiquitously expressed family member CAP1 (Jang et al. 2019), while recent studies revealed arrhythmia, cardiac conduction defects as well as dilated cardiomyopathy in systemic and heart-specific CAP2 mutant mice (Peche et al. 2013; Field et al. 2015; Stockigt et al. 2016). Additionally, skeletal muscle development and myofibril differentiation was retarded in systemic CAP2 mutants, which displayed a myopathy characterized by a large number of ring fibers associated with motor function deficits (Kepser et al. 2019). Together, these studies emphasized a pivotal role for CAP2 in striated muscles, in agreement with its abundant expression in heart and skeletal muscle (Peche et al. 2007; Field et al. 2015; Kepser et al. 2019). Heart defects in CAP2 mutant mice were associated with altered gene expression including an upregulation of genes whose expression is controlled by serum response factor (SRF), and they were partially restored upon SRF inhibition (Xiong et al. 2019), suggesting a causal relationship between SRF dysregulation and heart pathology. However, the mechanism underlying increased SRF activity upon CAP2 inactivation remained unknown.

SRF is a ubiquitously expressed and highly conserved transcription factor that was first identified in studies of fibroblast serum response. Its activity is mainly regulated by two classes of transcriptional coactivators, namely the ternary complex factors (TCFs) as well as myocardin and myocardin-related transcription factors (MRTFs) (Olson et al. 2010).

TCFs and MRTFs compete for a common surface domain on the DNA-binding domain of SRF, interact with SRF in a mutually exclusive manner and activate different sets of SRF-target genes (Esnault et al. 2014; Gualdrini et al. 2016). The TCF-SRF pathway is promoted by Ras and mitogen-activated protein kinases (MAPKs), induces expression primarily of immediate early genes (IEG) and has been implicated in cell-cycle re-entry and proliferation (Gualdrini et al. 2016). Instead, the MRTF-SRF pathway is controlled by the availability of G-actin and induces expression of cytoskeleton-related genes (Esnault et al. 2014). Specifically, G-actin binds to MRTF and promotes its translocation into the cytosol, thereby inhibiting MRTF-SRF-dependent gene expression (Olson et al. 2010). Hence, the actin regulator CAP2 may control SRF activity via a mechanism that involves actin and MRTF.

By exploiting mouse embryonic fibroblasts (MEFs) from systemic CAP2 mutant mice, we here i) tested whether CAP2 controls SRF activity in cell types others than heart cells and ii) aimed at deciphering the underlying mechanism. Reporter assays and quantitative PCR (qPCR) revealed reduced SRF activity in MEFs upon CAP2 inactivation. Impaired SRF activity in CAP2 mutant MEFs was associated with moderately increased G-actin and reduced nuclear MRTF-A levels. Further, MRTF-A distribution in mutant MEFs was normalized by pharmacological actin manipulation. While our data were in line with a role for CAP2 in regulating SRF activity via the actin-MRTF-A pathway in non-stimulated MEFs, serum stimulation equally induced nuclear MRTF-A translocation and SRF activity in control and CAP2 mutant MEFs.

Material and Methods

Preparation and culture of MEFs

MEFs were isolated from CAP2-KO mice and CTR littermates at E12.5 as previously described (Seiler et al. 2008; Rehklau et al. 2012). Briefly, dissected embryos were minced and treated with 0.25% trypsin (Invitrogen) after removal of the head and organs. After 15 min of incubation at 37°C, tissue was pulled through a 0.9-mm needle to obtain isolated cells. After washing twice with serum-free Dulbecco's modified Eagle's medium (DMEM; Invitrogen), isolated cells were cultured in DMEM containing 10% fetal calf serum (FCS; PAA). Primary MEFs (termed passage 0) were grown for 1 day. On the next day, MEF immortalization was started according to the 3-day transfer protocol (3T3) immortalization protocol that defined immortalization as completed after passage 12. MEFs were kept at 37°C and 5% CO_2 in DMEM containing 4.5 g/l glucose and 10% FCS, as well as penicillin (100 m/ml; PAA) and streptomycin (100 mg/ml; PAA). MEFs were passaged every 2–3 days. All experiments were performed with MEFs of P12–P40.

Generation of MEF cell line stably expressing MRTF-A-GFP

MRTF-A-GFP was stably expressed in MEF cells (CTR and CAP2-KO cell lines). For that, first HEK293T cells were transfected using the calcium phosphate method. For lentivirus production, HEKT293T cells were cotransfected with the lentiviral packaging vectors psPAX and pMDG.2 together with the pInducer-MRTF-A GFP plasmid as described before (Hinojosa et al. 2017). After 48 h, supernatants containing viral particles were harvested, filtered, and used to transduce MEF cells. Transduced MEF cells were selected by FACS-based cell sorting. Expression of MRTF-A–GFP from pInducer20 was induced by 333 ng/ml doxycycline.

Live cell imaging

To analyze MRTF-A subcellular localization upon serum stimulation, MEF cells stably expressing pIND20-MRTF-A-GFP were serum-deprived for 48 h and then live cell imaging was performed. Cells were stimulated 24 h before imaging with 333 ng/ml doxycycline to induce MRTF-A-GFP expression.

Serum stimulation was performed adding 20% serum directly to the cells under the microscope to follow the effects of the stimulation on MRTF-A translocation over time. Microscopic imaging was performed using confocal laser-scanning microscope (LSM 800, Carl Zeiss) and a 63x 1.4 NA oil objective lens (Carl Zeiss). Time-lapse microscopy was performed at 37°C in a CO2-humidified incubation chamber (Pecon, CO2, module S1) using ZEN software (Carl Zeiss).

SRF-luciferase reporter gene assay

To assess SRF activity, we generated MEF cell lines (CTR and CAP2-KO) expressing the firefly luciferase reporter where MRTF-SRF promoter 3Da.luc was linked to GFP. To generate the MEF cell lines stably expressing the MRTF-SRF luciferase reporter, first HEK293T cells were transfected using the calcium phosphate method. For lentivirus production, HEKT293T cells were cotransfected with the lentiviral packaging vectors psPAX and pMDG.2 together with the lentiviral vector FUGW expressing MRTF-SRF promoter 3Da.luc linked to GFP. Generation of the lentiviral luciferase reporter construct has been described before (Hinojosa et al. 2017). After 48 h, supernatants containing viral particles were harvested, filtered, and used to transduce MEF cells. Transduced MEF cells were selected by FACS-based cell sorting.

MEF cells expressing the MRTF-SRF luciferase reporter were serum-deprived overnight and stimulated either with or without 20% serum for 24 h or 48 h. Then, cells were lysed with 200 µl Triton lysis buffer on ice and collected in 1.5 ml Eppendorf tube, followed by 10 min centrifugation at 13 000 rpm at 4°C. The amount of firefly luciferase was measured luminometrically for each condition using a Glomax 96 Microplate Luminometer (Promega) (Baker et al. 2014).

Nucleofection

To study MEF morphology and CAP2 localization, MEF cells were transfected with either 3µg pEGFP-C1 (Clontech) or 3µg pEGFP-C1-MmCAP2 (kindly provided by Elena Marcello, Milano) using the 4D Nucleofector (Lonza) with the Amaxa P3 Primary Cell 4D Nucleofector X Kit (Lonza) according to the manufacturer's instructions.

Fixation and Immunohistochemistry

MEFs were plated on coverslips coated with 0,01 % calf skin collagen (Sigma Aldrich) in 0,1 M acetic acid. Coverslips were fixed with 4% PFA in PBS for 10 min and afterwards washed three times with PBS for 5 min each.

For immunohistochemistry, coverslips were treated for 1 hour with blocking solution and afterwards incubated over night at 4°C in carrier solution containing the primary antibody. After three washing steps of 5 min in PBS, coverslips were incubated for 2 hours at room temperature (RT) in carrier solution containing Alexa-488 conjugated secondary antibodies (1:200, Life Technologies). For phalloidin and DNase I treatment, coverslips were incubated for 2 hours at RT with both conjugates in PBS. Afterwards, coverslips were counterstained for 10 min at RT with the intercalating dye Hoechst 33342 (Invitrogen) diluted 1:1,000 in PBS. After two washing steps in PBS, coverslips were fixed on microscopic slides with Aqua-Poly/Mount (Polyscience Inc.). Images were acquired with a Leica SP5 confocal microscope using 20x and 40x objectives (N.A. 0.7, N.A. 1.3, respectively). Images were processed with Fiji software (ImageJ 1.51w) and analyzed by exploiting the cell counter plug-in.

Primary antibodies used for immunohistochemistry: mouse anti-MRTF-A (G8, Santa Cruz). To label F- and G-actin, we exploited rhodamine (1:200, R415, Invitrogen) phalloidin and Alexa-488 DNAse I conjugate (1:500, D12371, Invitrogen).

Treatment with LATB and JASP

Previous to treatment with LATB (Abcam, #ab1442091) or JASP (Abcam, #ab141409), pIND20-MRTF-A-GFP control and CAP2 mutant cells were activated 24 h before with 333 ng/ml doxycycline. Cells were treated for 4 h with either 25nM LATB, 25nM JASP or an equal volume of DMSO as control.

Immunoblot analysis

Immunoblots were performed as described before (Kepser et al. 2019). Briefly, generation of total protein from MEF cells was contained by homogenization of cells in lysis buffer containing protease inhibitor (Complete, Roche).

For determination of G/F-actin ratio fractionation was performed as described from Huang and coworkers (Huang et al. 2013).

Protein extracts were denatured at 95°C in Laemmli buffer, separated by SDS-page and blotted onto a polyvinylidene difluoride membrane (Merck) by using a Wet/Tank Blotting System (Biorad). Membranes were blocked for 1 hour and afterwards incubated with primary antibodies in blocking solution over night at 4°C. As secondary antibodies, horseradish peroxidase (HRP)-conjugated antibodies (1:20,000, Thermo Fisher Scientific) were used and detected by chemiluminescence with ECL Plus Western Blot Detection System (GE Healthcare). Primary antibodies used for immunoblots: rabbit anti-CAP2 (1:500, #15865-1-AP, Proteintech) mouse anti-actin (1:5,000, #NB600-535, Novus Biologicals), mouse anti-GAPDH (1:10,000, #MAB5718, R&D Systems)

Quantitative PCR

Total RNA from MEFs was isolated using peqGold Trifast (VWR) according to the manufacturer's instructions. To exclude DNA contamination, samples were treated with the TURBO DNA-free kit (Invitrogen), followed by reverse transcription using iScript cDNA synthesis kit (Bio-Rad) according to the manufacturer's protocol. Quantitative PCR (qPCR) was performed in the STEP-One Light cycler (ABI Systems) using the iTaq SYBR Green Supermix (Bio-Rad) for detection of target genes. Three technical replicates were averaged and normalized to GAPDH in order to determine mRNA levels. Relative changes were calculated using the ΔΔCt method. Primer sequences: *Srf* (forward (f): TTCCCGTCCGAGGAAACAT, reverse (r) GGCTCTTTTGACCCAGACCAT), *Vcl* (f: AGCCCAGATGCTTCAGTCAGA, r: GGTCAGATGTGCCAGAAAGGA), *c-Fos* (f: TTCCTACTACCATTCCCCAGCC, r: GATCTGCGCAAAAGTCCTGTG, *Gapdh* (f: CCCTTCATTGACCTCAACTA, r: CCAAAGTTGTCATGGATGAC), *Acta2* (f: GGCATCCACGAAACCACCTAT, r: CTGTGATCTCCTTCTGCATCCT), *Egr2* (f: TGCTAGCCCTTTCCGTTGA, r: TCTTTTCCGCTGTCCTCGAT), *Cyr61* (f: AATCGCAATTGGAAAAGGCA, r: TGAAAAGAACTCGCGGTTCG)

Results

CAP2 inactivation moderately increases G-actin levels in mouse fibroblasts

To study the cellular function of CAP2 in mammalian cells, we generated immortalized mouse embryonic fibroblasts (MEFs) from two $CAP2^{-/-}$ mice (termed KO) and two $CAP2^{+/+}$ control littermates (CTR) at embryonic day (E) 12.5. Immunoblots confirmed absence of CAP2 from both KO MEF lines (Fig. 1A). Due to the lack of specific antibodies suitable for immunocytochemistry, we examined subcellular CAP2 localization in MEFs by expressing a green fluorescent protein (GFP)-tagged CAP2 construct. GFP-CAP2 was homogenously distributed within the cytosol and largely absent from the nucleus (Fig. 1B). CAP2 inactivation in MEFs did not induce any obvious alterations as KO MEFs proliferated normally, adhered to cell culture dishes and did not differ from CTR MEFs in size or solidity index that we calculated to assess cellular morphology (Fig. 1C-E: size (in μm^2): CTR: 2,689.45±154.77, KO: 2,856.97±184.21, n≥25/3, P=0.500; solidity index (arbitrary units): CTR: 0.78±0.02, KO: 0.76±0.01, n≥25/3 cells, P=0.316). Together, CAP2 inactivation did not induce any obvious defects in cellular functions such as morphology, proliferation or adhesion.

Next, we studied whether CAP2 inactivation affected the actin cytoskeleton. To do so, we exploited fluorescent phalloidin that specifically labels F-actin and fluorescent DNase I that binds G-actin with high affinity (Cramer et al. 2002; Melak et al. 2017). In line with overall normal cellular functions, KO MEFs did not display any severe actin cytoskeleton defects (Fig. 1F). However, compared to CTR MEFs, fluorescent intensities of phalloidin and DNase I were both moderately increased in KO MEFs (Fig. 1G; DNase I: CTR: 237.41±11.62, KO: 366.63±19.83, n≥71/3, P<0.001; phalloidin: CTR: 292.02±21.41, KO: 444.60±12.09, n≥71/3, P<0.001). In CTR MEFs as well as in KO MEFs, DNase I fluorescence was much higher in the nucleus when compared to the cytosol and this likely did not reflect subcellular G-actin distribution. We therefore left aside the nucleus and determined phalloidin and DNase I fluorescence solely in the cytosol. Similar to our analysis of fluorescent intensity in entire MEFs, cytosolic phalloidin and DNase I fluorescence intensity was both higher in KO MEFs when compared to CTR MEFs (Fig. 1H; DNase I: CTR: 177.11±10.61, KO: 284.49±15.75, n≥71/3, P<0.001; phalloidin: CTR: 305.65±21.91, KO: 468.13±15.60, n≥71/3, P<0.001).

However, the G/F-actin ratio calculated from DNase I and phalloidin fluorescence intensities was not different between CTR and KO MEFs independent of considering fluorescence intensity in the cytosol or in the entire cells (Fig. 1I; total: CTR: 1.42±0.04, KO: 1.56±0.03, n≥71/3, P=0.497; cytosol: CTR: 2.15±0.05, KO: 2.19±0.04, n≥71/3, P=0.880). A normal G/F-actin ratio in KO MEFs was confirmed by immunoblots, for which we separated soluble protein from insoluble protein fractions including G-actin and F-actin, respectively (Fig. 1J-K; CTR: 1.83±0.47, KO: 1.76±0.26, n=5, P=0.916). Together, CAP2 inactivation did not induce severe defects in the actin cytoskeleton. However, it caused a moderate increase in G-actin and F-actin levels, which did not change the equilibrium between G-actin and F-actin.

CAP2 inactivation alters subcellular distribution of MRTF-A in mouse fibroblasts

MRTF-A is a transcriptional coactivator that shuttles between the cytosol and the nucleus. This shuttling depends on G-actin, because G-actin binding is necessary for nuclear MRTF-A export and interferes with accessibility of its nuclear localization sequence (Treisman 2013; Plessner and Grosse 2015). Hence, moderately increased G-actin levels in KO MEFs might be associated with altered subcellular MRTF-A distribution. To test this, we generated CTR and KO MEF lines that stably expressed GFP-tagged MRTF-A (MRTF-A-GFP) and grouped MEFs into three categories: 1) MEFs with mainly nuclear MRTF-A-GFP (nuclear), 2) MEFs with mainly cytosolic MRTF-A-GFP (cytosolic) and 3) MEFs with equal MRTF-A-GFP levels in both compartments (equal), similar to previous studies (Hinojosa et al. 2017). In KO MEFs, MRTF-A-GFP distribution was different from CTR MEFs, as indicated by an almost sevenfold increase in the cytosolic MRTF-A-GFP fraction and a sevenfold decrease in the nuclear MRTF-A-GFP fraction (Fig. 2A, C; (in %) CTR: nuclear: 68.04±3.74, cytosolic: 11.51±2.58, equal: 20.45±2.22, n=15/3, KO: nuclear: 9.00±2.09, cytosolic: 85.22±2.61, equal: 5.78±1.95, n=15/3, P<0.001). In an independent experiment, we determined localization of endogenous MRTF-A by immunocytochemistry and found very similar differences between CTR and KO MEFs (Fig. 2B-C; (in %) CTR: nuclear: 50.24±6.87, cytosolic: 25.23±3.60, equal: 24.53±4.77, n=6/3, KO: nuclear: 7.50±2.12, cytosolic: 75.97±4.38, equal: 16.53±3.24, n=6/3, P<0.001), thereby demonstrating that our GFP-tagged construct faithfully reflects MRTF-A localization and that our stably transfected MEF lines were valuable tools to study the mechanisms that control

MRTF-A localization. Together, increased actin levels in KO MEFs were associated with altered MRTF-A localization, and we therefore hypothesized that CAP2 controls MRTF-A localization in an actin-dependent mechanism.

CAP2 controls MRTF-A localization via an actin-dependent mechanism

To test this hypothesis, we exploited MRTF-A-GFP expressing MEF lines to determine MRTF-A localization upon pharmacological manipulation of the actin cytoskeleton. Latrunculin B (LATB) reportedly increased G-actin levels and promoted interaction of G-actin with MRTF-A (Morton et al. 2000). Hence, LATB treatment should increase cytosolic MRTF-A localization (Olson et al. 2010). Indeed, when compared to dimethyl sulfoxide (DMSO)-treated CTR MEFs, LATB increased threefold the CTR MEF fraction with cytosolic MRTF-A-GFP localization and it decreased eightfold the fraction with nuclear localization (Fig. 2D-E; DMSO: nuclear: 41.76±2.68, cytosolic: 29.40±2.64, equal: 28.85±2.25, LATB: nuclear: 4.95±2.36, cytosolic: 90.20±3.43, equal: 4.85±1.86, n=9/3, $P<0.01$). Instead, LATB failed in changing the subcellular MRTF-A-GFP distribution in KO MEFs (DMSO: nuclear: 6.74±1.43, cytosolic: 84.46±2.77, equal: 8.81±1.87, LATB: nuclear: 0.28±0.26, cytosolic: 98.35±0.64, equal: 1.38±0.66, n=9/3, $P=0.158$). Notably, subcellular MRTF-A distribution was not different between CTR and KO MEFs upon LATB treatment ($P=0.225$). Hence, LATB caused a subcellular MRTF-A distribution in CTR MEFs that was similar to that in KO MEFs.

Apart from LATB, we tested jasplakinolide (JASP) that stabilizes F-actin, reduces G-actin levels and that reportedly induced nuclear MRTF-A localization (Tsuji et al. 2009; Olson et al. 2010). As expected, JASP doubled the fraction of CTR MEFs with nuclear MRTF-A-GFP localization and reduced the fraction with cytosolic localization (Fig. 2D-E; JASP: nuclear: 83.69±2.61, cytosolic: 6.41±1.05, equal: 9.90±2.16, n=9/3, $P<0.01$). Similarly, JASP changed the subcellular MRTF-A-GFP distribution in KO MEF as indicated by a ninefold increased fraction with nuclear MRTF-A-GFP localization concomitant with a fourfold decreased cytosolic fraction (JASP: nuclear: 62.21±6.32, cytosolic: 22.28±5.95, equal: 15.50±2.19, n=9/3, $P<0.01$). Notably, the subcellular MRTF-A distribution did not differ between CTR and KO MEFs upon JASP treatment ($P=0.237$). Hence, pharmacological induced reduction of G-actin levels rescued MRTF-A localization in KO MEFs. We therefore concluded that CAP2 controlled MRTF-A localization via an actin-dependent mechanism.

CAP2 is dispensable for serum induced nuclear MRTF-A translocation

Serum stimulation reportedly induced nuclear MRTF-A translocation in fibroblasts (McGee et al. 2011; Esnault et al. 2014). By exploiting MRTF-A-GFP expressing MEF lines, we next tested whether CAP2 was relevant for serum-induced nuclear MRTF-A translocation. First, we starved MEFs in 0.3% fetal calf serum (FCS) for 48 h and, thereafter, determined nuclear translocation during the first six min of stimulation with 20% FCS by live-cell imaging. We restricted this analysis to CTR and KO MEFs of the cytosolic fraction to avoid any false interpretation due to different MRTF-A localization before stimulation. As obvious from the movies and image sequences (Fig. 3A, Movies S1-2), MRTF-A rapidly translocated into the nucleus of CTR and KO MEFs upon serum stimulation. Quantification of the latency of nuclear translocation revealed no difference between both groups (Fig 3B; (in s) CTR: 248.75±31.25, KO: 185.00±14.18, n=12/3, P=0.089). Next, we determined subcellular MRTF-A localization in all CTR and KO MEFs both upon 48 h of starving and upon 10 min of serum stimulation. Compared to basal conditions (Fig. 2C), the CTR MEF fraction with nuclear MRTF-A localization was reduced by 40%, and the fraction with cytosolic MRTF-A was increased threefold upon starvation (Fig. 3C-D; nuclear: 40.90±3.78, cytosolic: 34.73±5.02, equal: 24.38±3.63, n=25/3, P<0.001). As expected, serum stimulation induced a nuclear translocation of all MRTF-A in CTR MEFs, and we did not note CTR MFEs with predominantly cytosolic MRTF-A or equal localization in cytosol and nucleus (Fig. 3C-D; n=9/3, P<0.001). In contrast to CTR MEFs, starving did not alter MRTF-A localization in KO MEFs (nuclear: 1.67±1.07, cytosolic: 92.34±2.39, equal: 6.00±2.29, n=15/3, P<0.0543), but serum stimulation induced nuclear MRTF-A translocation in the majority of KO MEFs. However, unlike in FCS-stimulated CTR MEFs, we noted a fraction of 25% KO MEFs with equal localization of MRTF-A in cytosol and nucleus upon FCS stimulation (nuclear: 75.02±3.79, equal: 24.98±3.79, n=9/3, P<0.001). Upon serum stimulation, subcellular MRTF-A distribution was still different between CTR and KO MEFs (P<0.05). Together, serum stimulation induced nuclear MRTF-A translocation in KO MEFs with a latency similar to CTR MEFs. However, different from CTR MEFs, in a quarter of serum-stimulated KO MEFs MRTF-A was still present in the cytosol.

CAP2 inactivation reduces SRF activity in mouse fibroblasts

So far, we showed that CAP2 i) controls MRFT-A localization in MEFs in an actin-dependent mechanism and ii) was largely dispensable for serum-induced nuclear MRTF-A translocation. Next, we tested whether CAP2 was relevant for MRFT-A-dependent activation of SRF. To do so, we generated CTR and KO MEF lines that stably expressed a SRF reporter in which expression of firefly luciferase was controlled by three minimal c-Foc promotor sequences including serum response elements, but lacking TCF binding sites (Hinojosa et al. 2017). Luciferase activity was strongly reduced in KO MEFs and reached only half of that in CTR MEFs, thereby suggesting reduced SRF activity in KO MEFs (Fig. 4A; (arbitrary units) CTR: 48.19±6.94, KO: 27.28±1.81, n=6, P<0.05). Indeed, qPCR experiments revealed a reduction in mRNA levels of several established SRF downstream target genes including those encoding for c-Fos (*c-Fos*), vinculin (*Vcl*), smooth muscle α-actin (*Acta2*), Cyr61 (*Cyr61*) or SRF (*Srf*) itself (Fig. 4B). In these experiments, we found similar changes in both KO MEF lines generated (KO 1: *Cyr61*: 0.16±0.02, P<0.01; *c-Fos*: 0.16±0.03, P<0.05; *Acta2*: 0.29±0.05, P<0.05; *Vcl*: 0.20±0.05, P<0.05; *Srf*: 0.48±0.07, P=0.073, n=9; KO 2: *Cyr61*: 0.48±0.11, P<0.05; *Fos*: 0.11±0.02, P<0.05; *Acta2*: 0.11±0.02, P<0.05; *Vcl*: 0.24±0.06, P<0.05; *Srf*: 0.29±0.04, P<0.05, n=9). Notably, mRNA levels of *Egr2*, a SRF downstream target that is controlled by the TCF, but not by the MRTF-A pathway, was unchanged in both KO MEF lines (KO 1: 1.03±0.20, n=9, P=0.923; KO 2: 0.70±0.03, n=9, P=0.319). Together, altered MRTF-A localization in KO MEFs was associated with reduced SRF activity.

Next, we wanted to know whether serum-induced SRF activity depends on CAP2. To test this, we starved CTR and KO MEFs expressing the SRF reporter for 20 h before stimulation with 20% FCS for either 24 or 48 h. As expected, serum stimulation for either 24 or 48 h induced SRF activity in CTR MEFs (Fig. 4C; 24 h: 2.36±0.55, n=6, P<0.01; 48 h: 4.83±1.22, n=6, P<0.05). Very similar to CTR MEFs, serum stimulation induced SRF activity in KO MEFs (24 h: 2.86±0.81, n=6, P<0.05; 48 h: 6.06±1.69, n=6, P<0.05), and serum induced SRF activity was not different between groups (24 h: P=0.652; 48 h: P=0.601). Together, basal SRF activity was reduced in KO MEFs, but serum stimulation equally induced SRF activity in CTR and KO MEFs.

Discussion

The present study aimed at deciphering the CAP2-dependent mechanism relevant for the control of the transcription factor SRF. We chose mouse embryonic fibroblasts (MEFs) as a cellular model system for our study, because in these cells CAP2 is expressed at substantial levels and SRF-dependent gene regulation and upstream regulatory mechanisms have been intensively studied (Esnault et al. 2014). We found increased DNase I fluorescent intensity in CAP2 mutant MEFs, which was associated with a reduction in nuclear MRTF-A, reduced SRF activity and decreased expression of established MRTF-SRF target genes. While drug-induced increase in G-actin levels altered MRTF-A localization in control MEFs, it did not affect MRTF-A localization in mutant MEFs, which was normalized upon drug-induced decrease in G-actin levels. These data let us propose a model in which CAP2 controls SRF-dependent gene expression via regulating G-actin levels and nuclear MRTF-A localization.

This model is in good agreement with recent studies, which identified important functions for CAPs in controlling F-actin dynamics (Chaundhry et al. 2010; Jansen et al. 2014; Johnston et al. 2015; Kotila et al. 2018; Kotila et al. 2019; Mu et al. 2019; Shekhar et al. 2019). Specifically, these studies showed that CAPs can i) facilitate F-actin severing and actin subunit dissociation in synergy with ADF/cofilin and twinfilin (Chaundhry et al 2010; Jansen et al. 2014; Johnston et al. 2015; Kotila et al. 2018; Kotila et al. 2019; Shekhar et al. 2019), ii) catalyze ATP-for-ADP exchange on G-actin that is relevant for F-actin assembly (Moriyama and Yahara 2002; Chaudhry et al. 2007; Nomura et al. 2012; Jansen et al. 2014), and iii) inhibit activity of inverted formin 2 (INF2) that promotes F-actin assembly (Mu et al. 2019). Hence, by regulating various aspects of F-actin assembly and disassembly, CAPs control G-actin levels and, hence, interaction of G-actin with MRTF-A. Our finding of increased DNase I fluorescent intensity and reduced nuclear MRTF-A localization in CAP2 mutant MEFs, together with normalization of MRTF-A localization upon treatment with the F-actin stabilizing drug JASP emphasize that CAP2 inactivation increased G-actin levels in MEFs, suggesting that in MEFs CAP2 acts as a F-actin assembly factor rather than promoting F-actin disassembly.

We found reduced SRF activity in reporter assays as well as reduced expression of SRF target genes in CAP2 mutant MEFs.

Supportively, reduced expression of MRTF-SRF targets in CAP2 mutant MEFs have been noted recently by others (Xiong et al. 2019). Although SRF activity has not been systematically analyzed in skeletal muscle from CAP2 mutant mice, decreased mRNA levels of established MRTF-SRF targets such as *Acta1*, *Acta2* and *Actc1* suggest reduced SRF activity in skeletal muscles from CAP2 mutant embryos, too (Kepser et al. 2019), in which SRF dysregulation may contribute to retarded skeletal muscle development. Indeed, a crucial function for the MRTF-SRF pathway during late embryonic skeletal muscle development is evident from gene-targeted mice (Li et al. 2005; Cenik et al. 2016). Opposite to our findings in CAP2 mutant MEFs and to reduced expression of MRTF-SRF target genes in skeletal muscles from CAP2 mutant embryos (Kepser et al. 2019), a recent study reported upregulation of several MRTF-SRF target genes including *Acta1* and *Acta2* in heart tissue and isolated cardiomyocytes from CAP2 mutant mice, which was associated with increased nuclear MRTF levels. Interestingly, heart defects in CAP2 mutant mice including dilated cardiomyopathy and impaired cardiac conductance were partially restored upon pharmacological inhibition of MRTF-SRF activity, demonstrating that CAP2-dependent regulation of the MRTF-SRF pathway is physiologically relevant and that its dysregulation due to CAP2 inactivation contributes to pathological conditions (Xiong et al. 2019). The opposite effects of CAP2 inactivation on MRTF-SRF activity suggest different CAP2 activities towards F-actin dynamics in MEFs versus cardiomyocytes. Our data suggest that CAP2 promotes F-actin assembly in MEFs. Instead, it may primarily act as a F-actin disassembly factor in cardiomyocytes.

By chromatin immunoprecipitation combined with deep sequencing, previous studies convincingly demonstrated that serum-induced, SRF-mediated transcriptional response largely depends on the MRTF-SRF pathway (Esnault et al. 2014). In line with these data, we showed efficient MRTF-A translocation into the nucleus as well as elevated SRF activity upon serum stimulation in control MEFs. Interestingly, serum-stimulated nuclear MRTF-A translocation as well as SRF activation was similar to controls in CAP2 mutant MEFs. Hence, while we found a role for CAP2 in MRTF-A localization and SRF activity under basal conditions, in unstimulated MEFs, CAP2 was dispensable for serum stimulation of the MRTF-SRF pathway.

Via acting on transmembrane receptors including G-protein-coupled receptors, receptor tyrosine kinases or serine-threonine receptor kinases, extracellular signals are translated into intracellular signaling cascades that include Rho family small guanosine triphosphatases (GTPases) (Schiller 2006; Moustakas and Heldin 2008; Cotton and Claing 2009). Effectors of Rho GTPases include, among others, formins, Wiskott-Aldrich syndrome protein (WASP), WASP-family verprolin homologues (WAVEs) and actin-related protein 2/3 (ARP2/3) complex, which orchestrate actin polymerization (Jaffe and Hall 2005). Hence, Rho GTPase signaling promotes incorporation of G-actin into filaments that releases MRTF from G-actin complexes and stimulates MRTF-SRF-dependent gene expression (Olson et al. 2010). Rho GTPase signaling further shifts the F/G-actin equilibrium towards F-actin via activation of Rho-associated kinases (ROCKs) that in turn inhibits actin depolymerizing proteins of the ADF/cofilin family (Ohashi et al. 2000). ADF/cofilin cooperates with CAPs in actin dynamics (Chaudhry et al. 2010; Ono 2013; Jansen et al. 2014; Kotila et al. 2018; Kotila et al. 2019), and inhibition of ADF/cofilin activity upon serum stimulation may explain why CAP2 was dispensable for serum-induced stimulation of the MRTF-SRF pathway.

In summary, our data revealed that CAP2 controls in an actin-dependent mechanism the subcellular localization of MRTF and thereby SRF activity in unstimulated MEFs, while CAP2 was dispensable for serum-induced nuclear MRTF translocation and MRTF-SRF stimulation.

Acknowledgements

We thank Maria Bettina Kowalski, Denis Grabski and Andrea Wüstenhagen for excellent technical support. This work was supported by research grants of the Deutsche Forschungsgemeinschaft (DFG) and Fondazione Cariplo to MBR. LJK and LSH were supported by the DFG Research Training Group 'Membrane Plasticity in Tissue Development and Remodeling' (GRK 2213).

Author contributions

Experiments were designed and results were discussed by LJK, LSH, RG and MBR. Data were analyzed by LJK, LSH and MBR. Manuscript was written by MBR and LJK.

References

Baker, J. M. and F. M. Boyce (2014). "High-throughput Functional Screening using a Homemade Dual-glow Luciferase Assay." J Vis Exp **2014**(88): 50282.

Balcer, H. I., A. L. Goodman, A. A. Rodal, E. Smith, J. Kugler, J. E. Heuser and B. L. Goode (2003). "Coordinated regulation of actin filament turnover by a high-molecular-weight Srv2/CAP complex, cofilin, profilin, and Aip1." Curr Biol **13**(24):2159-69.

Bertling, E., P. Hotulainen, P. K. Mattila, T. Matilainen, M. Salminen and P. Lappalainen (2004). "Cyclase-associated protein 1 (CAP1) promotes cofilin-induced actin dynamics in mammalian nonmuscle cells." Mol Biol Cell **15**(5): 2324-2334.

Cenik, B. K., N. Liu, B. Chen, S. Bezprozvannaya, E. N. Olson and R. Bassel-Duby (2016). "Myocardin-related transcription factors are required for skeletal muscle development." Development **143**(15): 2853-2861.

Chaudhry, F., C. Guérin, M. von Witsch, L. Blanchoin and C. J. Staiger CJ (2007). "Identification of Arabidopsis cyclase-associated protein 1 as the first nucleotide exchange factor for plant actin." Mol Biol Cell **18**(8):3002-14

Chaudhry, F., K. Little, L. Talarico, O. Quintero-Monzon and B. L. Goode (2010). "A central role for the WH2 domain of Srv2/CAP in recharging actin monomers to drive actin turnover in vitro and in vivo." Cytoskeleton **67**(2):120-33..

Cotton, M. and A. Claing (2009). "G protein-coupled receptors stimulation and the control of cell migration." Cell Signal **21**(7):1045-53.

Cramer, L. P., L. J. Briggs and H. R. Dawe HR (2002). "Use of fluorescently labelled deoxyribonuclease I to spatially measure G-actin levels in migrating and non-migrating cells." Cell Motil Cytoskeleton **51**(1):27-38.

Esnault, C., A. Stewart, F. Gualdrini, P. East, S. Horswell, N. Matthews and R. Treisman (2014). "Rho-actin signaling to the MRTF coactivators dominates the immediate transcriptional response to serum in fibroblasts." Genes Dev **28**(9):943-58.

Field, J., D. Z. Ye, M. Shinde, F. Liu, K. J. Schillinger, M. Lu, T. Wang, M. Skettini, Y. Xiong, A. K. Brice, D. C. Chung and V. V. Patel (2015). "CAP2 in cardiac conduction, sudden cardiac death and eye development." Sci Rep **30**;5:17256.

Freeman, N. L. and J. Field (2000). "Mammalian homolog of the yeast cyclase associated protein, CAP/Srv2p, regulates actin filament assembly." Cell Motil Cytoskeleton **45**(2):106-20.

Gualdrini, F., C. Esnault, S. Horswell, A. Steward, N. Matthews and R. Treisman (2016). "SRF Co-factors Control the Balance between Cell Proliferation and Contractility." Mol Cell **64**: 1048-1061

Hinojosa, L. S., M. Holst, C. Baarlink and R. Grosse (2017). "MRTF transcription and Ezrin-dependent plasma membrane blebbing are required for entotic invasion." J Cell Biol **216**(10):3087-3095.

Huang, W., P. J. Zhu, S. Zhang, H. Zhou, L. Stoica, M. Galiano, K. Krnjević, G. Roman and M. Costa-Mattioli (2013) "mTORC2 controls actin polymerization required for consolidation of long-term memory." Nat Neurosci **16**(4):441-448

Hubberstey, A. V. and E. P. Mottillo (2002). "Cyclase-associated proteins: CAPacity for linking signal transduction and actin polymerization." FASEB J. **16**(6):487-99.

Jaffe, A. B. and A. Hall (2005). "Rho GTPases: biochemistry and biology." Annu Rev Cell Dev Biol **21**:247-69.

Jang, H. D., S. E. Lee, J. Yang, H. C. Lee, D. Shin, H. Lee, J. Lee, S. Jin, S. Kim, S. J. Lee, J. You, H. W. Park, K. Y. Nam, S. H. Lee, S. W. Park, J. S. Kim, S. Y. Kim, Y. W. Kwon, S. H. Kwak, H. M. Yang and H. S. Kim (2020). "Cyclase-associated protein 1 is a binding partner of proprotein convertase subtilisin/kexin type-9 and is required for the degradation of low-density lipoprotein receptors by proprotein convertase subtilisin/kexin type-9." Eur Heart J **41**(2): 239-252.

Jansen, S., A. Collins, L. Golden, O. Sokolova and B. L. Goode (2014). "Structure and mechanism of mouse cyclase-associated protein (CAP1) in regulating actin dynamics." J Biol Chem **289**(44):30732-42.

Johnston, A. B., A. Collins and B. L. Goode (2015). "High-speed depolymerization at actin filament ends jointly catalysed by Twinfilin and Srv2/CAP." Nat Cell Biol **17**(11):1504-11.

Kepser, L. J., F. Damar, T. De Cicco, C. Chaponnier, T. J. Proszynski, A. Pagenstecher and M. B. Rust (2019). "CAP2 deficiency delays myofibril actin cytoskeleton differentiation and disturbs skeletal muscle architecture and function." Proc Natl Acad Sci U S A **116**(17) 8397-8402

Kotila, T., K. Kogan, G. Enkavi, S. Guo, I. Vattulainen , B. L. Goode and P. Lappalainen (2018). "Structural basis of actin monomer re-charging by cyclase-associated protein." Nat Commun **9**(1):1892.

Kotila, T., H. Wioland, G. Enkavi, K. Kogan, I. Vattulainen, A. Jégou, G. Romet-Lemonne and P. Lappalainen (2019). "Mechanism of synergistic actin filament pointed end depolymerization by cyclase-associated protein and cofilin." Nat Commun **10**(1):5320.

Li, S., M. P. Czubryt, J. McAnally, R. Bassel-Duby, J. A. Richardson, F. F. Wiebel, A. Nordheim and E. N. Olson (2005). "Requirement for serum response factor for skeletal muscle growth and maturation revealed by tissue-specific gene deletion in mice." Proc Natl Acad Sci U S A **102**(4): 1082-1087.

McGee, K. M., M. K. Vartiainen, P. T. Khaw, R. Treisman and M. Bailly (2011). "Nuclear transport of the serum response factor coactivator MRTF-A is downregulated at tensional homeostasis." EMBO Rep **12**(9): 963-970.

Melak, M., M. Plessner and R. Grosse (2017). "Actin visualization at a glance." J Cell Sci **130**(3):525-530.

Moriyama, K. and I. Yahara (2002). "Human CAP1 is a key factor in the recycling of cofilin and actin for rapid actin turnover." J Cell Sci **115**(Pt 8):1591-601.

Morton, W. M., K. R. Ayscough and P. J. McLaughlin (2000). "Latrunculin alters the actin-monomer subunit interface to prevent polymerization." Nat Cell Biol **2**(6):376-8.

Moustakas, A. and C. H. Heldin (2008). "Dynamic control of TGF-beta signaling and its links to the cytoskeleton." FEBS Lett **582**(14):2051-65.

Mu, A., T.S. Fung, A. N. Kettenbach, R. Chakrabarti and H. N. Higgs (2019). "A complex containing lysine-acetylated actin inhibits the formin INF2." Nat Cell Biol **21**(5):592-602.

Nomura, K., K. Ono and S. Ono (2012). "CAS-1, a C. elegans cyclase-associated protein, is required for sarcomeric actin assembly in striated muscle." J Cell Sci **125**(Pt 17):4077-89.

Ohashi, K., K. Nagata, M. Maekawa, T. Ishizaki, S. Narumiya and K. Mizuno (2000). "Rho-associated kinase ROCK activates LIM-kinase 1 by phosphorylation at threonine 508 within the activation loop." J Biol Chem **275**(5):3577-82.

Olson, E. N. and A. Nordheim (2010). "Linking actin dynamics and gene transcription to drive cellular motile functions." Nat Rev Mol Cell Biol **11**(5): 353-365.

Ono, S. (2013). "The role of cyclase-associated protein in regulating actin filament dynamics - more than a monomer-sequestration factor." J Cell Sci **126**(Pt 15): 3249-3258.

Peche, V., S. Shekar, M. Leichter, H. Korte, R. Schroder, M. Schleicher, T. A. Holak, C. S. Clemen, Y. B. Ramanath, G. Pfitzer, I. Karakesisoglou and A. A. Noegel (2007). "CAP2, cyclase-associated protein 2, is a dual compartment protein." Cell Mol Life Sci **64**(19-20): 2702-2715.

Peche, V. S., T. A. Holak, B. D. Burgute, K. Kosmas, S. P. Kale, F. T. Wunderlich, F. Elhamine, R. Stehle, G. Pfitzer, K. Nohroudi, K. Addicks, F. Stockigt, J. W. Schrickel, J. Gallinger, M. Schleicher and A. A. Noegel (2013). "Ablation of cyclase-associated protein 2 (CAP2) leads to cardiomyopathy." Cell Mol Life Sci **70**(3): 527-543.

Plessner, M. and R. Grosse (2015). "Extracellular signaling cues for nuclear actin polymerization." Eur J Cell Biol **94**(7-9):359-62.

Rehklau, K., C. B. Gurniak, M. Conrad, E. Friauf, M. Ott and M. B. Rust (2012). "ADF/cofilin proteins translocate to mitochondria during apoptosis but are not generally required for cell death signaling." Cell Death Differ **19**(6):958-67.

Schiller, M. (2006). "Coupling receptor tyrosine kinases to Rho GTPases--GEFs what's the link." Cell Signal **18**(11):1834-43.

Seiler, A., M. Schneider, H. Förster, S. Roth, E. K. Wirth, C. Culmsee, N. Plesnila, E. Kremmer, O. Rådmark, W. Wurst, G. W. Bornkamm, U. Schweizer and M. Conrad (2008). "Glutathione peroxidase 4 senses and translates oxidative stress into 12/15-lipoxygenase dependent- and AIF-mediated cell death." Cell Metab **8**(3):237-48.

Shekhar, S., J. Chung, J. Kondev, J. Gelles and B. L. Goode (2019). "Synergy between Cyclase-associated protein and Cofilin accelerates actin filament depolymerization by two orders of magnitude." Nat Commun **10**(1):5319.

Stockigt, F., V. S. Peche, M. Linhart, G. Nickenig, A. A. Noegel and J. W. Schrickel (2016). "Deficiency of cyclase-associated protein 2 promotes arrhythmias associated with connexin43 maldistribution and fibrosis." Arch Med Sci **12**(1): 188-198.

Treisman, R. (2013). "Shedding light on nuclear actin dynamics and function." Trends Biochem Sci **38**(8):376-7.

Tsuji, T., T. Miyoshi, C. Higashida, S. Narumiya and N. Watanabe (2009). "An order of magnitude faster AIP1-associated actin disruption than nucleation by the Arp2/3 complex in lamellipodia." PLoS One **4**(3):e4921.

Xiong, Y., K. Bedi, S. Berritt, B. K. Attipoe, T. G. Brooks, K. Wang, K. B. Margulies and J. Field (2019). "Targeting MRTF/SRF in CAP2-dependent dilated cardiomyopathy." JCI Insight **4**(6): e124629.

Figure 1

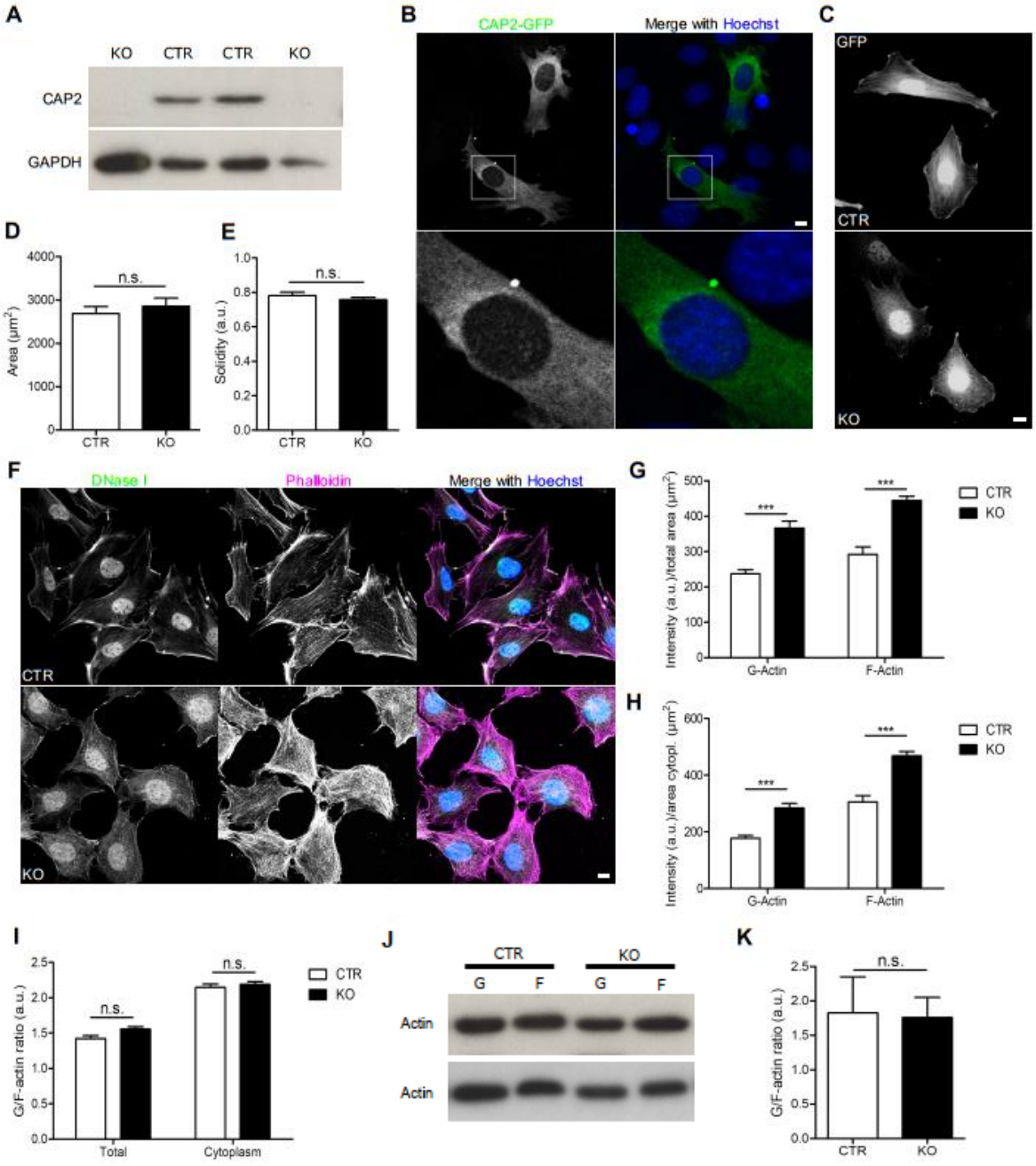
A
KO
CTR
CTR
KO
CAP2
GAPDH
B
CAP2-GFP
Merge with Hoechst
C
GFP
CTR
KO
D
Area (µm²)
n.s.
CTR
KO
E
Solidity (a.u.)
n.s.
CTR
KO
F
DNase I
Phalloidin
Merge with Hoechst
CTR
KO
G
Intensity (a.u.)/total area (µm²)
***
***
G-Actin
F-Actin
CTR
KO
H
Intensity (a.u.)/area cytopl. (µm²)
***
***
G-Actin
F-Actin
CTR
KO
I
G/F-actin ratio (a.u.)
n.s.
n.s.
Total
Cytoplasm
CTR
KO
J
CTR
KO
G
F
G
F
Actin
Actin
K
G/F-actin ratio (a.u.)
n.s.
CTR
KO

Figure 2

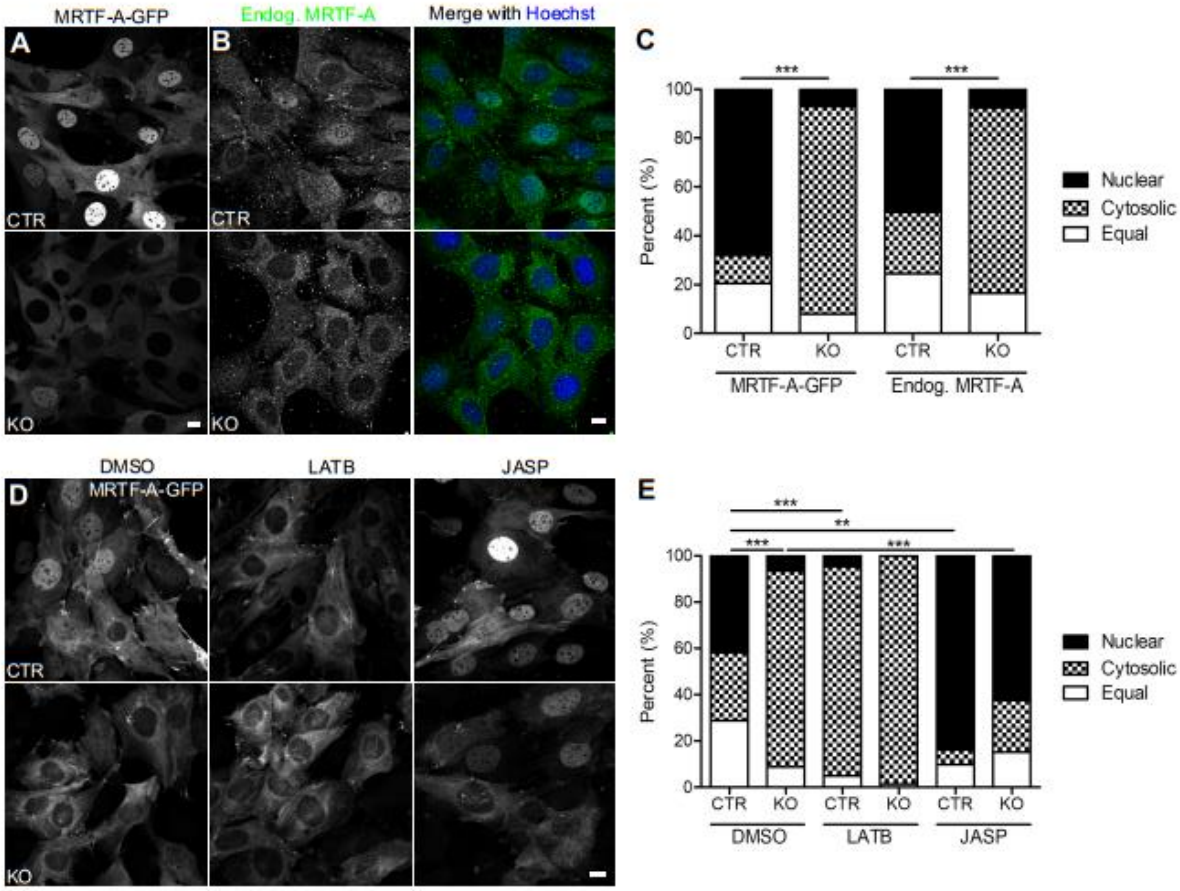
MRTF-A-GFP
Endog. MRTF-A
Merge with Hoechst
A
B
C
CTR
KO
***
Percent (%)
Nuclear
Cytosolic
Equal
MRTF-A-GFP
Endog. MRTF-A
DMSO
LATB
JASP
D
E
**
LATB
JASP

Figure 3

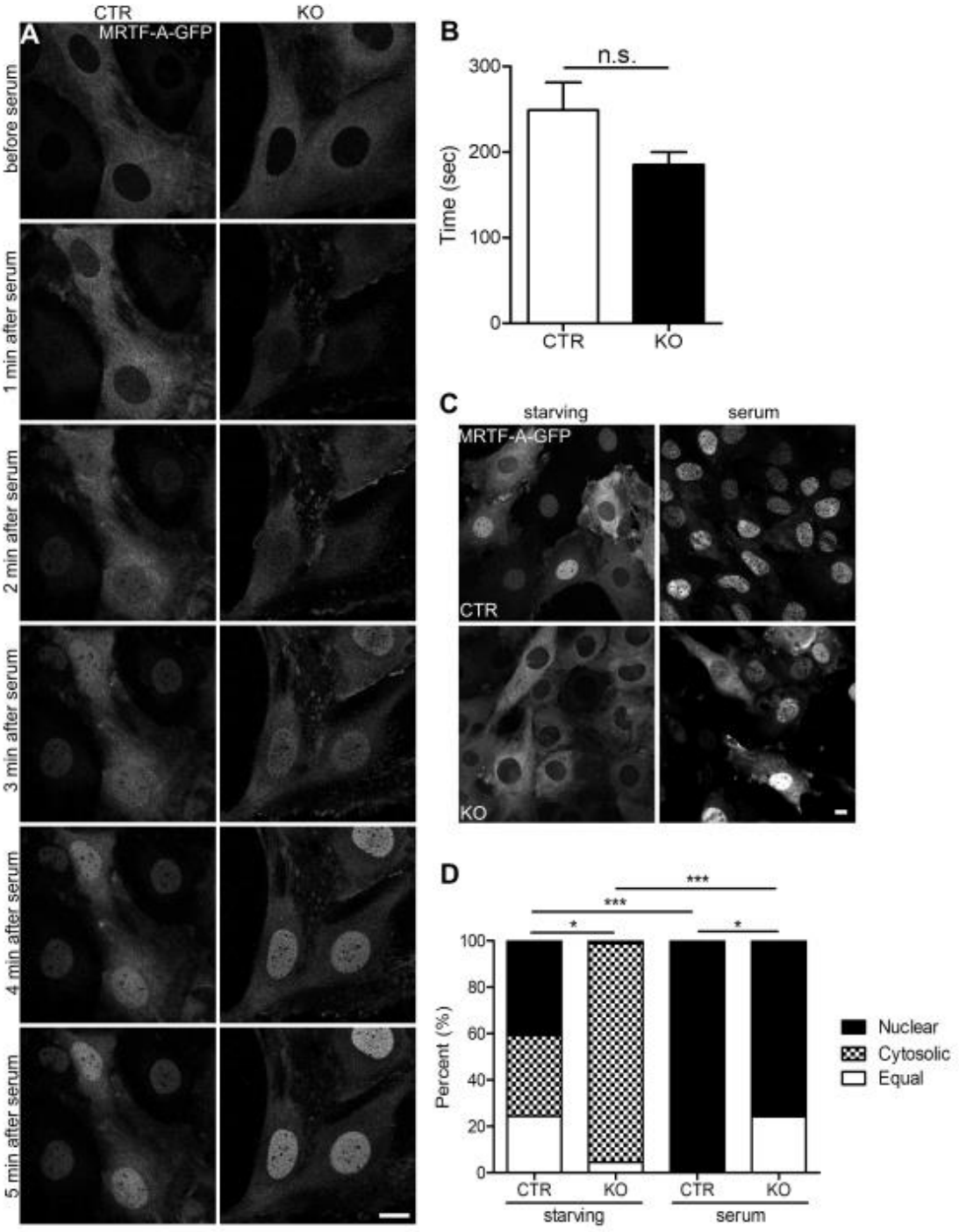
CTR
KO
A
MRTF-A-GFP
before serum
1 min after serum
2 min after serum
3 min after serum
4 min after serum
5 min after serum
B
n.s.
Time (sec)
300
200
100
0
CTR
KO
C
starving
serum
MRTF-A-GFP
CTR
KO
D
***
***
*
*
Percent (%)
100
80
60
40
20
0
CTR
KO
CTR
KO
starving
serum
Nuclear
Cytosolic
Equal

Figure 4

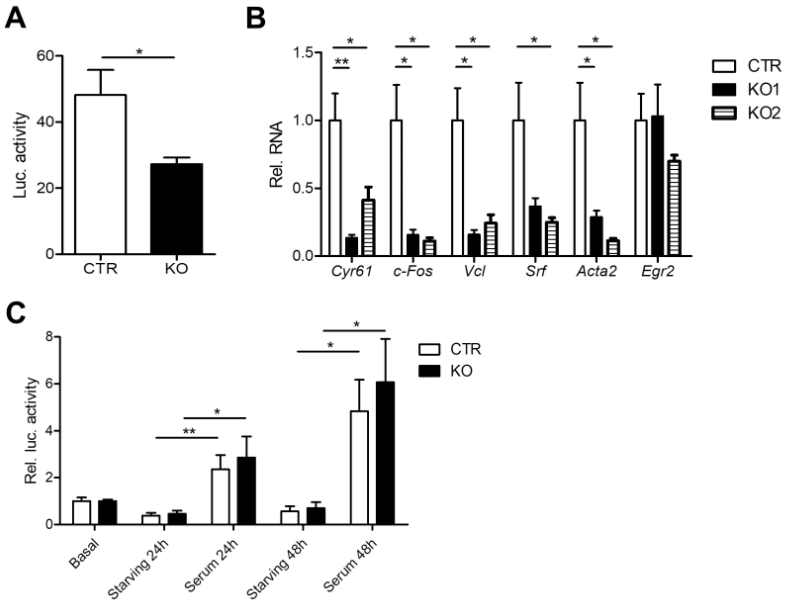
A
B
C
Luc. activity
CTR
KO
Rel. RNA
Cyr61
c-Fos
Vcl
Srf
Acta2
Egr2
CTR
KO1
KO2
Rel. luc. activity
Basal
Starving 24h
Serum 24h
Starving 48h
Serum 48h
CTR
KO

Figure legends

Figure 1. CAP2 inactivation increased G-actin levels in MEFs. (A) Immunoblots showing CAP2 expression in two CTR MEF lines and CAP2 inactivation in two KO MEF lines. GAPDH was used as loading control. **(B)** Representative micrograph showing localization of GFP-tagged CAP2 (green) in CTR MEFs. Merge micrograph includes counterstaining with DNA dye 4′,6-diamidino-2-phenylindole (DAPI, blue). Box indicates area shown at higher magnification. **(C)** Representative micrographs of GFP-transfected CTR and KO MEFs. **(D)** Area quantification of CTR and KO MEFs. **(E)** Solidity index of CTR and KO MEFs. **(F)** Representative micrographs of MEFs stained with fluorescent phalloidin and DNase I. **(G)** Whole cell fluorescence quantification for phalloidin and DNase I. **(H)** Quantification of phalloidin and DNase I fluorescence in cytosol. **(I)** Quantification of DNase I-to-phalloidin-ratio for whole cell and cytosolic fluorescence. **(J)** Immunoblots showing actin in soluble (G) and insoluble (F) protein fractions. **(K)** Quantification of G/F-actin ratio. Scale bars (in µm): 10 (B. C, F). *: P<0.05, **: P<0.01, ***: P<0.001, ns: not significant.

Figure 2. CAP2 controls MRTF-A localization via an actin-dependent mechanism in MEFs. (A) Representative micrographs of CTR and KO MEFs that stably expressed GFP-tagged MRTF-A (MRTF-A-GFP). **(B)** Representative micrographs of CTR and KO MEFs stained with an antibody against MRTF-A (green). MEFs were counterstained with the DNA-dye Hoechst (blue). **(C)** Categorization of MEFs according to the localization of MRTF-A-GFP or endogenous MRTF-A, i.e. fractions with mainly nuclear or cytosolic MRTF-A-GFP and fraction with equal levels in both compartments. **(D)** Representative micrographs of MRTF-A-GFP-expressing CTR and KO MEFs upon treatment with either DMSO, latrunculin B (LATB) or jasplakinolide (JASP). **(E)** Categorization of MEFs according to the localization of MRTF-A-GFP upon treatment with either DMSO, LATB or JASP. Scale bars (in µm): 10 (A, B, D). *: P<0.05, **: P<0.01, ***: P<0.001, ns: not significant.

Figure 3. CAP2 was dispensable for serum induced nuclear MRTF-A translocation in MEFs. (A) Image sequence of MRTF-A-GFP-expressing MEFs before and during serum stimulation. **(B)** Latency of nuclear MRTF-A translocation. **(C)** Representative micrographs of MRTF-A-GFP-expressing CTR and KO MEFs during starving and upon serum stimulation. **(D)** Categorization of MEFs according to the localization of MRTF-A-GFP or endogenous MRTF-A during starving and upon serum stimulation. Scale bars (in µm): 10 (A, C). *: P<0.05, **: P<0.01, ***: P<0.001, ns: not significant.

Figure 4. CAP2 inactivation reduced SRF activity in MEFs. (A) Firefly luciferase activity in CTR and KO MEFs that stably expressed a SRF reporter in which firefly luciferase expression was under control of SRF activity. **(B)** mRNA levels of selected SRF target genes in two KO MEF lines as determined by qPCR. **(C)** Luciferase expression in CTR and KO MEFs under basal conditions, during starving and upon serum stimulation for either 24 or 48 h. Values are normalized to basal levels. *: P<0.05, **: P<0.01, ***: P<0.001, ns: not significant.

List of Abbreviations

ACTA2	Actin Alpha 2
ADF	Actin Depolymerizing Factor
ADP	Adenosine Diphosphate
ARP	Actin Regulatory Protein
ATP	Adenosine Triphosphate
CAP	Cyclase Associated Protein
Cyr61	Cysteine-rich Angiogenic Inducer 61
E	Embryonic Day
EDL	Musculus Extensor Digitorum Longus
Egr2	Early Growth Response 2
EM	Electron Microscopy
ERK	Extracellular Signal-regulated Kinase
F-actin	Actin Filaments
G-actin	Monomeric/Globular Actin
GFP	Green Fluorescent Protein
JASP	Jasplakinolide
LATB	Latrunculin B
Lmod3	Leiomodin3
MADS	MCM1, Agamous, Deficiens, and SRF
MEF	Mouse Embryonic Fibroblast
MRTF	Myocardin Related Transcription Factor
P	Postnatal Day

QUAD	Musculus Quadriceps Femoris
SOL	Musculus Soleus
SRE	Serum Response Element
SRF	Serum Response Factor
TA	Musculus Tibialis Anterior
TCF	Ternary Complex Factor
α-SKA	α-Skeletal Muscle Actin
α-CAA	α-Cardiac Actin
α-SMA	α-Smooth Muscle Actin
β-CYA	β-Cytoplasmic Actin
γ-CYA	γ-Cytoplasmic Actin

List of Academic Teachers

My academic teachers at the Radboud University Nijmegen were:

Brouwer

Celikel

Deen

De Vrieze

Döller

Flik

Gielen

Halffman

Hendriks

Homberg

Leenaars

Lemmens

Leuven

Jenks

Jetten

Keltjens

Kiliaan

Klaren

Kozicz

Maassen

Martens

Oostendorp

Roubos

Scheenen

Schubert

Peters

Van der Flag

Van der Zee

Van Muijen

Van Opstal

Van Wezel

Visser

Zwart

Acknowledgements

An dieser Stelle möchte ich mich bei all denjenigen bedanken, die mich die letzten Jahre auf dem Weg zu meiner Doktorarbeit begleitet und unterstützt haben.

Zuerst gebührt mein Dank natürlich Prof. Dr. Marco Rust, der meine Doktorarbeit betreut und begutachtet hat. Danke für die hilfreichen Anregungen, die konstruktive Kritik und die spannenden Diskussionen. Ich habe sehr viel gelernt in meiner Zeit hier, nicht nur fachlich, sondern auch persönlich.

Birgit und Christian, sowie den technischen Mitarbeitern, danke ich für die lockere, entspannte Arbeitsatmosphäre und dass man mit jedem Problem immer zu Euch kommen konnte. Ein besonderer Dank gilt an dieser Stelle Bettina. Danke, dass Du meine manchmal etwas verrückten, kurzfristigen und komplizierten Experiment-Designs immer so gut und vor allem verlässlich durchgeführt hast. Besonders Deine Unterstützung bei den Western Blots werde ich Dir nie vergessen!

Kommen wir zum Rest der Rasselbande ☺

Isabell. Was kann ich sagen außer DANKE! Danke für die geile Zeit, den Spaß, die lustigen und legendären Aktionen während und nach der Arbeit, Deine Verrücktheit, aber vor allem auch für Deine Unterstützung in schwierigen Zeiten. Ich könnte ein ganzes Buch darüber schreiben wie besonders deine Freundschaft für mich ist, aber vieles sollte ich hier besser nicht im Detail ausführen (haha). Du bist meine absolute Lieblingskartoffel und ich weiß ganz genau, dass diese Freundschaft für die Ewigkeit ist. Auf viele weitere geile Jahre!!

Felix. Dir auch ein ganz besonderes Dankeschön! Danke für den ganzen Blödsinn den ich immer mit Dir machen konnte, aber auch für Deine Hilfe im Arbeitsalltag. Du hast es auch in den ausweglosesten Situationen geschafft mich wieder aufzumuntern und ohne Dich und Deine besondere Art hätte ich die ganzen Jahre vermutlich nicht überstanden.

Anika, Cara und Sophie. Auch Euch danke ich natürlich von Herzen für die geile Zeit, die Freundschaft und die Unterstützung. Ich habe so viel Spaß mit Euch gehabt und Ihr habt mir die Zeit im und außerhalb des Labors immer versüßt. Ich hoffe wir werden noch weiterhin viele coole Sachen miteinander erleben und uns nie aus den Augen verlieren. Anika, wir sehen uns auf dem nächsten Winzerfestumzug!

Sharof, Kerstin und Jan, Euch danke ich für die fachmännische Unterstützung und natürlich dafür, dass ich mit all meinen Fragen immer zu Euch kommen konnte und Ihr mir stets mit Rat und Tat zur Seite standet. Ihr habt mir viel beigebracht und durch Euer Feedback konnte ich mich stets weiter verbessern und wachsen. Und auch für all die lustigen Momente und Abende möchte ich mich natürlich bedanken. Es war mir sowohl im als auch außerhalb des Labors eine Freude mit Euch!

Fidan, auch Dir danke ich natürlich. Du warst die beste Masterstudentin, die man sich vorstellen kann. Danke für die langen, aber auch lustigen Abende im Labor und deine Freundschaft.

Canan, du hast mich mit offenen Armen in Marburg empfangen und mir meinen Start hier sooo extrem erleichtert! Vielen Dank Bärchen!

Das Wichtigste zum Schluss:

Ein ganz besonderer Dank gilt natürlich meinen Eltern und Thomas. Vor allem aber meiner Mama die mich immer wieder aufs Neue motiviert und vor allem auch beruhigt hat wenn ich mal wieder den Wald vor lauter Bäumen nicht gesehen habe. Ohne Euch und Eure Unterstützung wäre ich heute nicht da wo ich bin.

Ich danke Dir Sascha, für all die Liebe und Geduld die Du mir während der letzten Jahre entgegen gebracht hast. Ich weiß, es war nicht immer leicht mit mir, aber Du hast mich immer unterstützt und jetzt kann unser gemeinsames Leben endlich richtig beginnen ☺ Ich liebe Dich!!!